ASGI-TR-75-09
October 1975

DOT-TSC

OPTIMIZATION OF AUTOMOBILE CRUSH CHARACTERISTICS

TECHNICAL REPORT

A. H. Jazwinski, T. S. Englar, Jr.
and C. Hipkins

OCTOBER 1975

FINAL REPORT
Contract No. DOT-TSC-852

Prepared for

DEPARTMENT OF TRANSPORTATION
TRANSPORTATION SYSTEMS CENTER
Cambridge, Massachussetts 02142

"Prepared for the Department of Transportation, National Highway Traffic Safety Administration under Contract No. DOT-TSC-852. The opinions, findings, and conclusions expressed in this publication are those of the authors and not necessarily those of the National Highway Traffic Safety Administration."

TECHNICAL REPORT STANDARD TITLE PAGE

1. Report No.	2. Government Accession No.	3. Recipient's Catalog No.

4. Title and Subtitle	5. Report Date
OPTIMIZATION OF AUTOMOBILE CRUSH CHARACTERISTICS Technical Report	October 1975 6. Performing Organization Code

7. Author(s)	8. Performing Organization Report No.
A. H. Jazwinski, T. S. Englar, Jr. and C. Hipkins	ASGI-TR-75-09

9. Performing Organization Name and Address	10. Work Unit No.
Automated Sciences Group, Inc. 10210 Greenbelt Road, Suite 605 Seabrook, Maryland 20801	11. Contract or Grant No. DOT-TSC-852

12. Sponsoring Agency Name and Address	13. Type of Report and Period Covered
DEPARTMENT OF TRANSPORTATION Transportation Systems Center Cambridge, Mass. 02142	Final Report Sept. 12, 1974-Oct. 15, 1975 14. Sponsoring Agency Code

15. Supplementary Notes

16. Abstract

A methodology is developed for the evaluation and optimization of societal costs of two-vehicle automobile collisions. Costs considered in a Figure of Merit include costs of injury/mortality, occupant compartment penetration, collision damage repairs, and costs of engineering modifications. The Figure of Merit is developed in a statistical setting, taking into account present (or projected) vehicle population and collision mix statistics, including distributions of vehicle weight/size classes, collision modes, and collision speeds. The methodology is implemented with first-order cost models for the several cost components. Simplified models are utilized for two-vehicle collision dynamics, vehicle force-crush characteristics, and restraint systems. A computer program is developed for the optimization of vehicle force-crush characteristics and crush distance design to minimize the Figure of Merit.

17. Key Words	18. Distribution Statement
Crashworthiness Optimization Societal costs Automobile collisions Vehicle crush characteristics	

19. Security Classif. (of this report)	20. Security Classif. (of this page)	21. No. of Pages	22. Price
Unclassified	Unclassified		

Form DOT F 1700.7 (8-69)

TABLE OF CONTENTS

1. INTRODUCTION

The evaluation of vehicle structural performance characteristics during collision as they impact motor vehicle safety must be performed within a societal costs/goals framework which assigns values or costs to human suffering, injuries and fatalities resulting from collisions, and permits trade-offs between such costs and the more tangible costs of providing added safety. Clearly, the costs of added motor vehicle safety must be in some sense reasonable. Such evaluation must also be performed in a statistical setting which does not consider merely a single collision, but rather a current or projected motor vehicle population and mix of collision modes and collision speeds.

Such considerations lead naturally to the formulation of an objective function, or *Figure of Merit*, which evaluates alternative vehicle crush characteristics. This Figure of Merit serves as the cost function, or payoff, for the optimization of future motor vehicle crush characteristics.

1.1 OBJECTIVES

The overall objective of the present study is the development, for the Department of Transportation's Transportation Systems Center (TSC) and National Highway Traffic Safety Administration (NHTSA), of first order techniques and computer programs for the definition of optimum crush characteristics for future highway vehicles. This includes

(1) Definition of an analytic form of an idealized Figure of Merit which provides a first order representation of the total cost to society of all traffic accidents and the costs of structural design modifications for improved safety.

(2) A computational algorithm for determining optimum front, side and rear force-crush characteristics of future families of vehicles having different weight classes, for minimizing the above Figure of Merit.

(3) A computer program which implements this algorithm and calculates optimum force-crush characteristics of a possible future family of vehicles.

1.2 TECHNICAL RESULTS

A Figure of Merit which evaluates the total societal costs of two-vehicle collisions and the cost of engineering modifications to vehicle structures has been formulated. The cost of collisions includes costs of occupant injury/mortality, costs of occupant compartment penetration, and costs of collision damage repairs, as component costs. The Figure of Merit depends parametrically on parameters of the various component cost models and on statistics describing the vehicle population and colliding vehicle mix (vehicle weight/size classes, collision modes and collision speeds). It is a function of the vehicles' crush characteristics. The Figure of Merit provides a systematic, meaningful framework and methodology for the evaluation and optimization of vehicle crush characteristics.

As indicated above, the Figure of Merit depends on the several component cost models. Such first-order cost models have been developed. The Figure of Merit also depends on two-vehicle collision dynamic models and restraint system models. Simplified models have been employed in this area. The various models and simplifying assumptions and approximations are given in detail in the body of this report.

The methodology described above has been combined with a conjugate gradient optimization algorithm and implemented into the computer program OACC which is described in Ref. 1. In view of the simplified model chosen for vehicle crush characteristics, the design (or optimization) variables consist of spring constants and yield strengths of each weight/size class vehicle's three aspects (front, side, rear), and added crush distance for each weight/size class vehicle.

1.3 TECHNICAL APPROACH

As previously stated, the prime objective of this work is the development of *first order* techniques and computer programs for the definition of optimum vehicle crush characteristics. In line with this objective, the work focuses on a meaningful and systematic formulation of the Figure of Merit and its optimization, and a first order implementation of the resulting methodology which features a variety of simplifying approximations and assumptions. For example, the simplified model for vehicle force-crush characteristics (linear up to a yield point) permits closed form solution to much of the problem, as does the piecewise linear (force-deflection) restraint system model. The approach has been to obtain closed form solutions

wherever possible (not everywhere), thus avoiding numerical integration and gaining insight into the structure of the problem.

1.4 ORGANIZATION OF THE REPORT

An overview of the formulation of the Figure of Merit and its optimization is presented in Section 2. That section also summarizes all underlying assumptions and approximations and the salient features of the theory. Mathematical details have been relegated to appendices. These appendices are largely self-contained, including their own reference and bibliography sections. Section 2 also contains a discussion of the numerical optimization of the Figure of Merit, together with a sample case. Conclusions and recommendations are presented in Section 3.

2. TECHNICAL DISCUSSION

This section contains a formulation and description of the techniques developed for the optimization of automobile crush characteristics, including underlying assumptions and approximations. The analysis begins with the formulation of an objective function or *Figure of Merit* which provides a measure of total societal costs of two-vehicle collisions. The optimal vehicle force-crush characteristics are implicitly defined through the minimization of the Figure of Merit. The Figure of Merit is a *statistic* depending on the statistical description of the vehicle population and colliding vehicle mix.

These techniques have been implemented in a computer program which is described elsewhere [Ref. 1]. The numerical optimization problem is discussed here, together with a sample case.

This discussion essentially serves as a technical overview. Mathematical details are relegated to appendices.

2.1 FIGURE OF MERIT

Consider a population of N_v vehicles distributed among weight/size classes i (e.g. subcompact, compact, intermediate, standard) with distribution (probability mass) p(i). In a given time period (e.g. one year) there are N_c two-vehicle collisions in this population. Collisions are distributed among weight/size classes i, collision modes m (e.g. front, side, rear), and collision speeds V_{ci}. Collision mode "front" for a given vehicle means that its front end is involved in that collision. Collision speeds V_{ci} are indexed by i_{vc}.

Two types of cost are considered; costs associated with the colliding vehicle (sub) population, and costs associated with the total vehicle population. The former costs are costs resulting from collisions, while the latter costs are costs of engineering modifications to vehicle structures. Such modifications might be postulated in an attempt to trade costs of improved or added structure for costs associated with injuries, fatalities and damage resulting from collisions.

Let $p(i,m,j,n,i_{vc}|col)$ be the probability, conditioned on collision (col), that a weight/size class i vehicle, in collision mode m, collides with a weight/size class j vehicle, which is in collision mode n, at collision speed V_{ci}. This probability is conditioned on collision; that is, it refers to the sub-population of vehicles involved in collisions. Then let the cost $C^{i}_{im/jn/V_{ci}}$ ($C^{j}_{im/jn/V_{ci}}$) be the cost associated with vehicle i (vehicle j) resulting from the collision just described. Also, let $C_{E/i}$ be the cost of a postulated modification to a weight/size class i vehicle. Then a *Figure of Merit*, or total societal cost, can be defined in a general way as

$$C_T = N_c \sum_{i=1}^{I} \sum_{j=1}^{I} \sum_{m=1}^{M} \sum_{n=1}^{M} \sum_{i_{vc}=1}^{I_{vc}} p(i,m,j,n,i_{vc}|col) \times$$

$$\times \left[C^{i}_{im/jn/V_{ci}} + C^{j}_{im/jn/V_{ci}} \right] + N_v \sum_{i=1}^{I} p(i) C_{E/i} \qquad (2\text{-}1)$$

where I is the number of vehicle weight/size classes, M is the number of collision modes, and I_{vc} is the number of collision speed intervals or brackets.

The above definition of the Figure of Merit provides a very general and systematic framework for the evaluation (and optimization) of vehicle structural crush characteristics. Nothing has been said so far about models of two-vehicle collision, nor about the components of the costs defined above or their dependence on the vehicle crush characteristics. The Figure of Merit [Eqn. (1)] can accommodate models of virtually any degree of complexity. It is observed that the Figure of Merit depends on the statistics of the present (or projected) vehicle population and colliding vehicle mix (vehicle weight/size classes, collision modes and collision speeds).

In the present work, collision costs $C^{\ell}_{im/jn/V_{ci}}$ associated with vehicle ℓ (ℓ=i,j) consist of costs of *Injury/Mortality*

$$C^{\ell}_{IM/im/jn/V_{ci}} \qquad (2\text{-}2)$$

occupant compartment *penetration penalty*

$$C^{\ell}_{P/im/jn/V_{ci}} \qquad (2\text{-}3)$$

and cost of collision *Damage Repairs*

$$C^{\ell}_{R/im/jn/V_{ci}} \qquad (2\text{-}4)$$

Models for these costs are developed in Appendices F, C and G, respectively. The model for costs of engineering modifications is given in Appendix H (see also Appendix I). The statistics involved in the Figure of Merit are presented in Appendix E. Finally, the Figure of Merit with the various models incorporated is summarized in Appendices C and M.

The present analysis contains the following features, assumptions and approximations:

Vehicle Collision Model - A single mass, colinear, two-vehicle collision model is utilized for the vehicle crush dynamics (Appendix A).

Vehicle Crush Characteristics - Vehicle force-crush characteristics are assumed linear up to a yield point, and are therefore characterized by a spring constant k_{im} and yield force f_{im} (Appendices B and C). ["im" refers to weight/size class i vehicle's aspect m.] While these linear/yield force-crush characteristics are utilized in computing vehicle accelerations, they are approximated alternatively by parabolic or inverse tangent curves (Appendix B) for the purpose of computing vehicle crush distance.

Restraint System Model - A piecewise linear force-deflection characteristic models restraint systems (Appendix K). The model provides for a dead zone (slack distance), linear/yield restraint characteristics, and barrier impact. Solutions of restrained occupant motion for linear/yield vehicle force-crush characteristics are given in Appendix L.

Injury/Mortality Costs - Costs of injury/mortality are based on a generalized Calspan injury severity index (SI) and a translation of short-term injury severity into long-term societal costs (Appendix F). Injury/mortality costs are given in

Appendix C for an occupant "locked" to the vehicle, and in Appendix M for a restrained occupant.

Penetration Penalty - Occupant compartment penetration cost penalty (Appendix C) is applied in (optionally defined) low speed collisions as a means of providing a "soft" constraint on vehicle force-crush characteristics.

Repair Costs - Two models are available for collision damage repair costs (Appendix G). One measures repair costs as a function of crush distance; the other as a function of vehicle speed decrement. Repair costs are in both cases limited by the depreciated value of the vehicle.

Costs of Engineering Modifications - Costs of engineering modifications are measured in terms of added crush distance, added stiffness and added strength (Appendix H). The data in Appendix I is relevant to the establishment of an engineering costs model.

Optimization Variables - "Design" variables available for the optimization of the Figure of Merit consist of spring constants k_{im} and yield strengths f_{im}, i=1, I, m=1, M; and added crush distances (in excess of current designs). For the purpose of crush distance design (and engineering cost computation) the vehicles' three aspects (front, side, rear) are scaled in fixed ratios so that there is a single design variable δ_i^* for each weight/size class i vehicle (Appendix I).

Statistics - In specifying the vehicle population and collision mix statistics appearing in the Figure of Merit, a variety of approximations are made to utilize the available accident statistics. This is treated in detail in Appendix E.

2.2 OPTIMIZATION OF THE FIGURE OF MERIT

A review of the preceding section and related appendices shows that the Figure of Merit is a function of the vehicle crush characteristics f_{in}, k_{in} and design crush distances δ_i^* (i=1,...,I; n=1,...,M). The optimum crush characteristics are defined as those which minimize the Figure of Merit. Therefore the relevant optimization problem is

$$\min_{f_{in},k_{in},\delta_i^*} C_T(f_{in},k_{in},\delta_i^*) \tag{2-5}$$

The technique chosen for this (numerical) minimization is a modified Davidon conjugate gradient algorithm described in Appendix J. The gradient of the Figure of Merit required by this algorithm is given in Appendices D and N.

2.3 NUMERICAL OPTIMIZATION - SAMPLE CASE

A sample case of the automobile force-crush characteristics optimization program OACC is presented. This case is in a population of three weight/size classes (sub-compact, compact, intermediate) and two collision modes (front, side). As such, it is merely an example, not representative of the real world. The weight/size class and collision mode distributions are shown in Tables 1 and 2. Table 3 gives the distribution of occupants by vehicle weight/size class, and Table 4 shows the collision speed distributions. The assumed restraint system characteristics are given in Table 5 (see Figure 2 for reference). Other parameters associated with this sample case are described in Table 6. The objective is to optimize the vehicle force-crush characteristics f_{im}, k_{im}, δ_i^* (i=1,3; m=1,2) (see Figure 1 for reference).

Iteration was initiated with the vehicle force-crush characteristics shown by the solid lines in Figure 3, and with $\delta_1^* = 4.0$ ft, $\delta_2^* = 5.0$ ft, and $\delta_3^* = 6.0$ ft, which all exceed the currently available crush distances. The individual plots in Figure 3 are each labeled with the number pair (i,m). (i,m) = (2,1) refers to the compact's (2) front-end (1). Notice that the initial force-crush characteristics are generally softer for the larger vehicles. The costs associated with these initial force-crush characteristics are shown in Table 7 (Iteration #0). Substantial engineering costs are called for to pay for the added crush distances.

TABLE 7

Figure of Merit by Iteration

Iter #	CIM	CR	CP	CE	CT
0	3.15×10^8	0.130×10^8	0	1.10×10^8	4.38×10^8
1	3.15×10^8	0.130×10^8	0	0	3.28×10^8
29	1.24×10^8	0.174×10^8	0.0018×10^8	0.34×10^{-4}	1.41×10^8

CIM ~ Costs of Injury Mortality ($); CR ~ Repair Costs ($)

CP ~ Penetration Penalty ($); CE ~ Costs of Engineering Modifications ($)

CT ~ Total Costs - Figure of Merit ($)

TABLE 1

Weight/Size Class Distributions

i	1 Sub Compact	2 Compact	3 Intermediate
Weight* Range	$W \leq 2700$	$2700 < W \leq 3400$	$3400 < W \leq 4100$
Representative Weight* W_i	2300	3100	3800
p(i)	0.280	0.360	0.360
p(i|col)	0.280	0.360	0.360

*Weight in lbs.

TABLE 2

Collision Modes Distribution*

	Front	Side
Front	.300	.310
Side	.310	.080

*p(m,n|col) = p(n,m|col)

TABLE 3

Distribution of Occupants

i	1	2	3
O(i)	1.58	1.60	1.64

TABLE 4

Collision Speed Distributions*

i_{vc}	$p(i_{vc}\|1,1,col)$	$p(i_{vc}\|1,2,col)$	$p(i_{vc}\|1,3,col)$	$p(i_{vc}\|2,2,col)$	$p(i_{vc}\|2,3,col)$	$p(i_{vc}\|3,3,col)$
1	.075	.552	.389	.892	1.000	1.000
2	.234	.357	.253	.108	.000	.000
3	.321	.072	.204	.000	.000	.000
4	.233	.019	.154	.000	.000	.000
5	.099	.000	.000	.000	.000	.000
6	.038	.000	.000	.000	.000	.000

*$p(i_{vc}|m,n,col) = p(i_{vc}|n,m,col)$

ΔV_c = 20 mph, so that i_{vc} = 1 represents the speed range 0-20 mph with average speed V_{c1} = 10 mph, and so on.

$p(2|1,2,col)$ = probability that a collision between the front-end of one vehicle and the side of another vehicle (intersection collision) occurs at closing speeds in the range of 20-40 mph.

TABLE 5

Restraint System Parameters

Parameter \ Collison Mode	Front	Driver Side	Pass. Side
d_S	0.3	0.0	0.4
k_R	12,000	12,000	12,000
f_M	4,000	0	4,000
d_T	1.5	Varies with weight/ size class	
k_D	16,000	16,000	16,000

Wt./Size Class	Driver Side	Pass. Side
1	0.2	3.0
2	0.3	3.25
3	0.4	3.5

d_S ~ slack distance (ft)

k_R ~ restraint spring constant (lb/ft)

f_M ~ restraint yield force (lb)

d_T ~ total "headroom" (ft)

k_D ~ "barrier" spring constant (lb/ft)

TABLE 6

Other Sample Case Parameters

- $N_v = 1x10^8$ (total number of vehicles in the population)
- $N_c = 3x10^7$ (total number of colliding vehicles)
- Inverse tangent vehicle force-crush approximation employed for crush computations
- Injury/mortality cost model parameters are: $\alpha=2.5$; $c_{IM}=\$250K$; $r_{IM}=0.4x10^{-13}$
- Crush distance repair cost option employed with: $d=2.0$; $a=3.0$; $r_d=0.2$
- Penetration cost penalty employed with: $\bar{V}_{cm}=60mph$(all m); $c_P=\$1000K$; $k_1=0.6$, $k_2=0.7$
- Currently available crush distance data as developed in the report
- Crush distance design in the current crush distance ratio ($e_2=e_3=1.0$)
- Cost of engineering modifications contains only quadratic term in added crush distance
- $w_P=140$ lbs (average occupant weight)
- $p_{ds}=0.6$ (probability of driver's side involvement in a side involvement)
- All arbitrary weighting constants = 1.0

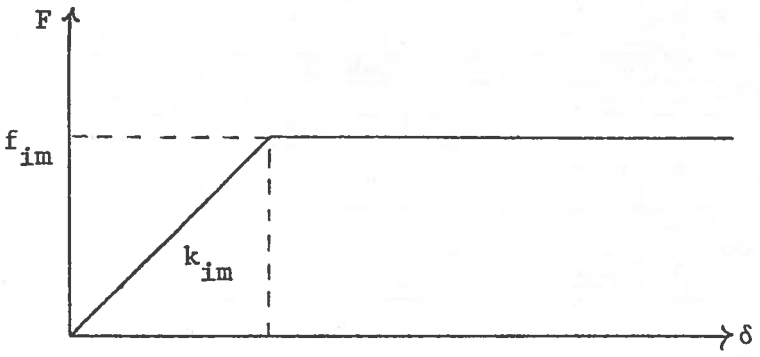

FIGURE 1

Vehicle Force-Crush Characteristics

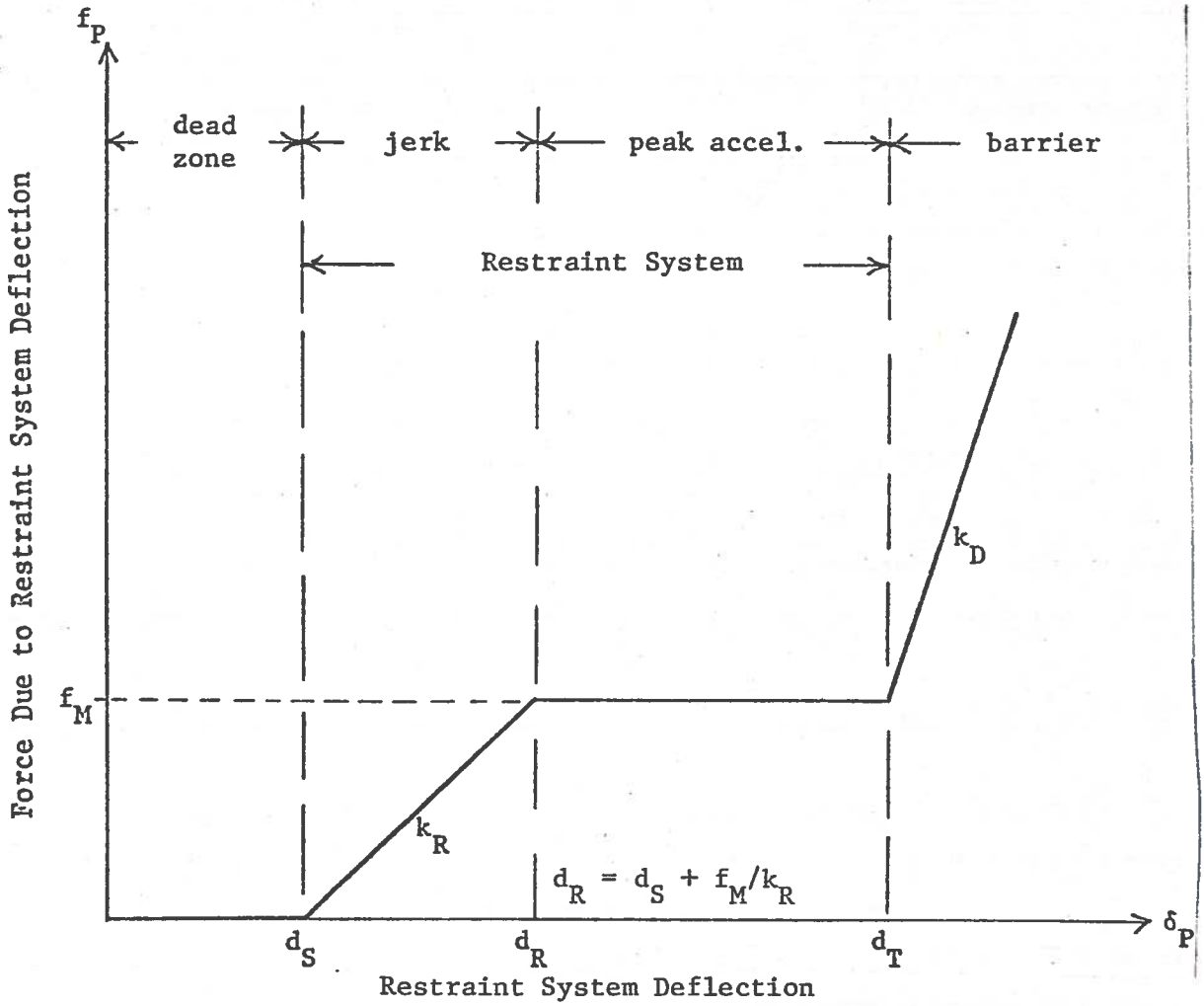

FIGURE 2

Restraint System Model

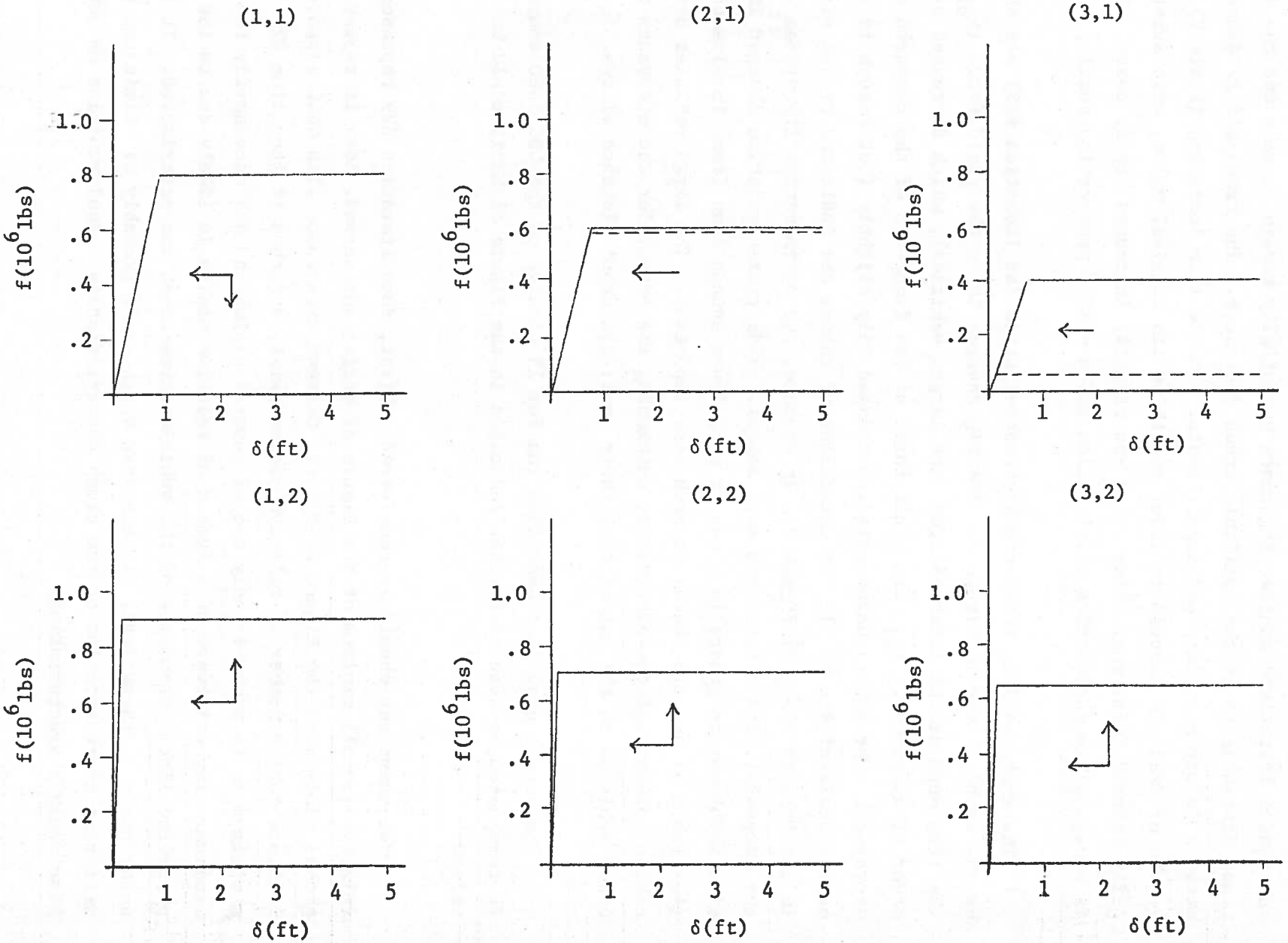

FIGURE 3 Nominal/Final Force-Crush Characteristics

The first iteration immediately drives the design crush distances (δ_i^*) below the available crush distances to reduce engineering costs to zero (Table 7). In subsequent iterations engineering costs essentially remain at zero and the design crush distances go to the available crush distances. The trade-off is essentially between Injury/Mortality and Repair costs. At the 29th iteration (Table 7), the Figure of Merit is reduced to about one-third its original value, with substantially reduced Injury/Mortality costs and slightly increased Repair costs. There is a negligible engineering modification and a slight penetration penalty.

The final vehicle force-crush characteristics (at Iteration #29) are shown by the dashed lines in Figure 3. The big change is in the yield force (f_{31}) of the front-end of the intermediates (the larges vehicles), which decreased by an order of magnitude. f_{21}, the yield force of the front-end of the compacts also decreased. The other characteristics changed only slightly (not enough to show on the scale of Figure 3); the directions of change are indicated by the arrows in the various plots of Figure 3. In essence, the optimization iterations made the largest vehicles' front-end much softer. Side characteristics changed little; side involvements generally occur at much lower speeds than front involvements (see Table 4) and are therefore much less important. The large vehicles are taking almost all the punishment, cushioning the impact for the occupants of other vehicles to the extent that their available crush distance allows.

The sample case just described ran for 15 minutes on the CDC 6600 computer. It terminated because no further reduction in the Figure of Merit could be obtained.

Two questions should be considered. First, does Iteration #29 represent a relative (local) minimum of the Figure of Merit; and second, does it represent a global minimum of the Figure of Merit? Current experience with OACC appears to indicate that a number of relative minima exist, and thus if Iteration #29 found a minimum, it is probably only one of several minima and not necessarily the global minimum. The existence of a number of relative minima is likely due to the piecewise linear structure of the vehicle force-crush characteristics. It is an unfortunate (mathematical) circumstance which could probably be eliminated by a different representation of the crush characteristics. Real vehicles do not have flat crush characteristics.

As to the first question, it is difficult to determine if Iteration #29 is precisely at a relative minimum, or in fact how far it might be from the minimum. The case terminated because no further reduction in the Figure of Merit could be obtained. The gradient of the Figure of Merit was substantially reduced in most components; however, quadratic convergence was not observed before the case terminated.

Numerical experiments have shown that (a) the problem is highly nonlinear, and (b) high computational accuracy is difficult to achieve without excessive computer running time. The latter difficulty is largely due to the numerical integration of the crush dynamics (computation of the final crush), particularly with the inverse tangent approximation to the force-crush characteristics. The high rates of change at the knee of the force-crush curve contribute to this problem. High computational accuracy is necessary for the precise location of a minimum which is usually exhibited by quadratic convergence of the Davidon conjugate gradient optimization algorithm. The accuracy problem would also likely be reduced by a different representation of the vehicle force-crush characteristics.

Much more experience with the OACC program is required to assess the questions discussed above, and whether or not this first-cut model of (linear/yield) vehicle force-crush characteristics can be useful in actual design studies. Certainly it can only be useful for high speed design. Such experiments and studies with OACC can indicate appropriate directions of further effort.

2.4 REFERENCES

1. C. Hipkins, C. L. Hammond, T. S. Englar, Jr. and A. H. Jazwinski, "USERS MANUAL FOR OACC - Optimization of Automobile Crush Characteristics," Automated Sciences Group, Inc. Report No. ASGI-TR-75-11, Contract No. DOT-TSC-852, October 1975.

3. CONCLUSIONS AND RECOMMENDATIONS

3.1 CONCLUSIONS

A systematic methodology has been developed for the evaluation and optimization of vehicle force-crush characteristics in a societal goals/costs framework. The Figure of Merit which evaluates societal costs of two-vehicle collisions and costs of structural vehicle modification is a statistical quantity depending on the vehicle population and collision mix statistics.

A first-order implementation of this methodology has been achieved with simplified cost models and collision dynamics. The computer program OACC optimizes vehicle force-crush characteristics within the framework of these first-order models. More experience with OACC is required to evaluate the problems of relative minima, nonlinearities and numerical accuracies, and to assess the present first-order representation of vehicle force-crush characteristics.

The present work must be viewed as a first step in the development of tools for the optimization of vehicle crush characteristics. Logical next steps and extensions of this work are described in the next section.

3.2 RECOMMENDATIONS

(1) *Validation and Calibration* - The simplified models and OACC software should be validated and the regions of model validity should be determined. This might be accomplished in several ways. Optimized vehicle force-crush characteristics can be input to more advanced collision simulation models to compare resulting injury severity. In addition, OACC generated costs of injury/mortality, vehicle damage repairs, etc. can be compared with independently collected (available) data on these costs. This would serve not only as a validation exercise, but can also be useful in calibrating the OACC cost models. The problems of existence of relative minima, nonlinearities and numerical accuracies should be investigated. The present first-order representation of vehicle force-crush characteristics should be evaluated. Parametric studies with OACC are required to gain insight and understanding of various cost tradeoffs, their reasonableness and relevance to the real world.

(2) *General Vehicle Force-Crush Characteristics* - The limitation of the present model to linear/yield vehicle force-crush characteristics should be removed. It appears that linear combinations (sums) of tabulated functions for the vehicle crush characteristics can provide the required flexibility of characterizing a variety of structural features, and at the same time can probably provide a solution to the problems of relative minima and numerical accuracy, generally conditioning the Figure of Merit optimization problem. This modeling

approach to vehicle force-crush characteristics would also facilitate establishment and improvement of the several cost models. With this approach, all analytical solutions would be abandoned in favor of numerical techniques.

(3) *Improved Cost Models* - Much work remains to be done in generalizing and improving the cost models. Injury/mortality/occupant compartment penetration cost models should be made more compatible with various restraint systems. The injury severity index is often an irrelevant measure, particularly for restrained occupants. Furthermore, a gap exists in the transition from the AIS short-term (48 hr) disposition of injury severity to the long-term (disability) point of view where significant costs exist. Repair and engineering modification cost models need substantial improvement. This should be pursued in conjunction with item (2) above. More detailed force-crush characteristics may permit low speed as well as high speed vehicle design. An improvement in the engineering costs model may have a substantial impact on the results.

(4) *Statistical Data* - Available statistics do not adequately describe the colliding vehicle mix (weight/size classes, collision modes, collision speeds). There may be deficiencies in the fundamental data collected; however, it is rather obvious that all relevant statistics have not been extracted from the data. An effort is required to analyze accident data and extract sufficient statistics from that data which will describe the colliding vehicle mix. Such an effort would also be useful in identifying data deficiencies and impacting data collection procedures. In addition, forecasting models should be developed for predicting future vehicle populations and collision mixes, based on various assumptions and policy decisions.

(5) *Collision Geometrics, Models and Modes* - Models might be developed and incorporated in the software to treat the important oblique collisions in addition to the colinear front, side and rear collision models presently considered. Oblique impacts demonstrate a weakness of structures in this mode, and thus the present treatment contains a significant deficiency in an area where important payoffs may be realized. More accurate, multi-mass collision models would permit better treatment of collision costs as well. Occupant mass effects (particularly significant in subcompacts) could be taken into account. This is of course a significant model sophistication and a substantial effort. In addition, collisions with trucks, obstacles and rollovers might be treated.

(6) *Optimization of Restraint Systems* - Currently, restraint system characteristics are specified and are not subject to optimization. It is possible to extend program capability to optimize the restraint force-deflection characteristics as well as those of the vehicles.

(7) *Numerical Optimization Techniques* - With further development, particularly along the lines of item (5), and possibly also item (2), the computing time of the program will grow. Different optimization algorithms might be researched for applicability and efficiency in this application area.

REPORT OF INVENTIONS APPENDIX

After a diligent review of the work performed under this contract, no new innovation, discovery, improvement, or invention was made.

APPENDIX A

SINGLE-MASS COLINEAR COLLISION MODEL

The following is a presentation and derivation of a single-mass colinear vehicle collision model. This model includes these features and simplifying assumptions:

- The automotive vehicle population is represented by a small number of distinct vehicle classes, based upon vehicle gross weight;
- Vehicles within each class have identical crush characteristics;
- All collisions considered are between pairs of vehicles, not necessarily from the same vehicle weight class;
- All collisions are colinear; the relative velocity vector of the colliding vehicle pair is aligned and passes through the centers of mass of the colliding vehicles;
- Collision modes represented include frontal, rear, and side impacts;
- Each vehicle is treated as a single inelastic mass;
- The force-deformation-deformation rate relations for each collision mode and for each vehicle weight class are considered to be specified functions.

The geometry of a typical collision mode (frontal-frontal) is represented in Figure A-1. Other collision modes are described by the same form of equations, and may be distinguished by means of subscripts. As shown in the figure, M_A and M_B are the respective vehicle masses, x_A and x_B are the vehicle displacements (measured positive to the right), δ_A and δ_B are the crush deformations experienced during collision by each vehicle, and Δ_A and Δ_B are the locations of the vehicle leading edges relative to the mass centers, prior to collision deformation.

During the collision, the vehicles decelerate according to Newton's laws of motion

$$M_A\ddot{x}_A = -F, \qquad M_B\ddot{x}_B = F \tag{A-1}$$

$$F_{BA} = -F, \qquad F_{AB} = F \tag{A-2}$$

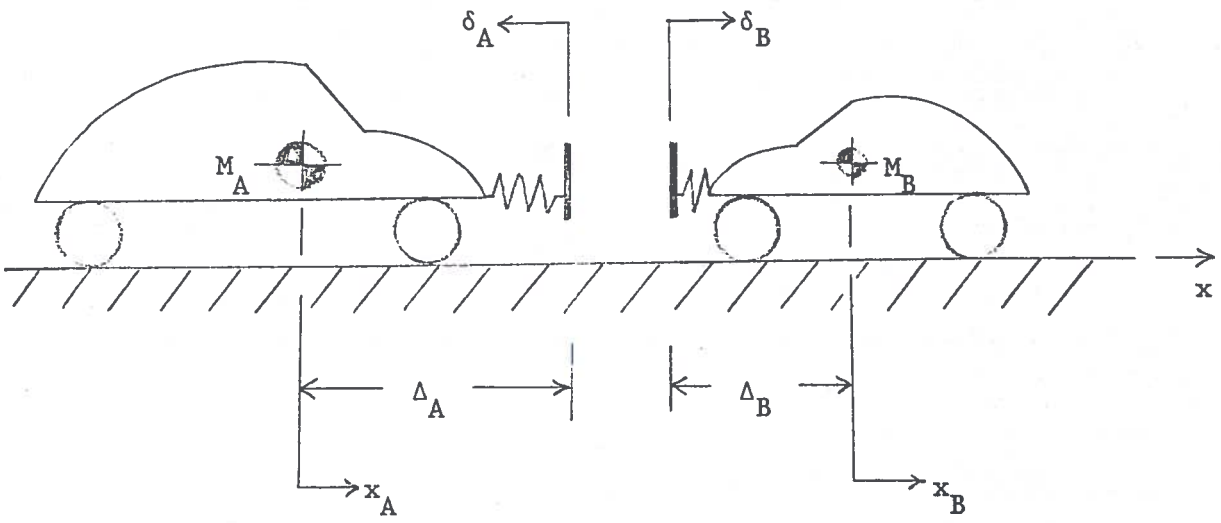

Figure A-1

Schematic of Frontal-Frontal Collision

Here the dots denote time derivatives, $\ddot{x}_A$ and $\ddot{x}_B$ are the vehicle accelerations, F is the mutual vehicle loading, F_{BA} is the force exerted by vehicle B on vehicle A, and F_{AB} is the reaction force acting on vehicle B. The forces are measured positive to the right. The crush distances, δ_A and δ_B, are measured rearward from the point of contact. The vehicle location coordinates, x_A and x_B, mark the positions of the respective mass centers. Thus, during collision, with the vehicles in contact, the following kinematic relationships apply

$$x_B = x_A + \Delta_A + \Delta_B - \delta_A - \delta_B \tag{A-3}$$

$$\dot{x}_B = \dot{x}_A - \dot{\delta}_A - \dot{\delta}_B \tag{A-4}$$

The initial conditions at the instant (t=0) the vehicles touch are

$$x_A(0) = 0 \qquad x_B(0) = \Delta_A + \Delta_B \tag{A-5}$$

$$\dot{x}_A(0) = V_A \qquad \dot{x}_B(0) = V_B \tag{A-6}$$

$$\delta_A(0) = 0 \qquad \delta_B(0) = 0 \tag{A-7}$$

The final speed, V_f, at the completion of the collision ($t=t_f$), when relative motion between the vehicles ceases, is found by equating the linear momentum, which is conserved, before and after collision. For a completely inelastic collision, the vehicles will move together as a single mass (M_A+M_B) with velocity V_f, after the relative motion ceases. Therefore,

$$(M_A + M_B)V_f = M_A V_A + M_B V_B \tag{A-8}$$

and

$$V_f = (M_A V_A + M_B V_B)/(M_A + M_B) \tag{A-9}$$

For convenience of notation, introduce the *reduced mass*

$$\mu = M_A M_B / (M_A + M_B) \tag{A-10}$$

and the *collision speed*

$$V_c = V_A - V_B \tag{A-11}$$

It remains to specify the dependence of the forces, F_{BA} and F_{AB}, acting on each vehicle, upon the vehicle crush distances, δ_A and δ_B, and upon the vehicle crush rates, $\dot{\delta}_A$ and $\dot{\delta}_B$. In general, the present model considers these relations to be of the form

$$F_{BA} = -f_A(\delta_A, \dot{\delta}_A) \tag{A-12}$$

$$F_{AB} = f_B(\delta_B, \dot{\delta}_B) \tag{A-13}$$

If the collision is to be inelastic, the force acting between the vehicles has a finite value only for compression,

$$F = \begin{cases} f(\delta, \dot{\delta}), & \dot{\delta} > 0 \\ 0, & \dot{\delta} \leq 0 \end{cases} \tag{A-14}$$

From Eqs. (A-2), (A-12) and (A-13), it is evident that

$$F = f_A(\delta_A, \dot{\delta}_A) \tag{A-15}$$

$$= f_B(\delta_B, \dot{\delta}_B) \tag{A-16}$$

It is sometimes useful to consider the time derivative

$$dF/dt = (\partial f_A/\partial \delta_A)\dot{\delta}_A + (\partial f_A/\partial \dot{\delta}_A)\ddot{\delta}_A \tag{A-17}$$

$$= (\partial f_B/\partial \delta_B)\dot{\delta}_B + (\partial f_B/\partial \dot{\delta}_B)\ddot{\delta}_B \tag{A-18}$$

Then Eqn. (A-16) may be replaced by the differential equation

$$(\partial f_A/\partial \dot{\delta}_A)\ddot{\delta}_A - (\partial f_B/\partial \dot{\delta}_B)\ddot{\delta}_B = (\partial f_B/\partial \delta_B)\dot{\delta}_B - (\partial f_A/\partial \delta_A)\dot{\delta}_A \tag{A-19}$$

It is convenient to introduce the total crush distance, c, and relative speed, $\dot{c}$, of the vehicles during the collision as new dependent variables. Then, with Eqs. (A-3) and (A-4), one finds

$$c = \delta_A + \delta_B = x_A - x_B + \Delta_A + \Delta_B \tag{A-20}$$

$$\dot{c} = \dot{\delta}_A + \dot{\delta}_B = \dot{x}_A - \dot{x}_B \tag{A-21}$$

and from Eqs. (A-1) and (A-16)

$$\ddot{c} = -f_A/\mu \tag{A-22}$$

The initial values of c and $\dot{c}$ at time t=0 are

$$c(0) = 0, \quad \dot{c}(0) = V_c \tag{A-23}$$

The completion of the inelastic collision process is noted when the relative speed, $\dot{c}$, between the vehicles vanishes

$$\dot{c}(t_f) = 0 \tag{A-24}$$

In the dynamic equations, the relations (A-20) and (A-21) are used as a means of substituting for δ_B and $\dot{\delta}_B$ in favor of c and $\dot{c}$. In these new variables, Eqn. (A-19) becomes

$$(\partial f_A/\partial \dot{\delta}_A + \partial f_B/\partial \dot{\delta}_B)\ddot{\delta}_A - (\partial f_B/\partial \dot{\delta}_B)\ddot{c}$$

$$= -(\partial f_A/\partial \delta_A + \partial f_B/\partial \delta_B)\dot{\delta}_A + (\partial f_B/\partial \delta_B)\dot{c} \tag{A-25}$$

The values of δ_B and $\dot{\delta}_B$ are found from

$$\delta_B = c - \delta_A, \quad \dot{\delta}_B = \dot{c} - \dot{\delta}_A \tag{A-26}$$

Similarly,

$$x_B = x_A - c + \Delta_A + \Delta_B, \quad \dot{x}_B = \dot{x}_A - \dot{c} \tag{A-27}$$

To summarize, the collision equations to be solved are

$$\ddot{c} = -f_A(\delta_A, \dot{\delta}_A)/\mu \tag{A-28}$$

$$f_A(\delta_A, \dot{\delta}_A) - f_B(c - \delta_A, \dot{c} - \dot{\delta}_A) = 0 \text{ [or Eqn. (A-25)]} \tag{A-29}$$

These equations, for c and δ_A, are subject to the initial conditions

$$\delta_A(0) = 0, \quad c(0) = 0, \quad \dot{c}(0) = V_c$$

$$f_A(0, \dot{\delta}_A(0)) - f_B(0, V_c - \dot{\delta}_A(0)) = 0 \tag{A-30}$$

The final time (collision time interval), t_f, is obtained from

$$\dot{c}(t_f) = 0 \tag{A-31}$$

Once these equations are solved, the remaining variables are obtained by means of the following relationships:

$$\ddot{x}_A(t) = -f_A[\delta_A(t), \dot{\delta}_A(t)]/M_A \tag{A-32}$$

$$\ddot{x}_B(t) = f_A[\delta_A(t), \dot{\delta}_A(t)]/M_B \tag{A-33}$$

$$\dot{x}_A(t) = V_A - M_A^{-1}\int_0^t f_A[\delta_A(\tau), \dot{\delta}_A(\tau)]d\tau \tag{A-34}$$

$$\dot{x}_B(t) = \dot{x}_A(t) - \dot{c}(t) \tag{A-35}$$

$$x_A(t) = \int_0^t \dot{x}_A(\tau)d\tau \tag{A-36}$$

$$x_B(t) = x_A(t) - c(t) + \Delta_A + \Delta_B \tag{A-37}$$

$$\dot{\delta}_B(t) = \dot{c}(t) - \dot{\delta}_A(t) \tag{A-38}$$

$$\delta_B(t) = c(t) - \delta_A(t) \tag{A-39}$$

APPENDIX B

SOME SPECIAL COLLISION SOLUTIONS

The collision dynamics developed in Appendix A may be solved in closed form for special forms of the force-deformation-deformation rate characteristics f_A and f_B; particularly when f_A and f_B are independent of the deformation (crush) rates. Several of these solutions are given in this appendix.

LINEAR FORCE-CRUSH CHARACTERISTICS

In this case

$$f_A(\delta_A) = k_A\delta_A, \quad f_B(\delta_B) = k_B\delta_B = k_B(c - \delta_A) \tag{B-1}$$

and Eqn. (A-28) becomes

$$\ddot{c} = -(k_A/\mu)\delta_A \tag{B-2}$$

From Eqs. (B-1) and (A-29)

$$\delta_A = [k_B/(k_A + k_B)]c = (\kappa/k_A)c \tag{B-3}$$

where κ, the *reduced stiffness*, is defined as

$$\kappa = k_A k_B/(k_A + k_B) \tag{B-4}$$

Then Eqn. (B-2) becomes

$$\ddot{c} = -(\kappa/\mu)c \tag{B-5}$$

which, with initial conditions (A-30), is easily seen to have the solution

$$c = \sqrt{\mu/\kappa}\, V_c \sin \sqrt{\kappa/\mu}\, t \tag{B-6}$$

Differentiating Eqn. (B-6)

$$\dot{c} = V_c \cos \sqrt{\kappa/\mu}\, t \tag{B-7}$$

and imposing the condition (A-31)

$$0 = V_c \cos \sqrt{\kappa/\mu}\, t_f \tag{B-8}$$

gives the collision time interval

$$t_f = \frac{\pi}{2} \sqrt{\mu/\kappa} \tag{B-9}$$

With the aid of Eqs. (B-3) and (A-26) the crush time histories are readily obtained as

$$\begin{aligned} \delta_A &= (1/k_A)\sqrt{\kappa\mu}\, V_c \sin \sqrt{\kappa/\mu}\, t \\ \delta_B &= (1/k_B)\sqrt{\kappa\mu}\, V_c \sin \sqrt{\kappa/\mu}\, t \end{aligned} \tag{B-10}$$

and the final crush deformations (at $t=t_f$)

$$\delta_A^f = (1/k_A)\sqrt{\kappa\mu}\, V_c, \quad \delta_B^f = (1/k_B)\sqrt{\kappa\mu}\, V_c \tag{B-11}$$

In this case the crush distances have the constant ratio

$$\delta_B/\delta_A = k_A/k_B \tag{B-12}$$

Also, the vehicle (center of mass) accelerations during the collision [Eqs. (A-32) and (A-33)] are easily found to be

$$\begin{aligned} \ddot{x}_A &= -(1/M_A)\sqrt{\kappa\mu}\, V_c \sin \sqrt{\kappa/\mu}\, t \\ \ddot{x}_B &= (1/M_B)\sqrt{\kappa\mu}\, V_c \sin \sqrt{\kappa/\mu}\, t \end{aligned} \tag{B-13}$$

and the magnitudes of the vehicle accelerations during collision are in the constant ratio

$$|\ddot{x}_B/\ddot{x}_A| = M_A/M_B \tag{B-14}$$

One can define the *collision intensities*, C_A and C_B, as

$$C_A = \int_0^{t_f} \ddot{x}_A^2 dt, \quad C_B = \int_0^{t_f} \ddot{x}_B^2 dt \tag{B-15}$$

and in this case obtain

$$C_A = (\pi/4)\mu\sqrt{k\mu}\, M_A^{-2} V_c^2, \quad C_B = (\pi/4)\mu\sqrt{k\mu}\, M_B^{-2} V_c^2 \tag{B-16}$$

It is seen that the collision intensities have the ratio

$$C_B/C_A = (M_A/M_B)^2 \tag{B-17}$$

When vehicles with identical crush characteristics collide (A=B), the expressions for collision intensity C and final crush δ^f are

$$C = (\pi/16)\sqrt{k/M}\, V_c^2, \quad \delta^f = (1/2)\sqrt{M/k}\, V_c \tag{B-18}$$

It is seen that there is a direct trade off between collision intensity as a measure of deceleration rate in the passenger compartment and maximum penetration δ^f into the vehicle. In fact,

$$C = (\pi/32)V_c^3/\delta^f \tag{B-19}$$

CONSTANT (HYDRAULIC) FORCE-CRUSH CHARACTERISTICS

In this case

$$f_A(\delta_A) = f_B(\delta_B) = f \text{ (constant)} \tag{B-20}$$

and Eqn. (A-28) becomes

$$\ddot{c} = -f/\mu \tag{B-21}$$

with solution

$$c = V_c t - \tfrac{1}{2}(f/\mu)t^2 \tag{B-22}$$

and [see Eqn. (A-31)]

$$t_f = \mu V_c / f \tag{B-23}$$

so that

$$c(t_f) = \tfrac{1}{2}\mu V_c^2 / f \tag{B-24}$$

In this case Eqn. (A-29) gives no information about the individual crush distances δ_A^f and δ_B^f, and it is not clear how to compute these crush distances.

The vehicle (center of mass) accelerations during the collision [Eqs. (A-32) and (A-33)] are

$$\ddot{x}_A = -f/M_A \tag{B-25}$$

$$\ddot{x}_B = f/M_B \tag{B-26}$$

and

$$|\ddot{x}_B/\ddot{x}_A| = M_A/M_B \tag{B-27}$$

The collision intensities [Eqn. (B-15)] are

$$C_A = \mu V_c f/M_A^2 \tag{B-28}$$

$$C_B = \mu V_c f/M_B^2 \tag{B-29}$$

and

$$C_B/C_A = (M_A/M_B)^2 \tag{B-30}$$

When vehicles with identical crush characteristics collide (A=B),

$$C = \tfrac{1}{2}V_c f/M, \quad \delta^f = (1/8)V_c^2 M/f \tag{B-31}$$

and

$$C = (1/16)V_c^2/\delta^f \tag{B-32}$$

LINEAR FORCE-CRUSH CHARACTERISTICS UP TO A YIELD POINT

In this case the force-crush characteristic is linear up to a yield point δ^y, whereafter the force level is constant, as shown for vehicle A below

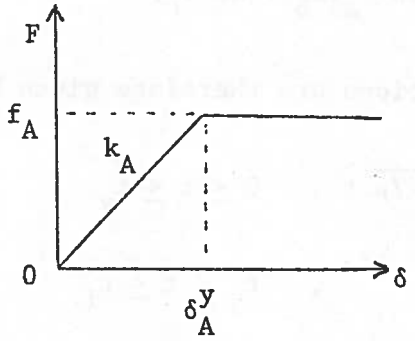

$$k_A = f_A/\delta_A^y$$

This characteristic may be defined by the yield force f_A and stiffness k_A.

As long as $\delta_A \leq \delta_A^y$ *and* $\delta_B \leq \delta_B^y$, the collision proceeds as in the case of linear force-crush characteristics [Eqs. (B-1)-(B-13)]. There are two distinct cases to consider: (a) motion stops while both $\delta_A \leq \delta_A^y$ and $\delta_B \leq \delta_B^y$, in which case the motion is already completely defined by Eqs. (B-1)-(B-13); and (b) motion stops only after $\delta_A > \delta_A^y$ or $\delta_B > \delta_B^y$, which means that the yield force f_A or f_B has been reached before motion stops. In view of Eqn. (B-11), case (a) is defined by the condition

$$V_c \leq f_A/\sqrt{\kappa\mu} \qquad \textit{and} \qquad V_c \leq f_B/\sqrt{\kappa\mu} \tag{B-33}$$

or, more compactly, by

$$V_c \leq \min(f_A,f_B)/\sqrt{\kappa\mu} \tag{B-34}$$

where "min" is the minimum operator. Case (b), then, is defined by

$$V_c > \min(f_A,f_B)/\sqrt{\kappa\mu} \tag{B-35}$$

Case (b) is now considered. Let t_y be the time when $F = \min(f_A,f_B)$. From Eqn. (B-10),

$$\min(f_A,f_B) = \sqrt{\kappa\mu}\, V_c \sin\sqrt{\kappa/\mu}\, t_y \tag{B-36}$$

so that

$$t_y = \sqrt{\mu/\kappa} \sin^{-1}[\min(f_A,f_B)/\sqrt{\kappa\mu}\, V_c] \tag{B-37}$$

The vehicle (center of mass) accelerations are therefore given by

$$\ddot{x}_A = \begin{cases} -M_A^{-1}\sqrt{\kappa\mu}\, V_c \sin\sqrt{\kappa/\mu}\, t\ , & 0 \leq t \leq t_y \\ -M_A^{-1} \min(f_A,f_B)\ , & t_y < t \leq t_f \end{cases}$$

$$\ddot{x}_B = \begin{cases} M_B^{-1}\sqrt{\kappa\mu}\, V_c \sin\sqrt{\kappa/\mu}\, t\ , & 0 \leq t \leq t_y \\ M_B^{-1} \min(f_A,f_B)\ , & t_y < t \leq t_f \end{cases} \tag{B-38}$$

where the collision time interval, t_f, is yet to be determined. To compute the crush deformations, two sub-cases are considered:

Case (b1): $f_A \neq f_B$; assume for simplicity that $f_B < f_A$

Case (b2): $f_A = f_B$

In case (b1), A no longer deforms for $t > t_y$ and, clearly,

$$\delta_A^f = f_B/k_A \tag{B-39}$$

$$\dot{c} = \dot{\delta}_B, \quad t_y < t \leq t_f \tag{B-40}$$

and from Eqn. (A-28)

$$\ddot{c} = \ddot{\delta}_B = -f_B/\mu \ , \quad t_y < t \leq t_f \tag{B-41}$$

so that

$$\dot{c} = \dot{c}(t_y) - (f_B/\mu)(t - t_y) \ , \quad t_y < t \leq t_f \tag{B-42}$$

From Eqs. (B-42), (B-7) and (A-24)

$$0 = V_c \cos\sqrt{\kappa/\mu}\ t_y - (f_B/\mu)(t_f - t_y) \tag{B-43}$$

so that

$$t_f = t_y + [\mu/\min(f_A,f_B)]V_c \cos\sqrt{\kappa/\mu}\ t_y \tag{B-44}$$

Now from Eqs. (B-40) and (B-42)

$$\dot{\delta}_B = \dot{c}(t_y) - (f_B/\mu)(t - t_y) \ , \quad t_y < t \leq t_f \tag{B-45}$$

$$\delta_B^f = f_B/k_B + \dot{c}(t_y)(t_f - t_y) - \tfrac{1}{2}(f_B/\mu)(t_f - t_y)^2 \tag{B-46}$$

and with Eqs. (B-7) and (B-37)

$$\delta_B^f = f_B/k_B + \tfrac{1}{2}[\kappa\mu V_c^2 - f_B^2]/\kappa f_B \tag{B-47}$$

In case (b2), δ_A^f and δ_B^f cannot be readily separated from the total crush.

PARABOLIC FORCE-CRUSH CHARACTERISTICS

This force-crush characteristic (for vehicle A) is of the form

$$f_A(\delta_A) = c_A \delta_A^{\frac{1}{2}} \tag{B-51}$$

and is shown below compared with the linear/yield characteristic

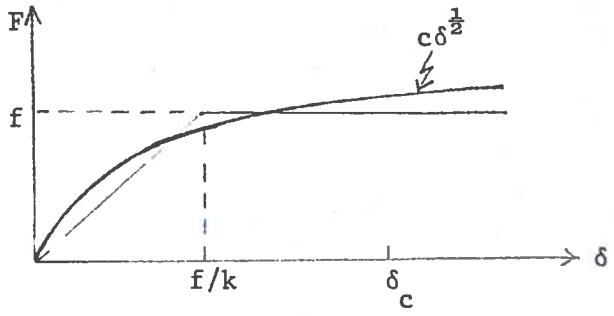

In this case Eqn. (A-29) gives

$$(c_A^2 + c_B^2)\delta_A = c_B^2 c \tag{B-52}$$

and Eqn. (A-28) becomes

$$\ddot{c} = -\frac{c_A c_B}{\mu[c_A^2 + c_B^2]^{\frac{1}{2}}} c^{\frac{1}{2}}, \quad c(0) = 0, \ \dot{c}(0) = V_c \tag{B-53}$$

While a complete solution to (B-53) has not been obtained, yet it is possible to determine $c(t_f)$ and therefore δ_A^f and δ_B^f. Letting

$$\lambda = c_A c_B/\mu[c_A^2 + c_B^2]^{\frac{1}{2}} \tag{B-54}$$

Eqn. (B-53) becomes

$$\ddot{c} = -\lambda c^{\frac{1}{2}} \tag{B-55}$$

Let $p = \dot{c}$; then

$$p \frac{dp}{dc} = \dot{c} \frac{d\dot{c}}{dc} = \dot{c} \frac{\ddot{c}}{\dot{c}} = \ddot{c} \tag{B-56}$$

so that Eqn. (B-55) becomes

$$p \frac{dp}{dc} = -\lambda c^{\frac{1}{2}} \tag{B-57}$$

or

$$pdp = -\lambda c^{\frac{1}{2}} dc \tag{B-58}$$

Integrating this gives

$$\tfrac{1}{2}(p^2 - V_c^2) = -\frac{2}{3}\lambda c^{3/2} \tag{B-59}$$

or

$$\dot{c}^2 = V_c^2 - \frac{4}{3}\lambda c^{3/2} \tag{B-60}$$

Then applying Eqn. (A-31) gives

$$c^{3/2}(t_f) = \frac{3V_c^2}{4\lambda} \tag{B-61}$$

and

$$c(t_f) = \left[\frac{3}{4} V_c^2 \frac{\mu(c_A^2 + c_B^2)^{\frac{1}{2}}}{c_A c_B}\right]^{2/3} \tag{B-62}$$

Finally, using Eqn. (B-52) and the fact that $c_A^2\delta_A = c_B^2\delta_B$ gives

$$\delta_A^f = \frac{c_B^2}{c_A^2 + c_B^2} \left[\frac{3}{4} V_c^2 \frac{\mu(c_A^2 + c_B^2)^{\frac{1}{2}}}{c_A c_B} \right]^{2/3} \tag{B-63}$$

$$\delta_B^f = \frac{c_A^2}{c_A^2 + c_B^2} \left[\frac{3}{4} V_c^2 \frac{\mu(c_A^2 + c_B^2)^{\frac{1}{2}}}{c_A c_B} \right]^{2/3} \tag{B-64}$$

As the figure below Eqn. (B-51) might suggest, the parabolic force-crush characteristics can quite well approximate the linear/yield characteristics, or vice versa. This can be formally accomplished by requiring equal areas under both characteristics for some characteristic length δ_c. For $\delta_c \gtrsim f/k$,

$$\int_0^{\delta_c} c\delta^{\frac{1}{2}}\, d\delta = f\delta_c - \tfrac{1}{2}f^2/k \tag{B-65}$$

from which is obtained the relation

$$c = \frac{3}{2}\, \delta_c^{-3/2} [f\delta_c - \tfrac{1}{2}f^2/k] \tag{B-66}$$

For $\delta_c < f/k$,

$$\int_0^{\delta_c} c\delta^{\frac{1}{2}}\, d\delta = \tfrac{1}{2}\delta_c^2 k \tag{B-67}$$

so that

$$c = \frac{3}{4}\, \delta_c^{\frac{1}{2}} k \tag{B-68}$$

INVERSE TANGENT FORCE-CRUSH CHARACTERISTICS

Another approximation to the linear/yield characteristic is given by the inverse tangent

$$F = a \tan^{-1}[g(\delta)] \tag{B-69}$$

as shown below

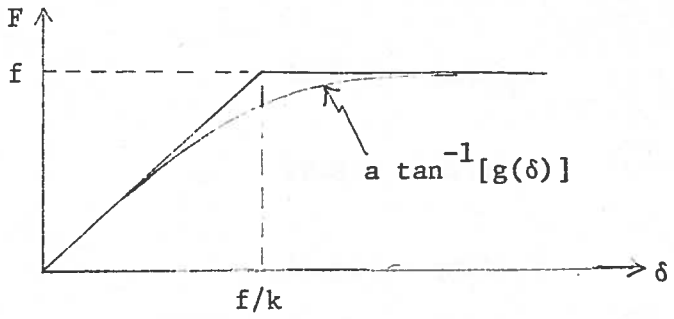

With $a = 2f/\pi$,

$$\lim_{g\to\infty} F = f \tag{B-70}$$

The function g should be monotone increasing and, in order to give a good approximation, should increase faster than $(\pi k/2f)\delta$. With $b = (\pi k/2f)$, the following g functions give successively better approximations.

$$\begin{aligned} g_1 &= b\delta \\ g_3 &= b\delta + \frac{b^3}{3}\delta^3 \\ g_5 &= b\delta + \frac{b^3}{3}\delta^3 + \frac{b^5}{7.5}\delta^5 \\ g_7 &= b\delta + \frac{b^3}{3}\delta^3 + \frac{b^5}{7.5}\delta^5 + \frac{17b^7}{315}\delta^7 \end{aligned} \tag{B-71}$$

These functions have the properties

$$\lim_{\delta\to\infty} F = f; \quad F'(0) = k \tag{B-72}$$

and, for small δ,

$$F(g_i) \triangleq F_i(\delta) = k\delta + o(\delta^{i+1}) \tag{B-73}$$

The goodness of these approximations may be measured by the speed of approach to f:

$$F_1(f/k) = 0.639f$$

$$F_3(f/k) = 0.786f$$

$$F_5(f/k) = 0.849f \qquad \text{(B-74)}$$

$$F_7(f/k) = 0.884f$$

These approximations may be improved by increasing the initial slop (which is k) so as to match the area under the approximating characteristics with that of the linear/yield characteristic over the interval [0,f/k]. This is accomplished by letting

$$b = \frac{\pi ck}{2f} \qquad \text{(B-75)}$$

with c>1. The appropriate values of c for the several functions F_i are

i	c
1	1.5571
3	1.1573
5	1.0753
7	1.0442

Closed form solution of the crush dynamics is not available with these inverse tangent force-crush characteristics, and one has to resort to numerical solution [Eqs. (A-28)-(A-31)]:

$$\ddot{c} = -F_{iA}(k_A, f_A, \delta_A)/\mu \qquad \text{(B-76)}$$

$$F_{iA}(k_A, f_A, \delta_A) - F_{iB}(k_B, f_B, c-\delta_A) = 0 \qquad \text{(B-77)}$$

$$c(0) = 0 \ , \quad \dot{c}(0) = V_c \qquad \text{(B-78)}$$

$$\dot{c}(t_f) = 0 \qquad \text{(B-79)}$$

APPENDIX C

FIGURE OF MERIT

WITH NO RESTRAINT SYSTEM MODEL

This appendix summarizes the equations for the computation of the Figure of Merit (total societal cost) of two-vehicle collisions in the case of no restraint system. That is, the occupant rides down the vehicle acceleration. The component costs considered are Injury/Mortality costs, Penetration Penalty costs, Repair costs, and costs of Engineering modifications. The reader should refer to appendices E-H and the main discussion for descriptions of the component costs and vehicle mix statistics.

The Figure of Merit is defined as

$$C_T = N_c \sum_{i=1}^{I} \sum_{j=1}^{I} \sum_{m=1}^{M} \sum_{n=1}^{M} \sum_{i_{vc}=1}^{I_{vc}} p(i|col)p(j|col)p(m,n|col)\times$$

$$\times\, p(i_{vc}|m,n,col)[C^{i}_{im/jn/V_{ci}} + C^{j}_{im/jn/V_{ci}}] \qquad \text{(C-1)}$$

$$+ N_v \sum_{i=1}^{I} p(i)C_{E/i}$$

Here indices (i,j) refer to vehicle weight/size classes, indices (m,n) refer to collision modes (front, side, rear), and the index i_{vc} refers to the collision speeds (V_{ci}). The functions p( ) are probability mass functions describing the vehicle mix (Appendix E), N_c is the total number of (two-vehicle) collisions, and N_v is the total number of vehicles. $C^{i(j)}_{im/jn/V_{ci}}$ is the cost, associated with the class i(j) vehicle, when a weight/size class i vehicle, in collision mode m, collides with a weight/size class j vehicle, which is in mode n, at collision speed V_{ci}. $C_{E/i}$ is the cost of engineering modifications for a weight/size class i vehicle.

In component form, the Figure of Merit is written as

$$C_T = C_{IM} + C_P + C_R + C_E \qquad \text{(C-2)}$$

where C_{IM} is the total societal cost of injury/mortality, C_P is the total penetration penalty cost, C_R is the total repair cost, and C_E is the total cost of engineering modifications. Since, as will be seen, the penetration penalty may be thought of as a device for constraining the vehicle force-crush characteristics, it is also of interest to compute

$$C_T' = C_{IM} + C_R + C_E \tag{C-3}$$

The component costs in Eqn. (C-2) are written below, where, to save space, the summation indices and arguments, which are identical to those in Eqn. (C-1), have been omitted

$$C_{IM} = N_c \sum \cdots \sum p \cdot\cdot p[C^i_{IM/im/jn/V_{ci}} + C^j_{IM/im/jn/V_{ci}}] \tag{C-4}$$

$$C_P = N_c \sum \cdots \sum p \cdot\cdot p[C^i_{P/im/jn/V_{ci}} + C^j_{P/im/jn/V_{ci}}] \tag{C-5}$$

$$C_R = N_c \sum \cdots \sum p \cdot\cdot p[C^i_{R/im/jn/V_{ci}} + C^j_{R/im/jn/V_{ci}}] \tag{C-6}$$

$$C_E = N_v \sum_{i=1}^{I} p(i) C_{E/i} \tag{C-7}$$

In the above, $C^i_{IM/im/jn/V_{ci}}$ is the injury/mortality cost component of $C^i_{im/jn/V_{ci}}$, and so on.

INJURY/MORTALITY COST OF EACH COLLISION

This cost (see Appendix F) is modeled as

$$C^i_{IM/im/jn/V_{ci}} + C^j_{IM/im/jn/V_{ci}}$$

$$= w_{IM}(i) O(i) c_{IM}[1 - \exp(-r_{IM}(SI_i)^4)] \tag{C-8}$$

$$+ w_{IM}(j) O(j) c_{IM}[1 - \exp(-r_{IM}(SI_j)^4)]$$

Here $w_{IM}(\ell)$ are arbitrary weighting factors, $O(\ell)$ is the average number of occupants in the weight/size class ℓ vehicle, c_{IM} and r_{IM} are constants, and SI_ℓ is the injury *severity index* associated with vehicle ℓ,

$$SI_\ell = \int_0^{t_f} \frac{a^\alpha(t)}{O_{\ell/im/jn/V_{ci}}} dt \qquad (\ell=i,j) \qquad \text{(C-9)}$$

The severity index SI_ℓ is an integral over the collision time interval of the magnitude of the vehicle ℓ occupant acceleration taken to the power α. Note that the severity index must be put in the units $g^\alpha \times sec$.

In the present model the occupant acceleration is taken as the vehicle acceleration, which is computed based on the linear/yield model of vehicle force-crush characteristics (Appendix B). The severity index is obtained in closed form:

For $V_{ci} \leq \min(f_{im},f_{jn})/\sqrt{\kappa\mu}$,

$$SI_\ell = [M_\ell^{-1}\sqrt{\kappa\mu}\, V_{ci}]^\alpha \int_0^{t_f} \sin^\alpha \sqrt{\kappa/\mu}\, t\, dt \qquad \text{(C-10)}$$

$$t_f = \frac{\pi}{2}\sqrt{\mu/\kappa} \qquad \text{(C-11)}$$

For $V_{ci} > \min(f_{im},f_{jn})/\sqrt{\kappa\mu}$,

$$SI_\ell = [M_\ell^{-1}\sqrt{\kappa\mu}\, V_{ci}]^\alpha \int_0^{t_y} \sin^\alpha \sqrt{\kappa/\mu}\, t\, dt$$

$$+ [M_\ell^{-1}\min(f_{im},f_{jn})]^\alpha [\sqrt{\mu/\kappa}\,/\min(f_{im},f_{jn})] \times \qquad \text{(C-12)}$$

$$\times [\kappa\mu V_{ci}^2 - \min^2(f_{im},f_{jn})]^{\frac{1}{2}}$$

$$t_y = \sqrt{\mu/\kappa}\,\sin^{-1}[\min(f_{im},f_{jn})/\sqrt{\kappa\mu}\,V_{ci}] \qquad \text{(C-13)}$$

In the above,

$$\mu = M_iM_j/(M_i + M_j), \quad \kappa = k_{im}k_{jn}/(k_{im} + k_{jn}) \qquad \text{(C-14)}$$

M_i is the mass of the class i vehicle, and f_{im}, k_{im} define the force-crush characteristics of the class i vehicle in mode m.

The integrals in Eqs. (C-10) and (C-12) are computed in terms of

$$I[x;\alpha] \triangleq \int_0^x \sin^{\alpha}\tau d\tau$$

$$\approx x^{\alpha+1}\left[\frac{1}{\alpha+1} - \alpha x^2\left[\frac{1}{6(3+\alpha)} - x^2\left[\frac{(5\alpha-2)}{360(5+\alpha)} - \frac{0.8834x^2}{(7+\alpha)}\times\right.\right.\right. \qquad \text{(C-15)}$$

$$\left.\left.\left.\times\left[\frac{35\alpha^2-42\alpha+16}{45360}\right]\right]\right]\right]$$

by noting that

$$\int_0^T \sin^{\alpha}\sqrt{\kappa/\mu}\,t\,dt = \sqrt{\mu/\kappa}\int_0^{\sqrt{\kappa/\mu}\,T} \sin^{\alpha}\tau d\tau \qquad \text{(C-16)}$$

Thus

$$\int_0^{t_f} \sin^{\alpha}\sqrt{\kappa/\mu}\,t\,dt = \sqrt{\mu/\kappa}\,I[\tfrac{\pi}{2};\alpha] \qquad \text{(C-17)}$$

$$\int_0^{t_y} \sin^{\alpha}\sqrt{\kappa/\mu}\,t\,dt = \sqrt{\mu/\kappa}\,I[\sin^{-1}[\min(f_{im},f_{jn})/\sqrt{\kappa\mu}\,V_{ci}];\alpha] \qquad \text{(C-18)}$$

PENETRATION COST PENALTY IN EACH COLLISION

This cost penalty is defined as

$$C^{i}_{P/im/jn/V_{ci}} + C^{j}_{P/im/jn/V_{ci}}$$

$$= \left\{ \begin{array}{ll} 0 & ; \text{ for } V_{ci} > \bar{V}_{cm} \text{ ; otherwise:} \\ 0 & ; \ \delta^{fi}_{im/jn/V_{ci}} \leq k_m \delta^{*}_{im} \\ w_P(i) c_P [\delta^{fi}_{im/jn/V_{ci}} - k_m \delta^{*}_{im}]^2 & ; \ \delta^{fi}_{im/jn/V_{ci}} > k_m \delta^{*}_{im} \end{array} \right\} \qquad \text{(C-19)}$$

$$+ \left\{ \begin{array}{ll} 0 & ; \text{ for } V_{ci} > \bar{V}_{cn} \text{ ; otherwise:} \\ 0 & ; \ \delta^{fj}_{im/jn/V_{ci}} \leq k_n \delta^{*}_{jn} \\ w_P(j) c_P [\delta^{fj}_{im/jn/V_{ci}} - k_n \delta^{*}_{jn}]^2 & ; \ \delta^{fj}_{im/jn/V_{ci}} > k_n \delta^{*}_{jn} \end{array} \right\}$$

This cost penalizes intrusion into the occupant compartment by penalizing excessive final crush $\delta^{fi}_{im/jn/V_{ci}}$ of vehicle i and $\delta^{fj}_{im/jn/V_{ci}}$ of vehicle j. This at the same time implicitly constrains the vehicle force-crush characteristics (f,k) [excludes solution (f→0, k→0) which would tend to minimize injury/mortality costs]. Note that there is no penetration penalty for collision speeds in excess of specified speeds $\bar{V}_{cm}$ which depend on the collision mode m. Only when the final crush exceeds $k_m \delta^{*}_{im}$ ($k_n \delta^{*}_{jn}$) is the penalty imposed. In this latter expression δ^{*}_{im}, δ^{*}_{jn} are the "designed" crush distances given by

$$\delta^{*}_{im} = e_m b_m \delta^{*}_{i} + (1-e_m)\bar{\delta}_{im} \ , \quad \delta^{*}_{jn} = e_n b_n \delta^{*}_{j} + (1-e_n)\bar{\delta}_{jn} \qquad \text{(C-20)}$$

and k_m, k_n are fractions defining the effective crush distance; that is, of the distance δ^{*}_{im}, only $k_m \delta^{*}_{im}$ is the effective crush distance of vehicle i in collision mode m. In Eqn. (C-19), $w_P(\ell)$ [ℓ=i,j] are arbitrary weighting factors

and c_p is a large number ($3K, say).

Consider Eqn. (C-20) for the designed crush distances. δ^*_ℓ are actually the design variables, and as will be seen, if m = 1 denotes the frontal collision mode, then δ^*_ℓ are the design frontal crush distances for vehicle weight/size classes ℓ. The balance of Eqn. (C-20) scales the side and rear (m=2,3) crush distance design via the constants b_m, and the constants e_m permit the removal from optimization (design) of the side and rear crush distances. $\bar{\delta}_{im}$ is the "currently available" crush distance of weight/size class i vehicle in mode m. Eqn. (C-20) and crush distance data are developed in Appendix I.

The final crush distances, $\delta^{fi}_{im/jn/V_{ci}}$ and $\delta^{fj}_{im/jn/V_{ci}}$, of vehicles i and j, respectively, are computed, alternately using the inverse tangent force-crush approximation (Appendix B), or using the parabolic force-crush characteristics (Appendix B) as they approximate the linear/yield force-crush characteristics [Eqs. (B-66) and (B-68)] with $\delta_c = \delta_{cf}\bar{\delta}$, δ_{cf} a specified constant. In the case of the parabolic approximation

$$\delta^{fi}_{im/jn/V_{ci}} = \frac{c^2_{jn}}{c^2_{im}+c^2_{jn}}\left[\frac{3}{4}V^2_{ci}\,\frac{\mu(c^2_{im}+c^2_{jn})^{\frac{1}{2}}}{c_{im}c_{jn}}\right]^{\frac{2}{3}} \qquad \text{(C-21)}$$

$$\delta^{fj}_{im/jn/V_{ci}} = \frac{c^2_{im}}{c^2_{im}+c^2_{jn}}\left[\frac{3}{4}V^2_{ci}\,\frac{\mu(c^2_{im}+c^2_{jn})^{\frac{1}{2}}}{c_{im}c_{jn}}\right]^{\frac{2}{3}} \qquad \text{(C-22)}$$

where

$$c_{\eta\xi} = \frac{3}{2}(\delta_{cf}\bar{\delta}_{\eta\xi})^{-3/2}[f_{\eta\xi}\delta_{cf}\bar{\delta}_{\eta\xi} - \tfrac{1}{2}f^2_{\eta\xi}/k_{\eta\xi}] \quad (\delta_{cf}\bar{\delta}_{\eta\xi} \geq f_{\eta\xi}/k_{\eta\xi}) \qquad \text{(C-23)}$$

$$c_{\eta\xi} = \frac{3}{4}(\delta_{cf}\bar{\delta}_{\eta\xi})^{1/2}k_{\eta\xi} \quad (\delta_{cf}\bar{\delta}_{\eta\xi} < f_{\eta\xi}/k_{\eta\xi}) \qquad \text{(C-24)}$$

$\eta\xi$ = im and jn. In the case of the inverse tangent approximation, the final crush distances are obtained by numerical integration.

REPAIR COST OF EACH COLLISION

Two optional forms of repair cost are provided (see Appendix G) and these are

$$C^{i}_{R/im/jn/V_{ci}} + C^{j}_{R/im/jn/V_{ci}}$$

$$= w_R(i)C_{VD}(i)[1-\exp(-d\delta^{fi}_{im/jn/V_{ci}}/\bar{\delta}_{im})] \qquad \text{(C-25)}$$

$$+ w_R(j)C_{VD}(j)[1-\exp(-d\delta^{fj}_{im/jn/V_{ci}}/\bar{\delta}_{jn})]$$

and

$$C^{i}_{R/im/jn/V_{ci}} + C^{j}_{R/im/jn/V_{ci}}$$

$$= \left\{ \begin{array}{ll} w_R(i)\dfrac{c_{RC}}{V^2_{ch}}\left(\dfrac{M_j V_{ci}}{M_i+M_j}\right)^2, & \text{if} \leq C_{VD}(i) \\ C_{VD}(i), & \text{otherwise} \end{array} \right\}$$

$$+ \left\{ \begin{array}{ll} w_R(j)\dfrac{c_{RC}}{V^2_{ch}}\left(\dfrac{M_i V_{ci}}{M_i+M_j}\right)^2, & \text{if} \leq C_{VD}(j) \\ C_{VD}(j), & \text{otherwise} \end{array} \right\} \qquad \text{(C-26)}$$

The costs in Eqn. (C-25) depend on the final crush distances, while the costs in Eqn. (C-26) are independent of crush distance and also of collision mode. $w_R(\ell)$, ℓ = i,j, are arbitrary weighting constants; d, c_{RC} and V_{ch} are constants; and $C_{VD}(\ell)$, ℓ = i,j, are depreciated values of class ℓ vehicles.

COST OF ENGINEERING MODIFICATION

This cost, as described in Appendix H, is modeled as:

$$C_{E/i} = \left\{ \begin{array}{ll} w_E(i)C_{E1}(i)(\delta^*_i-\bar{\delta}_{il})^{\gamma} + w_E(i)C_{E2}(i)(\delta^*_i-\bar{\delta}_{il})^2 & ; \quad \delta^*_i > \bar{\delta}_{il} \\ 0 & ; \quad \delta^*_i \leq \bar{\delta}_{il} \end{array} \right\}$$

$$+ w_E(i)C_{E3}(i)\sum_{m=1}^{M} \left\{ \begin{array}{ll} s_m(f_{im}-\bar{f}_{im})^2 & ; \quad f_{im} > \bar{f}_{im} \\ 0 & ; \quad f_{im} \leq \bar{f}_{im} \end{array} \right\}$$

$$+ w_E(i) C_{E4}(i) \sum_{m=1}^{M} \begin{cases} s_m (k_{im} - \bar{k}_{im})^2 & ; \quad k_{im} > \bar{k}_{im} \\ 0 & ; \quad k_{im} \leq \bar{k}_{im} \end{cases} \qquad \text{(C-27)}$$

Here $w_E(i)$ are arbitrary weighting constants; C_{E1}, C_{E2}, C_{E3}, and C_{E4} are coefficients depending on the weight/size class i; s_m are scaling constants depending on the collision mode; γ is a constant close to 1 (e.g. 1.05); $\bar{k}_{im}$ and $\bar{f}_{im}$ are nominal (reference) values of the spring constants and yield strengths; δ_i^* is the design (frontal) crush distance for weight/size class i vehicles; and $\bar{\delta}_{il}$ is the available frontal crush distance for weight/size class i vehicles (see Appendix I).

SUMMARY COMMENTS

A review of this appendix shows that the Figure of Merit, once all constants are specified, is a function of the force-crush characteristics

$$f_{\eta\xi} \ , \quad k_{\eta\xi} \qquad \text{(C-28)}$$

and the design crush distances

$$\delta_\eta^* \qquad \text{(C-29)}$$

Here η refers to the weight/size class, and ξ refers to the collision mode. The gradient of the Figure of Merit (partial derivatives with respect to the variables in Eqs. (C-28) and (C-29)) is given in Appendix D.

APPENDIX D

GRADIENT OF THE FIGURE OF MERIT (C)

This appendix lists the equations for the partial derivatives of the Figure of Merit defined in Appendix C with respect to the variables $f_{\eta\xi}$, $k_{\eta\xi}$, δ^*_η [see SUMMARY COMMENTS, Appendix C]. From Eqn. (C-1), for any variable β,

$$\frac{\partial C_T}{\partial \beta} = N_c \sum\cdots\sum p\cdot\cdot p\left[\frac{\partial (C^i_{IM}+C^j_{IM})}{\partial \beta} + \frac{\partial (C^i_P+C^j_P)}{\partial \beta} + \frac{\partial (C^i_R+C^j_R)}{\partial \beta}\right] + N_v \sum_{i=1}^{I} p(i)\frac{\partial C_{E/i}}{\partial \beta} \tag{D-1}$$

where C^i_P is an abbreviation for $C^i_{P/im/jn/V_{ci}}$, and so on. The partials on the right-hand side of Eqn. (D-1) are given below.

$$\frac{\partial (C^i_{IM}+C^j_{IM})}{\partial \delta^*_\eta} = 0, \quad \text{all } \eta \tag{D-2}$$

For $V_{ci} \leq \min(f_{im}, f_{jn})/\sqrt{\kappa\mu}$, Eqs. (D-3)-(D-7):

$$\frac{\partial (C^i_{IM}+C^j_{IM})}{\partial f_{\eta\xi}} = 0, \text{ all } \eta\xi \tag{D-3}$$

$$\frac{\partial (C^i_{IM}+C^j_{IM})}{\partial k_{\eta\xi}} = 0, \ \eta\xi \neq im, \ \eta\xi \neq jn \tag{D-4}$$

$$\frac{\partial (C^i_{IM}+C^j_{IM})}{\partial k_{\eta\xi}} = 4c_{IM}r_{IM}\left[w_{IM}(i)O(i)e^{-r_{IM}(SI_i)^4}(SI_i)^3\frac{\partial SI_i}{\partial k_{\eta\xi}} + w_{IM}(j)O(j)e^{-r_{IM}(SI_j)^4}(SI_j)^3\frac{\partial SI_j}{\partial k_{\eta\xi}}\right] \tag{D-5}$$

where

$$\frac{\partial SI_{\ell}}{\partial k_{\eta\xi}} = \frac{(\alpha-1)}{2\kappa}[M_{\ell}^{-1}\sqrt{\kappa\mu}\, V_{ci}]^{\alpha}\sqrt{\mu/\kappa}\, I[\tfrac{\pi}{2};\alpha]\, \frac{\partial \kappa}{\partial k_{\eta\xi}}\ , \quad (\ell=i,j) \tag{D-6}$$

$$\frac{\partial \kappa}{\partial k_{im}} = \frac{\kappa^2}{k_{im}^2}\ , \qquad \frac{\partial \kappa}{\partial k_{jn}} = \frac{\kappa^2}{k_{jn}^2} \tag{D-7}$$

For $V_{ci} > \min(f_{im}, f_{jn})/\sqrt{\kappa\mu}$, Eqs. (D-8)-(D-15):

$$\frac{\partial (C_{IM}^{i}+C_{IM}^{j})}{\partial f_{\eta\xi}} = 0, \quad \eta\xi\neq im, \ \eta\xi\neq jn \tag{D-8}$$

$$\frac{\partial (C_{IM}^{i}+C_{IM}^{j})}{\partial k_{\eta\xi}} = 0, \quad \eta\xi\neq im, \ \eta\xi\neq jn \tag{D-9}$$

$$\begin{aligned}\frac{\partial (C_{IM}^{i}+C_{IM}^{j})}{\partial f_{\eta\xi}} = 4c_{IM}r_{IM}[&w_{IM}(i)O(i)e^{-r_{IM}(SI_i)^4}(SI_i)^3\frac{\partial SI_i}{\partial f_{\eta\xi}} \\ &+ w_{IM}(j)O(j)e^{-r_{IM}(SI_j)^4}(SI_j)^3\frac{\partial SI_j}{\partial f_{\eta\xi}}]\end{aligned} \tag{D-10}$$

where

$$\frac{\partial SI_{\ell}}{\partial f_{\eta\xi}} = (\alpha-1)\sqrt{\mu/\kappa}\,\frac{[M_{\ell}^{-1}\min(f_{im},f_{jn})]^{\alpha}}{\min^2(f_{im},f_{jn})}\,[\kappa\mu V_{ci}^2-\min^2(f_{im},f_{jn})]^{\frac{1}{2}}\times$$

$$\times\ \frac{\partial}{\partial f_{\eta\xi}}\min(f_{im},f_{jn}) \qquad (\ell=i,j) \tag{D-11}$$

$$\frac{\partial}{\partial f_{im}} \min(f_{im}, f_{jn}) = \begin{cases} 1, \text{ if } i=j \textit{ and } m=n \\ \text{If } i\neq j \textit{ and/or } m\neq n: \\ 1, \text{ if } f_{im}<f_{jn} \textit{ and } f_{jn}-f_{im}>\varepsilon f_{jn} \\ 0, \text{ if } f_{im}>f_{jn} \textit{ and } f_{im}-f_{jn}>\varepsilon f_{im} \\ \dfrac{2f_{jn}^2}{(f_{im}+f_{jn})^2}, \text{ if } f_{im}<f_{jn} \textit{ and } f_{jn}-f_{im}\leq\varepsilon f_{jn} \\ \qquad\qquad \textit{or} \\ \qquad \text{if } f_{im}>f_{jn} \textit{ and } f_{im}-f_{jn}\leq\varepsilon f_{im} \end{cases} \tag{D-12}$$

$$\frac{\partial}{\partial f_{jn}} \min(f_{im}, f_{jn}) = \begin{cases} 1, \text{ if } i=j \textit{ and } m=n \\ \text{If } i\neq j \textit{ and/or } m\neq n: \\ 1, \text{ if } f_{im}>f_{jn} \textit{ and } f_{im}-f_{jn}>\varepsilon f_{im} \\ 0, \text{ if } f_{im}<f_{jn} \textit{ and } f_{jn}-f_{im}>\varepsilon f_{jn} \\ \dfrac{2f_{im}^2}{(f_{im}+f_{jn})^2}, \text{ if } f_{im}<f_{jn} \textit{ and } f_{jn}-f_{im}\leq\varepsilon f_{jn} \\ \qquad\qquad \textit{or} \\ \qquad \text{if } f_{im}>f_{jn} \textit{ and } f_{im}-f_{jn}\leq\varepsilon f_{im} \end{cases} \tag{D-13}$$

[For the purpose of differentiating the min function, if f_{im} and f_{jn} are sufficiently close (specified ε), min(x,y) is replaced by the approximation $2xy/(x+y)$.]

$$\frac{\partial(C_{IM}^i+C_{IM}^j)}{\partial k_{\eta\xi}} = 4c_{IM}r_{IM}[w_{IM}(i)O(i)e^{-r_{IM}(SI_i)^4}(SI_i)^3\frac{\partial SI_i}{\partial k_{\eta\xi}} + w_{IM}(j)O(j)e^{-r_{IM}(SI_j)^4}(SI_j)^3\frac{\partial SI_j}{\partial k_{\eta\xi}}] \tag{D-14}$$

where

$$\frac{\partial SI_{\ell}}{\partial k_{\eta\xi}} = \frac{(\alpha-1)}{2\kappa}[M_{\ell}^{-1}\sqrt{\kappa\mu}\,V_{ci}]^{\alpha}\sqrt{\mu/\kappa}\;I[\sin^{-1}(\frac{\min(f_{im},f_{jn})}{\sqrt{\kappa\mu}\,V_{ci}});\alpha]\;\frac{\partial\kappa}{\partial k_{\eta\xi}} \qquad \text{(D-15)}$$

$(\ell=i,j)$

and where $\partial\kappa/\partial k_{\eta\xi}$ is given in Eqn. (D-7).

$$\frac{\partial(C_P^i+C_P^j)}{\partial\delta_{\eta}^*} = 0,\ \eta\neq i,\ \eta\neq j \qquad \text{(D-16)}$$

$$\frac{\partial(C_P^i+C_P^j)}{\partial f_{\eta\xi}} = \frac{\partial(C_P^i+C_P^j)}{\partial k_{\eta\xi}} = 0,\ \eta\xi\neq im,\ \eta\xi\neq jn \qquad \text{(D-17)}$$

$$\frac{\partial(C_P^i+C_P^j)}{\partial\delta_{\eta}^*} = \left\{\begin{array}{ll} 0 & ;\ V_{ci}>\bar{V}_{cm}\ ;\ \text{otherwise:} \\ 0 & ;\ \delta^{fi}\leq k_m\delta_{im}^* \\ -2c_P k_m e_{bm} w_P(i)[\delta^{fi}-k_m\delta_{im}^*]\,\dfrac{\partial\delta_i^*}{\partial\delta_{\eta}^*} & ;\ \delta^{fi}>k_m\delta_{im}^* \end{array}\right\} \qquad \text{(D-18)}$$

$$+\left\{\begin{array}{ll} 0 & ;\ V_{ci}>\bar{V}_{cn}\ ;\ \text{otherwise:} \\ 0 & ;\ \delta^{fj}\leq k_n\delta_{jn}^* \\ -2c_P k_n e_{bn} w_P(j)[\delta^{fj}-k_n\delta_{jn}^*]\,\dfrac{\partial\delta_j^*}{\partial\delta_{\eta}^*} & ;\ \delta^{fj}>k_n\delta_{jn}^* \end{array}\right\}$$

where

$$\frac{\partial\delta_i^*}{\partial\delta_i^*} = \frac{\partial\delta_j^*}{\partial\delta_j^*} = 1\ ,\quad \frac{\partial\delta_i^*}{\partial\delta_j^*} = \frac{\partial\delta_j^*}{\partial\delta_i^*} = 0 \qquad \text{(D-19)}$$

$$\frac{\partial(c_p^i+c_p^j)}{\partial f_{\eta\xi}} = \left\{ \begin{array}{ll} 0 & ; \; V_{ci} > \bar{V}_{cm} \; ; \; \text{otherwise:} \\ 0 & ; \; \delta^{fi} \leq k_m \delta^*_{im} \\ 2c_p w_p(i)[\delta^{fi} - k_m \delta^*_{im}] \dfrac{\partial \delta^{fi}}{\partial f_{\eta\xi}} & ; \; \delta^{fi} > k_m \delta^*_{im} \end{array} \right\} \tag{D-20}$$

$$+ \left\{ \begin{array}{ll} 0 & ; \; V_{ci} > \bar{V}_{cn} \; ; \; \text{otherwise:} \\ 0 & ; \; \delta^{fj} \leq k_n \delta^*_{jn} \\ 2c_p w_p(j)[\delta^{fj} - k_n \delta^*_{jn}] \dfrac{\partial \delta^{fj}}{\partial f_{\eta\xi}} & ; \; \delta^{fj} > k_n \delta^*_{jn} \end{array} \right\}$$

where, in case of the parabolic force-crush approximation [in case of the inverse tangent approximation, see Eqs. (D-40)-(D-44)]

$$\frac{\partial \delta^{fi}}{\partial f_{\eta\xi}} = \frac{\partial \delta^{fi}}{\partial c_{im}} \frac{\partial c_{im}}{\partial f_{im}} \frac{\partial f_{im}}{\partial f_{\eta\xi}} + \frac{\partial \delta^{fi}}{\partial c_{jn}} \frac{\partial c_{jn}}{\partial f_{jn}} \frac{\partial f_{jn}}{\partial f_{\eta\xi}} \tag{D-21}$$

$$\frac{\partial \delta^{fj}}{\partial f_{\eta\xi}} = \frac{\partial \delta^{fj}}{\partial c_{im}} \frac{\partial c_{im}}{\partial f_{im}} \frac{\partial f_{im}}{\partial f_{\eta\xi}} + \frac{\partial \delta^{fj}}{\partial c_{jn}} \frac{\partial c_{jn}}{\partial f_{jn}} \frac{\partial f_{jn}}{\partial f_{\eta\xi}} \tag{D-22}$$

$$\frac{\partial \delta^{fi}}{\partial c_{im}} = -\frac{2(c_{im}^2+\frac{1}{3}c_{jn}^2)}{c_{im}(c_{im}^2+c_{jn}^2)} \delta^{fi} \; ; \; \frac{\partial \delta^{fi}}{\partial c_{jn}} = \frac{4}{3} \frac{c_{jn}}{c_{im}^2+c_{jn}^2} \delta^{fj} \tag{D-23}$$

$$\frac{\partial \delta^{fj}}{\partial c_{im}} = \frac{4}{3} \frac{c_{im}}{c_{im}^2+c_{jn}^2} \delta^{fi} \; ; \; \frac{\partial \delta^{fj}}{\partial c_{jn}} = -\frac{2(c_{jn}^2+\frac{1}{3}c_{im}^2)}{c_{jn}(c_{im}^2+c_{jn}^2)} \delta^{fj} \tag{D-24}$$

$$\frac{\partial c_{\eta\xi}}{\partial f_{\eta\xi}} = \left\{ \begin{array}{ll} \frac{3}{2}(\delta_{cf}\bar{\delta}_{\eta\xi})^{-3/2}[\delta_{cf}\bar{\delta}_{\eta\xi} - f_{\eta\xi}/k_{\eta\xi}] & ; \; \delta_{cf}\bar{\delta}_{\eta\xi} \geq f_{\eta\xi}/k_{\eta\xi} \\ 0 & ; \; \delta_{cf}\bar{\delta}_{\eta\xi} < f_{\eta\xi}/k_{\eta\xi} \end{array} \right\} \tag{D-25}$$

$\eta\xi$ = im and jn.

$$\frac{\partial f_{im}}{\partial f_{im}} = \frac{\partial f_{jn}}{\partial f_{jn}} = 1 \; ; \quad \frac{\partial f_{im}}{\partial f_{jn}} = \frac{\partial f_{jn}}{\partial f_{im}} = 0 \tag{D-26}$$

$$\frac{\partial (C_P^i + C_P^j)}{\partial k_{\eta\xi}} = \text{same as Eqn. (D-20) with partials with respect to } k_{\eta\xi} \tag{D-27}$$

where, in case of the parabolic force-crush approximation [in case of the inverse tangent approximation, see Eqs. (D-40)-(D-44)]

$$\frac{\partial \delta^{fi}}{\partial k_{\eta\xi}} = \frac{\partial \delta^{fi}}{\partial c_{im}} \frac{\partial c_{im}}{\partial k_{im}} \frac{\partial k_{im}}{\partial k_{\eta\xi}} + \frac{\partial \delta^{fi}}{\partial c_{jn}} \frac{\partial c_{jn}}{\partial k_{jn}} \frac{\partial k_{jn}}{\partial k_{\eta\xi}} \tag{D-28}$$

$$\frac{\partial \delta^{fj}}{\partial k_{\eta\xi}} = \frac{\partial \delta^{fj}}{\partial c_{im}} \frac{\partial c_{im}}{\partial k_{im}} \frac{\partial k_{im}}{\partial k_{\eta\xi}} + \frac{\partial \delta^{fj}}{\partial c_{jn}} \frac{\partial c_{jn}}{\partial k_{jn}} \frac{\partial k_{jn}}{\partial k_{\eta\xi}} \tag{D-29}$$

where see Eqs. (D-23) and (D-24), and

$$\frac{\partial c_{\eta\xi}}{\partial k_{\eta\xi}} = \begin{cases} \frac{3}{4}(\delta_{cf}\bar{\delta}_{\eta\xi})^{-3/2}(f_{\eta\xi}/k_{\eta\xi})^2 \; ; & \delta_{cf}\bar{\delta}_{\eta\xi} \geq f_{\eta\xi}/k_{\eta\xi} \\ \frac{3}{4}(\delta_{cf}\bar{\delta}_{\eta\xi})^{1/2} \; ; & \delta_{cf}\bar{\delta}_{\eta\xi} < f_{\eta\xi}/k_{\eta\xi} \end{cases} \qquad \eta\xi = \text{im and jn} \tag{D-30}$$

$$\frac{\partial k_{im}}{\partial k_{im}} = \frac{\partial k_{jn}}{\partial k_{jn}} = 1 \; ; \quad \frac{\partial k_{im}}{\partial k_{jn}} = \frac{\partial k_{jn}}{\partial k_{im}} = 0 \tag{D-31}$$

For the repair cost option of Eqn. (C-25),

$$\frac{\partial (C_R^i + C_R^j)}{\partial \delta_\eta^*} = 0, \text{ all } \eta \tag{D-32}$$

$$\frac{\partial (C_R^i + C_R^j)}{\partial f_{\eta\xi}} = \frac{\partial (C_R^i + C_R^j)}{\partial k_{\eta\xi}} = 0, \; \eta\xi \neq im, \; \eta\xi \neq jn \tag{D-33}$$

$$\frac{\partial(C_R^i+C_R^j)}{\partial f_{\eta\xi}} = \frac{dw_R(i)}{\bar{\delta}_{im}} C_{VD}(i) e^{-\frac{d\delta^{fi}}{\bar{\delta}_{im}}} \frac{\partial \delta^{fi}}{\delta f_{\eta\xi}} + \frac{dw_R(j)}{\bar{\delta}_{jn}} C_{VD}(j) e^{-\frac{d\delta^{fj}}{\bar{\delta}_{jn}}} \frac{\partial \delta^{fj}}{\partial f_{\eta\xi}} \tag{D-34}$$

$$\frac{\partial(C_R^i+C_R^j)}{\partial k_{\eta\xi}} = \text{same as Eqn. (D-34) with partials with respect to } k_{\eta\xi} \tag{D-35}$$

where see Eqs. (D-21)-(D-26) and (D-28)-(D-31) for the parabolic force-crush approximation, and Eqs. (D-40)-(D-44) for the inverse tangent approximation.

For the repair cost option of Eqn. (C-26) all the partial derivatives are identically zero.

$$\frac{\partial C_{E/i}}{\partial \delta_\eta^*} = \begin{cases} w_E(i) C_{E1}(i) \gamma (\delta_i^* - \bar{\delta}_{i1})^{\gamma-1} \frac{\partial \delta_i^*}{\partial \delta_\eta^*} + 2 w_E(i) C_{E2}(i) (\delta_i^* - \bar{\delta}_{i1}) \frac{\partial \delta_i^*}{\partial \delta_\eta^*}; & \delta_i^* > \bar{\delta}_{i1} \\ 0 & ; \ \delta_i^* \leq \bar{\delta}_{i1} \end{cases} \tag{D-36}$$

$$\frac{\partial \delta_i^*}{\partial \delta_i^*} = 1, \quad \frac{\partial \delta_i^*}{\partial \delta_\eta^*} = 0, \quad \eta \neq i \tag{D-37}$$

$$\frac{\partial C_{E/i}}{\partial f_{\eta\xi}} = w_E(i) C_{E3}(i) \sum_{m=1}^{M} \begin{cases} 2 s_m (f_{im} - \bar{f}_{im}) \frac{\partial f_{im}}{\partial f_{\eta\xi}} & ; \ f_{im} > \bar{f}_{im} \\ 0 & ; \ f_{im} \leq \bar{f}_{im} \end{cases} \tag{D-38}$$

$$\frac{\partial C_{E/i}}{\partial k_{\eta\xi}} = w_E(i) C_{E4}(i) \sum_{m=1}^{M} \begin{cases} 2s_m (k_{im} - \bar{k}_{im}) \dfrac{\partial k_{im}}{\partial k_{\eta\xi}} & ; \quad k_{im} > \bar{k}_{im} \\ 0 & ; \quad k_{im} \leq \bar{k}_{im} \end{cases} \tag{D-39}$$

With the inverse tangent approximation, the partial derivatives of the final crush, δ^{fi} and δ^{fj}, are obtained as numerical solutions of variational equations. For any parameter λ, from Eqn. (B-76),

$$\begin{aligned} &\frac{d}{dt}\frac{\partial c}{\partial \lambda} = \frac{\partial \dot{c}}{\partial \lambda} \quad , \quad \frac{\partial c}{\partial \lambda}(0) = 0 \\ &\frac{d}{dt}\frac{\partial \dot{c}}{\partial \lambda} = \frac{\partial \ddot{c}}{\partial \lambda} = -\frac{1}{\mu}\left[\frac{\partial F_A}{\partial \lambda} + \frac{\partial F_A}{\partial \delta_A}\frac{\partial \delta_A}{\partial \lambda}\right] \quad , \frac{\partial \dot{c}}{\partial \lambda}(0) = 0 \end{aligned} \tag{D-40}$$

The $[\partial \delta_A / \partial \lambda]$ in Eqn. (D-40) is eliminated in favor of $[\partial c / \partial \lambda]$ by differentiating Eqn. (B-77):

$$\frac{\partial \delta_A}{\partial \lambda} = \left[\frac{\partial F_A}{\partial \delta_A} + \frac{\partial F_B}{\partial (c - \delta_A)}\right]^{-1} \left[-\frac{\partial F_A}{\partial \lambda} + \frac{\partial F_B}{\partial \lambda} + \frac{\partial F_B}{\partial (c - \delta_A)}\frac{\partial c}{\partial \lambda}\right] \tag{D-41}$$

Equations (D-40) are integrated, with $\lambda = f_A$, f_B, k_A and k_B to the final time defined by Eqn. (B-79). Then

$$\frac{\partial \delta_A^f}{\partial \lambda} \tag{D-42}$$

is computed from Eqn. (D-41), and since

$$\delta_B^f = c^f - \delta_A^f \quad , \tag{D-43}$$

$$\frac{\partial \delta_B^f}{\partial \lambda} = \frac{\partial c^f}{\partial \lambda} - \frac{\partial \delta_A^f}{\partial \lambda} \tag{D-44}$$

APPENDIX E

VEHICLE MIX STATISTICS

The Figure of Merit can be very generally defined as

$$C_T = N_c \sum_{i=1}^{I} \sum_{j=1}^{I} \sum_{m=1}^{M} \sum_{n=1}^{M} \sum_{i_{vc}=1}^{I_{vc}} p(i,m,j,n,i_{vc}|col)[C^{i}_{im/jn/V_{ci}} + C^{j}_{im/jn/V_{ci}}] + N_v \sum_{i=1}^{I} p(i) C_{E/i} \qquad \text{(E-1)}$$

The indices (i,j) refer to vehicle weight/size classes; indices (m,n) refer to collision modes; and the index i_{vc} refers to the collision speed interval. The speed V_{ci} in interval i_{vc} is given by

$$V_{ci} = (i_{vc}-1)\Delta V_c + \Delta V_c/2 \qquad \text{(E-2)}$$

where ΔV_c is the length of a speed interval. N_c is the number of (two-vehicle) collisions and N_v is the total number of vehicles. In the Figure of Merit, the probability (mass) function $p(i,m,j,n,i_{vc}|col)$ is the probability, conditioned on collision (col), that a weight/size class i vehicle in collision mode m collides with a weight/size class j vehicle which is in collision mode n, at collision speed V_{ci}. The probability function is conditioned on collision; that is, it refers to the sub-population of vehicles which are involved in collisions. The cost $C^{i(j)}_{im/jn/V_{ci}}$ is the cost, associated with vehicle i(j), of the collision just described [see Appendices C, F and G]. The second term in Eqn. (E-1) is the total cost of engineering modifications; p(i) is the (unconditional) *traffic distribution* of vehicles by weight/size class i, and $C_{E/i}$ is the cost of engineering modifications to a weight/size class i vehicle [see Appendix H].

It is seen that the Figure of Merit is the total societal cost of two-vehicle collisions, including the cost of engineering modifications (designed to relieve other costs). This appendix describes the statistics of the problem; that is, the two probability functions appearing in Eqn. (E-1).

APPROXIMATIONS OF THE COLLISION PROBABILITY FUNCTION

The collision probability function $p(i,m,j,n,i_{vc}|col)$ may be rewritten to put it in a form more compatible with the kind of collision statistics which are available. Using standard rules of conditional probabilities [Ref. 1],

$$\begin{aligned} & p(i,m,j,n,i_{vc}|col) \\ & \quad = p(m,n,i_{vc}|i,j,col)p(i,j|col) \\ & \quad = p(i_{vc}|m,n,i,j,col)p(m,n|i,j,col)p(i,j|col) \\ & \quad = p(i_{vc}|m,n,i,j,col)p(m,n|i,j,col)p(i|j,col)p(j|col) \end{aligned} \tag{E-3}$$

The first probability function in Eqn. (E-3), $p(i_{vc}|m,n,i,j,col)$, is the *collision speed distribution*. In general, the collision speed distribution depends on the collision modes (m,n) and weight/size classes (i,j). $p(m,n|i,j,col)$ is the *collision modes distribution*, and in general depends on the weight/size classes (i,j). $p(i|j,col)$ is the *conditional weight/size class distribution* of collisions (given the weight/size class (j) of the other vehicle), and $p(j|col)$ is the *weight/size class distribution* of collisions.

The limited published statistics [e.g. Refs. 2-4] indicate that the theoretical dependence of collision speeds on vehicle weight/size classes (as well as on collision modes) is a real one, and even a significant one; as is the dependence of collision modes on vehicle weight/size classes, and the dependence of the weight/size class distribution on the weight/size class of the other vehicle [$p(i|j,col)$ dependence on j]. While these dependencies exist in the accident data files, the relevant statistics apparently have not been extracted. Therefore, of necessity, the following approximations are made:

$$p(i_{vc}|m,n,i,j,col) \approx p(i_{vc}|m,n,col) \tag{E-4}$$

$$p(m,n|i,j,col) \approx p(m,n|col) \tag{E-5}$$

$$p(i|j,col) \approx p(i|col) \tag{E-6}$$

so that the collision probability function is approximated as

$$p(i,m,j,n,i_{vc}|col) \approx p(i_{vc}|m,n,col)p(m,n|col)p(i|col)p(j|col) \tag{E-7}$$

and this approximation is utilized in the working definition of the Figure of Merit [Eqn. (C-1), Appendix C].

COLLISION SPEED DISTRIBUTION

The only source of statistics on vehicle collision speeds appears to be Ref. 2, which gives these statistics for the CPIR3 data file. Vehicle speed distributions from Ref. 2 are reproduced in Figures E1-E6. It is noted that these are distributions of vehicle speeds, *not* of collision speeds (closing speeds). The distributions of collision speeds for the various collision modes are computed from the vehicle speed statistics.

Consider head-on collisions [(m,n) = (1,1)]. The collision speed is the sum of the individual vehicle speeds, and as is well known [Ref. 1], for continuous distributions has the distribution (probability density function)

$$f_s(x) = \int_{S_1} f_1(t)f_2(x-t)dt \tag{E-8}$$

where f_1, f_2 are the individual vehicle speed distributions, and S_1 is the sample space for the first random variable (with distribution f_1). In the present instance, however, the distributions are discrete (Figure E1), and considerable modification of Eqn. (E-8) is required.

Let q_0 be the fraction of struck cars which are standing still. Let q_i, i=1, 10, be the fraction of struck cars which have speed in the interval (10i-10,10i), where the speed is measured in mph. Clearly,

$$\sum_{i=0}^{10} q_i = 1 \tag{E-9}$$

A similar distribution is defined for the striking car, with notation p_i, where of course $p_0 = 0$. Then the probability of the collision speed interval

FIGURES E1-E6

Vehicle Speed Distributions

FIGURE E1

Head-Ons, All Vehicles

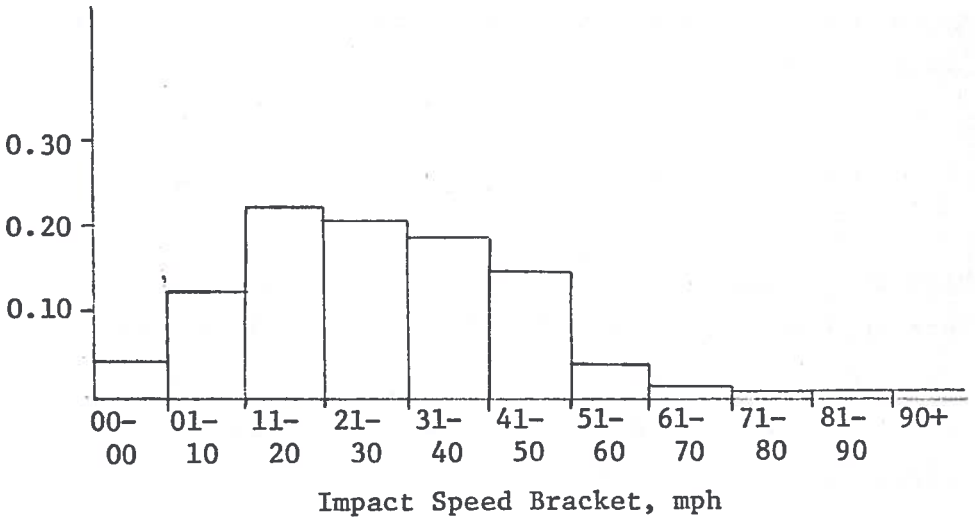

FIGURE E2

Sideswipes, All Vehicles

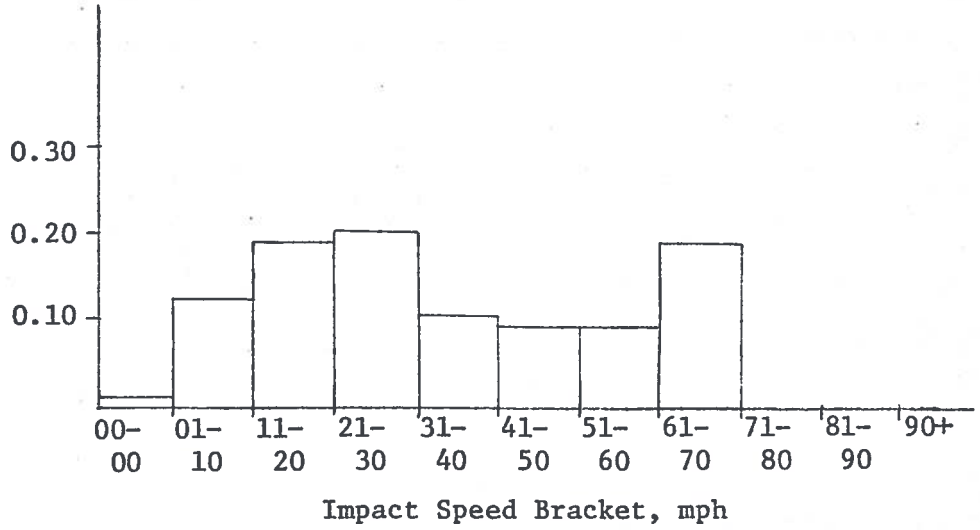

FIGURE E3

"L" OR "T" INTERSECTION COLLISIONS

Vehicle Striking with Front

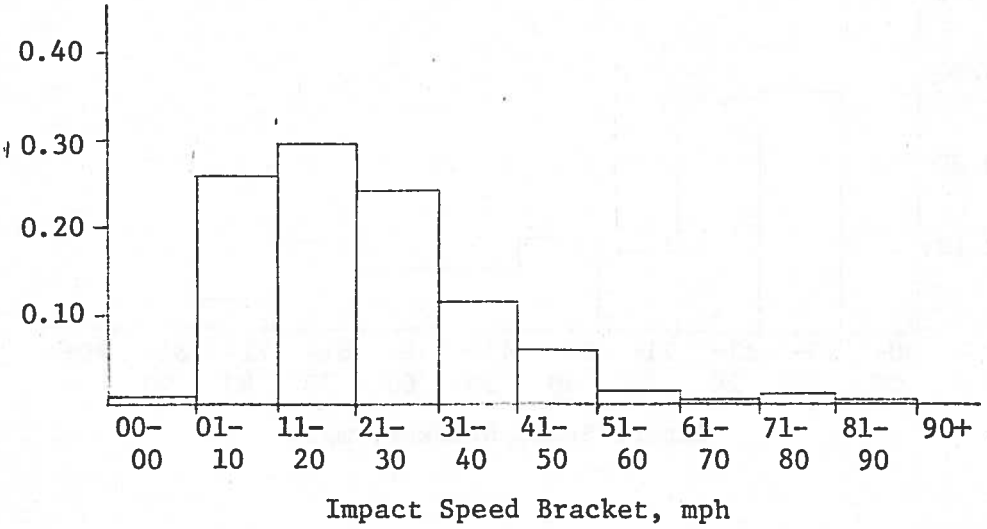

FIGURE E4

"L" OR "T" INTERSECTION COLLISIONS

Vehicle Struck in Side

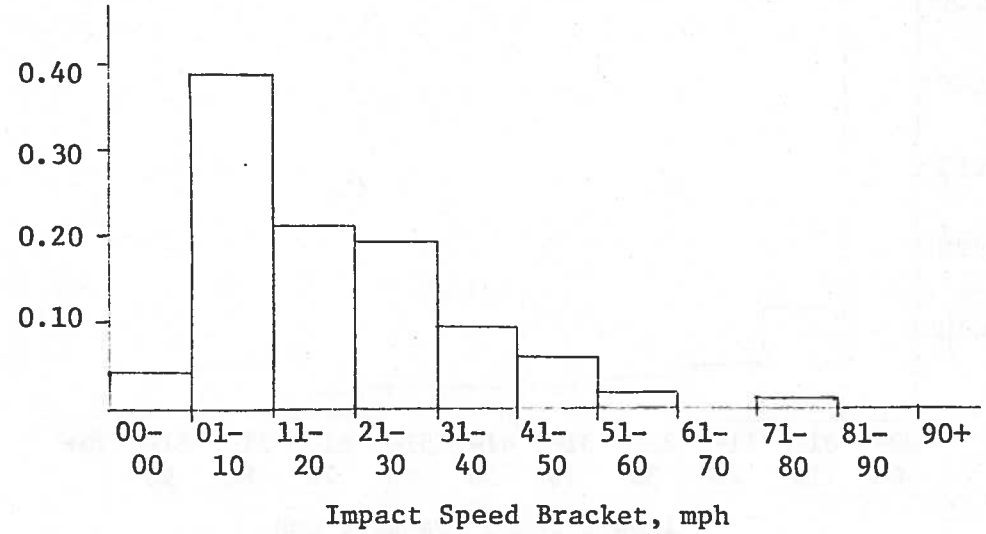

FIGURE E5

REAR-ENDS, Vehicle Striking with Front

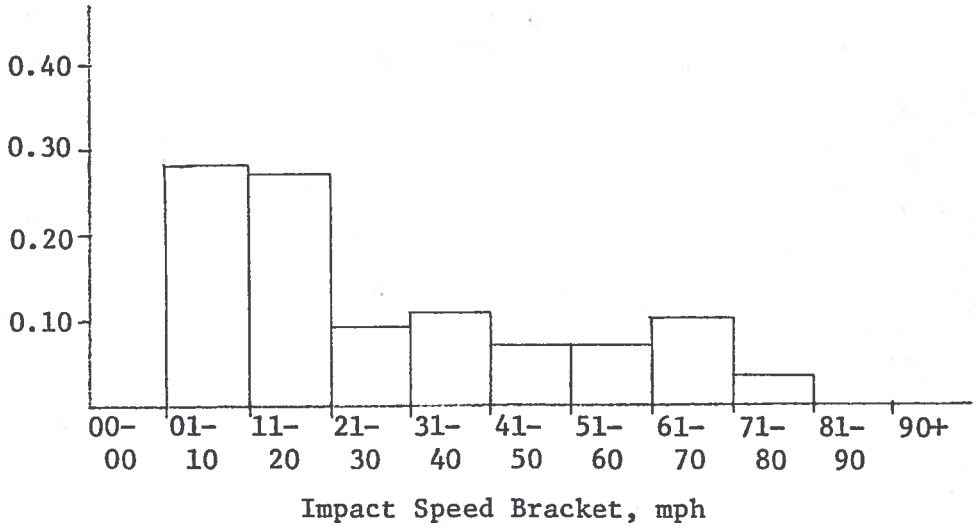

FIGURE E6

REAR-ENDS, Vehicle Struck in Rear

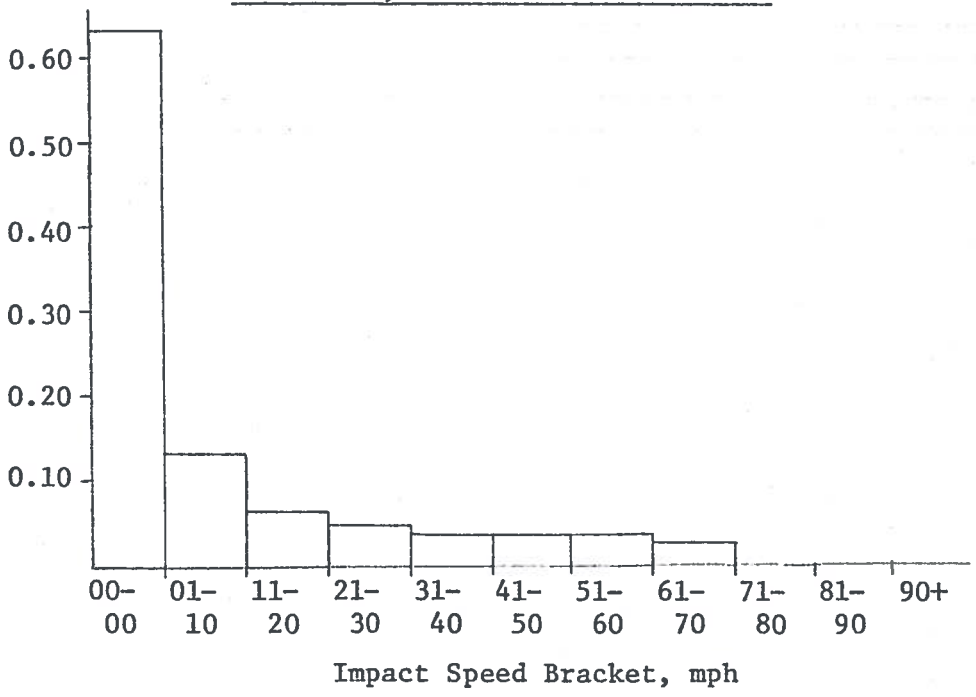

[10m-20,10m] for head-on collisions is

$$\Pr[10m-20,10m] = \sum_{i=1}^{m-1} q_i p_{m-i} \tag{E-10}$$

which is the discrete analog of Eqn. (E-8). Thus

$$\Pr[20,40] = q_1 p_3 + q_2 p_2 + q_3 p_1 \tag{E-11}$$

However, the probability of the interval [10m-10, 10m+10] is

$$\Pr[10m-10,10m+10] = \sum_{i=1}^{m} q_i p_{m+1-i} \tag{E-12}$$

and the probability of the interval [10m-10,10m] is

$$\Pr[10m-10,10m] = q_0 p_m \tag{E-13}$$

In the present case, probabilities of collision speeds for head-on collisions in intervals [10m-10,10m] are required. To compute these probabilities, all three of the intervals [Eqs. (E-10), (E-12) and (E-13)] must be considered. For simplicity, the assumption is made that in the intervals [10m-20,10m] the speeds are uniformly distributed. Then

$$\begin{aligned} &\Pr[10m-10 \leq V_c < 10m] \\ &= q_0 p_m + \tfrac{1}{2} \sum_{i=1}^{m-1} q_i p_{m-i} + \tfrac{1}{2} \sum_{i=1}^{m} q_i p_{m+1-i} \end{aligned} \tag{E-14}$$

This assumption of uniformity in the intervals tends to "smear" the probability in cases where adjacent intervals have different probabilities. However, a more detailed analysis using 5 mph intervals justifies this assumption.

Using the probabilities p_i, q_i from Figure E1, and Eqn. (E-14), the collision speed distribution for head-ons [(m,n) = (1,1)] was generated and is given in Table E1. The bracket [90, ∞] in Figure E1 was replaced by [90,100].

For intersection collisions [(m,n) = (1,2)], it is assumed that all the

TABLE E1

Collision Speed Distributions*

i_{vc}	$p(i_{vc}\|1,1,col)$	$p(i_{vc}\|1,2,col)$	$p(i_{vc}\|1,3,col)$	$p(i_{vc}\|2,2,col)$	$p(i_{vc}\|2,3,col)$	$p(i_{vc}\|3,3,col)$
1	0.019	0.261	0.034	0.666	1.000	1.000
2	0.056	0.291	0.355	0.226	0.0	0.0
3	0.098	0.242	0.098	0.092	0.0	0.0
4	0.136	0.115	0.155	0.016	0.0	0.0
5	0.162	0.060	0.104	0.0	0.0	0.0
6	0.159	0.012	0.100	0.0	0.0	0.0
7	0.135	0.005	0.112	0.0	0.0	0.0
8	0.098	0.007	0.042	0.0	0.0	0.0
9	0.063	0.007	0.0	0.0	0.0	0.0
10	0.036	0.0	0.0	0.0	0.0	0.0
11	0.018	0.0	0.0	0.0	0.0	0.0
12	0.010	0.0	0.0	0.0	0.0	0.0
13	0.006	0.0	0.0	0.0	0.0	0.0
14	0.003	0.0	0.0	0.0	0.0	0.0
15	0.001	0.0	0.0	0.0	0.0	0.0

*$p(i_{vc}|m,n,col) = p(i_{vc}|n,m,col)$

ΔV_c = 10 mph, so that [see Eqn. (E-2)] i_{vc} = 1 represents the speed range 0-10 mph with average speed V_{c1} = 5 mph, and so on.

closing (collision) speed is contributed by the striking vehicle. Thus

$$\Pr[10m-10 \leq V_c < 10m] = p_m \tag{E-15}$$

where the p_i are obtained from Figure E3. The results are given in Table E1.

Rear-end collisions [(m,n) = (1,3)] are similar to head-ons, except that the collision speed is the difference in speeds between the striking and struck vehicles. For continuous random variables, the density function for the difference is

$$f_d(x) = \int_{S_1} f_1(t) f_2(x+t)\,dt \tag{E-16}$$

[compare with Eqn. (E-8)]. Corresponding to this, the discrete probabilities are

$$\Pr[10m-20,10m] = \sum_{i=1}^{11-m} q_i p_{i+m-1} \tag{E-17}$$

In the same way as for head-ons, then,

$$\begin{aligned} &\Pr[10m-10 \leq V_c < 10m] \\ &= q_0 p_m + \tfrac{1}{2} \sum_{i=1}^{11-m} q_i p_{m+i-1} + \tfrac{1}{2} \sum_{i=1}^{10-m} q_i p_{m+i} \end{aligned} \tag{E-18}$$

Using probabilities p_i from Figure E5, and q_i from Figure E6, and Eqn. (E-18), the collision speed distribution for rear-ends [(m,n) = (1,3)] was computed and is given in Table E1.

The appropriate data does not exist to completely define the collision speed distribution for sideswipes [(m,n) = (2,2)], and approximating assumptions must be made. First, it is assumed that the speed of the struck vehicle is irrelevant. Second, it is assumed that the striking vehicle contributes the entire closing speed by projecting its own velocity through an angle θ onto the struck vehicle. The sine of the angle θ is assumed to be uniformly distributed in [0,0.5], so that

$$\Pr\left[\frac{i-1}{10} \leq \sin\theta < \frac{i}{10}\right] = 0.2, \quad i = 1,5 \qquad \text{(E-19)}$$

Given these assumptions, as well as the usual one that speeds are uniformly distributed in each interval, and given the p_i from Figure E2,

$$\Pr[20 \leq V_c < 30] = 0.2\left[\frac{5}{9}\, p_5 + p_6 + \frac{4}{9}\, p_6 + \frac{6}{11}\, p_7 + \frac{8}{10}\, p_7 + \frac{1}{9}\, p_7\right] \qquad \text{(E-20)}$$

and so on, applying standard rules of interval arithmetic. [A vehicle going [50,60] mph and striking at an angle whose sine falls in [0.3,0.4] has a closing speed in the interval [15,24] mph, and 4/9 of these cases are allotted to the interval [20,30].] The results are given in Table E1.

The collision modes (2,3) and (3,3), side-rear and rear-rear, respectively, are essentially low-speed, parking lot "fender benders", and all the probability mass is assumed concentrated in the lowest speed interval [0,10] (see Table E1).

COLLISION MODES DISTRIBUTION

The collision modes distribution, $p(m,n|\text{col})$, is available from several data files [Refs. 2 and 3]. Very significant discrepencies however exist between the available statistics. For example, the marginal probability

$$p(\text{front}|\text{col}) = \sum_{n=1}^{M} p(\text{front},n|\text{col}) = \begin{cases} 0.58 \text{ [Ref. 2, Table 7]} \\ 0.54 \text{ [Ref. 2, Table 8]} \\ 0.35 \text{ [Ref. 3, Table 4]} \end{cases} \qquad \text{(E-21)}$$

This is the "total involvement" of the front end in two-vehicle collisions.

The collision modes distribution from Table 7 of Ref. 2 (CPIR3 data, 835 two-vehicle collisions) is presented in Table E2.

TABLE E2

Collision Modes Distribution*

	Front	Side	Rear
Front	0.205	0.278	0.0945
Side	---	0.038	0.005
Rear	---	---	0.002

*$p(m,n|col) = p(n,m|col)$

WEIGHT/SIZE CLASS DISTRIBUTION OF COLLISIONS AND TRAFFIC

Surprisingly, these statistics are apparently not readily available because of inconsistent classifications of vehicles by weight/size class [Refs. 4-7]. Table E3 contains these statistics extracted from Ref. 4 (Washtenaw County, Michigan, 1972). However, these data are very approximate as they are extracted from graphs and charts. In fact, these data seem to contradict the authors' conclusion that small car involvement in accidents is greater than their share of the traffic mix.

TABLE E3

Weight/Size Class Distributions

i	1 Sub Compact	2 Compact	3 Intermediate	4 Full Size
Weight* Range	$W \leq 2700$	$2700 < W \leq 3400$	$3400 < W \leq 4100$	$W > 4100$
Representative Weight* W_i	2300	3100	3800	4300
p(i)	0.260	0.306	0.320	0.114
$p(i|col)$	0.208	0.354	0.359	0.079

*Weight in lbs.

DISTRIBUTION OF OCCUPANTS

The Injury/Mortality cost model (Appendix F) requires data on the average number of occupants by vehicle weight/size class i. These data, extracted from Ref. 4 (Washtenaw County, Michigan), are tabulated below.

TABLE E4

Distribution of Occupants

i	1	2	3	4
O(i)	1.58	1.60	1.64	1.67

*See Table E3 for corresponding vehicle weights.

REFERENCES

1. A. H. Jazwinski, Stochastic Processes and Filtering Theory, Academic Press, Inc., New York, 1970.
2. "A Characterization of Collisions, Resulting Damage and Occupant Injury," NHTSA Staff Report, Prepared by the Research Institute, Office of Accident Investigation and Data Analysis, August 1972.
3. W. W. Sorenson, R. E. Gardner and J. Casassa, II (State Farm Mutual Automobile Insurance Co.), "Patterns of Automobile Crash Damage," SAE Paper No. 740065, 1974.
4. J. O'Day, D. H. Golomb and P. Cooley, "A Statistical Description of Large and Small Car Involvement in Accidents," The University of Michigan, Highway Safety Research Institute, HIT Lab Report, Vol. 3, No. 9, May 1973.
5. "Two Car Collision Study" State of New York, Department of Motor Vehicles, Report No. DOT HS-800977, November 1973.
6. H. W. Case, A. Bury and J. D. Baird, "Accident Frequency as Related to Vehicle Size," UCLA Institute of Transportation and Traffic Engineering, Report No. UCLA-ENG-7261, August 1972.
7. "Major Specifications for '74 U.S. Makes," Automotive News (1974 Almanac Issue), April 1974.

APPENDIX F

COSTS OF INJURY/MORTALITY

The specification of the cost of injury/mortality in an automobile collision is a very difficult problem. It involves two relationships: (a) the relation between societal costs and level or index of injury/mortality; and (b) the relation between that level or index and the collision dynamics (acceleration, impulse, etc.). In the present work, a severity index (SI), similar to the Calspan index, is adopted for (b). The relation for (a) is based on work at NHTSA and relations between injury severity and costs of disability (lost time). This appendix presents a general discussion of injury/mortality costs and then summarizes the model adopted for the present work.

GENERAL DISCUSSION

There is need for versatile indices which measure the degree of injury likely to result from impulses applied in the testing of automotive structures. The diverse ways in which bodily injuries can occur make it unlikely that a single rigorously quantitative index can exist. However, relatively simple measures have been developed to approximate a force/injury severity relationship. Groups at Holloman Air Force Base and Wayne State University have accumulated data on animals and human volunteers. Since head injuries are the most frequently serious, the first severity models have dealt with head injury data and consequent internal stress.

It has been impractical to obtain force readings which are directly associated with the injury. As a result, the overall head acceleration, an indirect measure, has come into use. While acceleration does not consistently represent the diversity of kinematics and injury mechanisms involved, it does provide a basis for judging head impact severity from an internal injury standpoint. Once a pulse depicting a blow has been given, its severity should be assessed from the standpoint of waveform or profile. Area under the g-time pulse has been suggested as a simple way of recognizing that injury hazard generally increases with increasing time of exposure to a loading upon the body. A weighting factor can be employed to fit the biomechanics data pertinent to injury.

A simple weighting factor is one which exponentially weights the intensity scale. This takes into account time dependency of damage, as follows. First, one can visualize a hypothetical completely brittle material which fails suddenly if the loading exceeds a certain level. At the other extreme would be a completely viscous material for which percentage increments of load intensity would be just as damaging as corresponding increments of time duration of loading, with failure defined as some excessive degree of shear strain. Examination of the biomechanics literature indicates that animal tissues fall somewhere between these two extremes in their failure properties.

A systematic study of the role of load duration in animal impact injury was made by Wayne State University [Ref. 1]. Impact sled tests were also made [Ref. 2], studying human tolerance to impact. A Wayne State University "Tolerance Curve" was suggested as in Figure F1. The ordinate is the deceleration level (or average deceleration level) and the abscissa displays the pulse time. It should be clear that the higher the deceleration level the shorter the pulse length, and vice versa.

If it is assumed that the area under the force-time curve is constant (i.e. impulse) for injury initiation, this would suggest that the product of deceleration level times time is a constant; that is,

$$a\,t = \text{constant} \qquad \text{(F-1)}$$

This equation has been superposed as a dashed line on Figure F1. The constant is selected so that the curve passes through the suggested tolerance curve at the point noted.

The critical question in the selection of an approximate criterion or tolerance curve for unrestrained occupants is as follows: when the head impacts an object, be it the windshield, instrument panel, door post, or whatever; what impulse level could be tolerated without permanent brain damage or skull fracture? The "second collision" has been characterized as the one in which the occupant strikes the interior of the car, but in fact the critical collision might be termed the "third collision" in which the brain tissue sitting in the skull cavity sloshes to a halt. It is noted that these considerations are

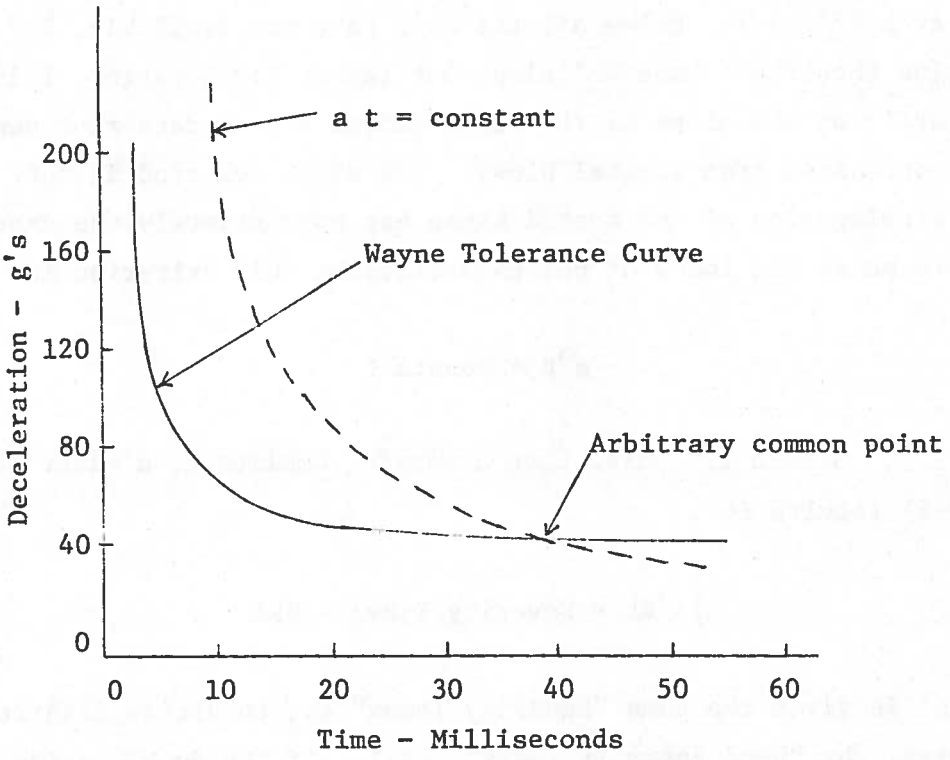

FIGURE F1

Comparison of Wayne Tolerance Curve
with Constant Pulse Area Criterion

probably not relevant to restrained occupants.

A mathematical model to describe the possibility of incipient head injury has been presented in Ref. 3. If the deceleration-time pulse were the only determining factor and the impulse associated with the injury level were approximately constant, then Eqn. (F-1) would be valid and could be plotted on a log-log curve as a 45° line. Using all the data that was available, Ref. 3 found that the line should not have 45° slope but rather 1:2.5 ratio. This was based primarily on the slope of the Wayne animal impact data representing dangerous concussion from frontal blows. The slope selected in Ref. 2 for spineward acceleration of the seated human has approximately the same value. For a square pulse the locus of points satisfying this criterion is

$$a^{\alpha}t = \text{constant} \tag{F-2}$$

where $\alpha = 2.5$. Should the pulse have a varying amplitude, a minor modification of Eqn. (F-2) results in

$$\int a^{\alpha} dt = \text{Severity Index} = \text{HSI} \tag{F-3}$$

The constant is given the name "Severity Index" or, to distinguish it from other indexes, the "Head Severity Index" (HSI). If the deceleration is given in g's, then this impulse criterion is set up in such a way that a value of approximately 1000 units is the borderline between fatal and nonfatal impacts.

In a Calspan study on injury severity in railway collisions [Ref. 4], the HSI has been modified to include a variety of injuries. For example, chest injury criteria are presented in terms of acceleration along all three axes,

$$C_R = (C_X^2 + C_Y^2 + C_Z^2)^{\frac{1}{2}} \tag{F-4}$$

and a "Chest Severity Index" CSI, is defined as

$$\text{CSI} = \int C_R^{2.5} dt \tag{F-5}$$

The Calspan study takes the train structural properties and occupant loading situation as inputs to obtain the relative impact velocity of the passenger.

The impact velocity is then used to define a deceleration time history of the occupant. From this a severity index is assigned based on a compilation of the HSI, CSI, and other injury criteria. This severity index is defined as

$$SI = \int a_0^{2.5}(t)dt \qquad \text{(F-6)}$$

where $a_0(t)$ is the occupant deceleration.

The Calspan Severity Index (SI) has been applied to the American Medical Association's Abbreviated Injury Scale (AIS), as shown in Table F1. Note that the AIS is based on previously normal life expectancy of the victim, and on assessment of his injuries *within 48 hours of the accident.* In use, the injury encountered in each body area is assigned to one of nine injury-severity categories that have been established on the bases of the energy absorbed by the victim and the threat to his life. Then the most severe (highest-numbered) injury in any body area is used as the overall degree of injury for the victim. An injury is not classified as fatal unless the victim dies within 24 hours following the accident. In effect, the progressive stages of injury in the scale are assigned severity indexes of 250 to over 2,000. This was done through consideration of the head and chest injuries described under each injury category, and evaluation of those injuries in terms of the index numbers and injury data upon which the indexes were formulated.

To assess societal costs of motor vehicle injuries it is necessary to have severity measurements based not only on the nature of the injury but on some notion of the permanence of the injury. Estimation of medical costs is dependent not only on the initial expenditures, but on the continuing expenditures over the remaining lifetime. Some estimate of the permanence of an injury is vital to the measurement of wage losses.

In the comprehensive report [Ref. 5], NHTSA presents a broad study of societal costs of motor vehicle accidents, which considers a very complete spectrum of accident cost components. Injury severity is approached from a *long-term view,* in these categories:

No injury (property damage only)
No permanent disability
Partial disability

TABLE F1

Relation Between Calspan Severity Index and the AIS

AIS	Injury Severity Category	SI
0	No Injury	< 250
1	Minor Injuries	250 to 500
2	Moderate Injuries	500 to 1000
3	Severe Injuries (Non Life-Threatening)	1000 to 1500
4	Serious Injuries (Life-Threatening, Survival Probable)	1500 to 2000
5	Critical (Survival Uncertain)	over 2000
6	Fatal (Within 24 Hours)	over 2000
7	Fatal (Within 24 Hours)	over 2000
8	Fatal	over 2000
9	Fatal	over 2000

Permanent and total disability

Fatality

Contrast the above list with the AIS 48-hour perspective:

No injury

Minor

Moderate

Severe (not life-threatening)

Serious (life-threatening, survival probable)

Critical (survival uncertain)

Fatal

Note that a victim suffering a major bodily airway obstruction would be considered "Critical" on the AIS. Yet if the victim survives with his earning power intact, the NHTSA study would treat the injury as a relatively minor encounter ("No permanent disability"). Some of the NHTSA results are presented in Table F2.

As a totally different approach to the costs of mortality, it is interesting to cite results based on Ref. 6, which takes a gross economic approach to these costs - the gross discounted average output method. If d is the average life expectancy of an individual, GNP the gross national product, E the total employed population, and r the discount rate (to compensate for present value of future earnings), then the average gross present value of an individual is (approximately) given by

$$G = \sum_{n=1}^{d} GNP/E(1+r)^n \qquad (F-7)$$

With GNP = $\$1.42 \times 10^{12}$, E = 8.6×10^{7}, r = 0.07, and d = 30, we get G = \$204,765. Compare this with the NHTSA result of \$200,700. (Table F2).

It remains to relate the Calspan Severity Index (SI) to dollar costs. This requires identifying the (tenuous) connection between short- and long-term dispositions of injury severity. Ref. 7 relates costs of injury to the AIS by considering the results of the NHTSA study [Ref. 5] and the railroad industry's records of work time lost as a function of injuries. These results are reproduced in Figure F2, and suggest a cubic relationship with a discontinuity (drop) at AIS = 6 (fatality). Combining this relationship with the relation between the AIS and the SI (Table F1), results in Figure F3.

TABLE F2

Average Costs of Motor Vehicle Accidents (NHTSA), 1971

Accident Type	Persons	
	Number	Ave. Cost/Person
Fatality	55,000	$200,700.
Permanent and total disability	8,000	260,300.
Partial disability	250,000	67,100.
No permanent disability	3,545,000	2,465.
Property damage only	----	----
Total	3,858,000	----
Average	----	10,000.

*Total may not add due to rounding.

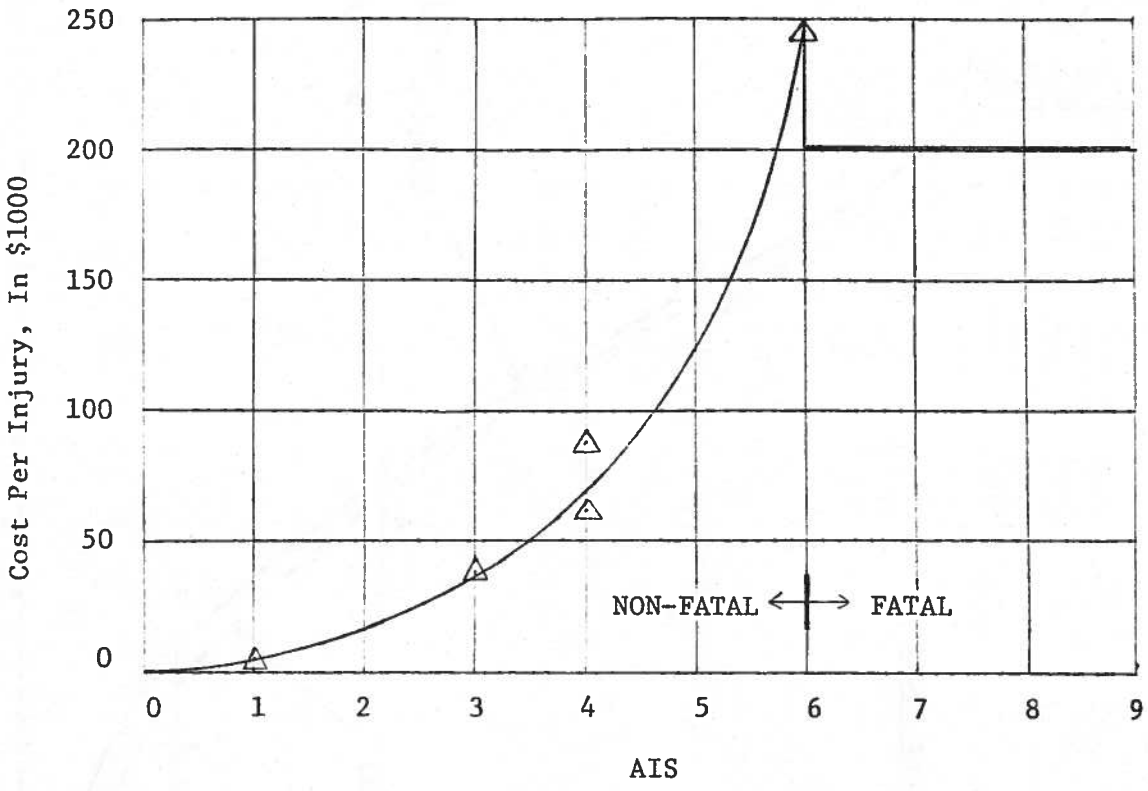

FIGURE F2

Cost of Injury by the AIS

FIGURE F3

Injury/Mortality Cost Model

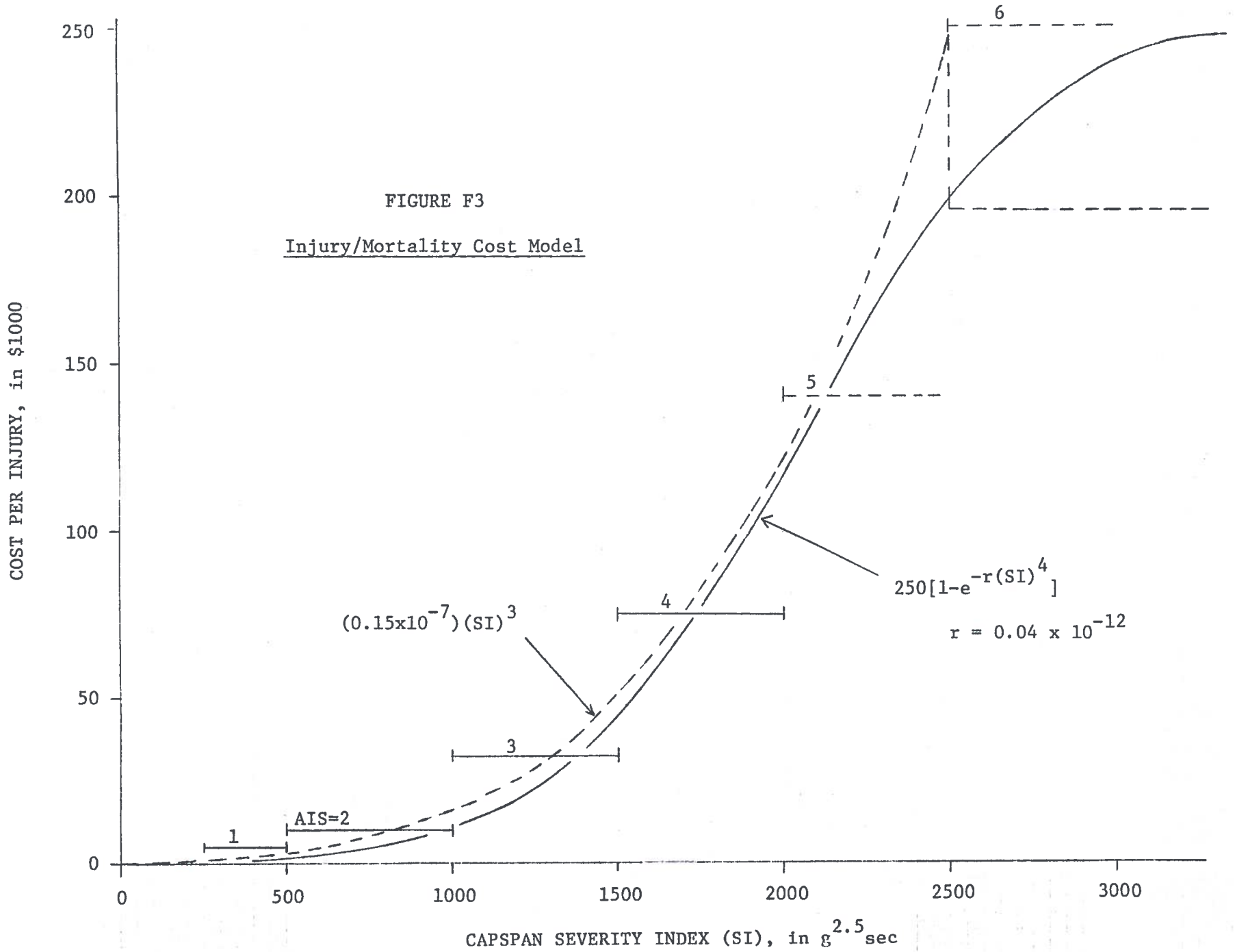

The suggested cubic cost-SI relation is plotted in Figure F3. Also plotted is the exponential relationship

$$C(\$K) = 250[1-e^{-r(SI)^4}] \ , \quad r = 0.04 \times 10^{-12} \qquad \text{(F-8)}$$

Because of the inherant uncertainties, and for convenience, the relationship in Eqn. (F-8) is adopted for the present work.

INJURY/MORTALITY COST MODEL

On the basis of the foregoing discussion, the injury/mortality cost model of Appendix C [Eqs. (C-8) - (C-9)] is adopted. The cost associated with vehicle i is

$$C^{i}_{IM/im/jn/V_{ci}} = w_{IM}(i)O(i)c_{IM}[1-\exp(-r_{IM}(SI_i)^4)] \qquad \text{(F-9)}$$

where the Severity Index (SI_i) is

$$SI_i = \int_0^{t_f} a^{\alpha}_{(t)_{Oi/im/jn/V_{ci}}} dt \qquad \text{(F-10)}$$

Here $w_{IM}(i)$ is an arbitrary weighting constant depending on the vehicle weight/size class i; O(i) is the average number of occupants in a weight/size class i vehicle; c_{IM} and r_{IM} are constants; t_f is the collision time interval; and $a_{(t)_{Oi/im/jn/V_{ci}}}$ is the acceleration magnitude of the occupant of vehicle i. Note that SI must be put in the units $g^{\alpha}\times sec$.

REFERENCES

1. H. R. Lissner, et al, "Experimental Studies on the Relationship Between Acceleration and Intracranial Pressure Changes in Man," Surgery, Gynecology and Obstetrics, September 1960.

2. A. Eiband, "Human Tolerance to Rapidly Applied Accelerations: A Survey of the Literature," NASA Memorandum 5-19-59 E, June 1959.

3. C. W. Gadd, "Use of a Weighted Impulse Criterion for Estimating Injury Hazard," Proceedings of the 10th Stapp Car Crash Conference, 1966.

4. H. Weinstock, Private Communication.

5. ···, "Societal Costs of Motor Vehicle Accidents," U. S. Department of Transportation, NHTSA, Preliminary Report, April 1972.

6. V. F. Babkov, "Temporary Manual for the Consideration of Losses to the People's Economy from Road Accidents," Ministry of Road Construction, Moscow, 1970.

7. R. Petersen and D. Friedman, "Interim Report on Accident Analysis," Minicars, Inc., HS-113-3-746.

BIBLIOGRAPHY

V. F. Babkov, "Temporary Manual for the Consideration of Losses to the People's Economy from Road Accidents," Ministry of Road Construction, Moscow, 1970.

··· "Biomechanics and its Application to Automotive Design," SAE Publication P-49, New York, January 1973.

D. Burke, "Accident Costs: Some Estimates for Use in Engineering-Economy Studies," Highway Research Record, 1973.

A. K. Clarke, "The Cost to the Community of Automobile Accidents," SAE-Australasia, 1969.

R. F. F. Dawson, "Cost of Road Accidents in Great Britain," Ministry of Transport, England, 1967.

R. F. F. Dawson, "Current Costs of Road Accidents in Great Britain," Department of the Environment, England, 1971.

··· "Economic Consequences of Automobile Accident Injuries," U.S. Department of Transportation, Automobile Insurance and Compensation Study, 1970.

A. Eiband, "Human Tolerance to Rapidly Applied Accelerations: A Summary of the Literature," NASA Memorandum 5-19-59 E, June 1959.

··· "Estimating the Costs of Accidents," National Safety Council, Chicago, 1970.

C. W. Gadd, "Use of a Weighted Impulse Criterion for Estimating Injury Hazard," Proceedings of the 10th Stapp Car Crash Conference, 1966.

P. B. Goodwin, "On the Evaluation of Human Life in Accident Studies," University College, London, 1973.

··· "Human Tolerance to Impact Conditions as Related to Motor Vehicle Design," SAE Handbook Supplement J885, 1964.

··· ["Injury Severity in Railway Collisions"?] Partial xerox copy of report, Calspan Corporation, Buffalo, New York.

H. R. Lissner, et al, "Experimental Studies on the Relationship Between Acceleration and Intracranial Pressure Changes in Man," Surgery, Gynecology and Obstetrics, September 1960.

H. R. Lissner and E. S. Gurdjian, "Experimental Cerebral Concussion," ASME Paper No. 60-WA-273, November 1960.

A. D. Little, "Cost-Effectiveness in Traffic Safety," Washington, D.C., 1968.

E. J. Mishan, "Evaluation of Life and Limb: A Theoretical Approach," Journal of Political Economy, 1971.

Nicholas Perrone, "Biomechanical Problems Related to Vehicle Impact," Paper presented at Symposium on the Foundations and Objectives of Biomechanics, University of California, San Diego, July 1970.

D. J. Reynolds, "The Cost of Road Accidents," Journal of the Royal Statistical Society, 1956.

G. Anthony Ryan and John W. Garrett, "A Quantitative Scale of Impact Injury," Report VJ-1823-R34, Calspan Corporation, Buffalo, New York, October 1968.

... "Societal Costs of Motor Vehicle Accidents," NHTSA, Washington, D.C., 1972.

John D. States, "The Abbreviated and the Comprehensive Research Injury Scales," Proceedings of the 13th Stapp Car Crash Conference, SAE. New York, 1969.

R. Winfrey, "Economic Analysis for Highways," Pennsylvania, 1969.

APPENDIX G
REPAIR COSTS

Two repair cost models are given in Appendix C [Eqs. (C-25) and (C-26)]. The first model [Eqn. (C-25)] measures repair costs as a function of crush deformation; $\delta^{fi}_{im/jn/V_{ci}}$ of vehicle i, and $\delta^{fj}_{im/jn/V_{ci}}$ of vehicle j. No attempt is made in this model to accurately represent repair costs of minor accidents (fender benders). To attempt to do so would be inconsistent with the gross model chosen for vehicle force-crush characteristics and the collision model itself, and would require extensive and detailed modeling of vehicle structures (bumpers, etc.). Rather, the model gives a reasonable relationship (exponential) between crush deformation and repair cost, up to a maximum repair cost which is the depreciated value of the vehicle. The vehicle i component of this model [from Eqn. (C-25)] is

$$C^{i}_{R/im/jn/V_{ci}} = w_R(i)C_{VD}(i)[1-\exp(-d\delta^{fi}_{im/jn/V_{ci}}/\bar{\delta}_{im})] \qquad (G\text{-}1)$$

Here $w_R(i)$ is an arbitrary weighting constant; $C_{VD}(i)$ is the depreciated value of a weight/size class i vehicle,

$$C_{VD}(i) = (1-r_d)^a C_V(i) \qquad (G\text{-}2)$$

where r_d is the depreciation rate, a the average age of the traffic mix, and $C_V(i)$ the new class i vehicle cost (see Appendix H); d is a constant; δ^{fi} is the (final) crush; and $\bar{\delta}_{im}$ is the available crush distance of a weight/size class i vehicle in mode m (see Appendix I).

It is of interest to see the effect of the choice of the constant d on the repair cost in Eqn. (G-1) in terms of the repair cost as a percentage of the vehicle depreciated value when the final crush equals the available crush. This is shown below:

d	C_R/C_{VD} for $\delta^f = \overline{\delta}$
1.6	0.80
2.0	0.86
3.0	0.95

The second repair cost model [Eqn. (C-26) of Appendix C] models repair cost as a (quadratic) function of the speed decrement suffered by the vehicle, up to the vehicle depreciated value, and for vehicle i is

$$C^i_{R/im/jn/V_{ci}} = \left\{ \begin{array}{ll} w_R(i) \dfrac{c_{RC}}{V_{ch}^2} \left(\dfrac{M_j V_{ci}}{M_i+M_j}\right)^2 & , \text{ if } \leq C_{VD}(i) \\ \\ C_{VD}(i) & , \text{ otherwise} \end{array} \right\} \qquad \text{(G-3)}$$

Note that (Appendix A)

$$\left(\frac{M_j V_{ci}}{M_i+M_j}\right)^2 = (V_i - V_f)^2 \qquad \text{(G-4)}$$

Typical values for the constants c_{RC} and V_{ch} might be, c_{RC} = \$1.5K, V_{ch} = 15 mph. Note that again this is a rather gross model, and the repair cost is independent of collision mode and *does not* depend on the details of the collision dynamics (e.g. vehicle force-crush characteristics).

APPENDIX H

COSTS OF ENGINEERING MODIFICATIONS

Costs of engineering modifications are measured in terms of added crush distance over and above the crush distance currently available, and added stiffness and yield strength. Added crush distance is related to added vehicle weight and the added weight is related to added cost.

Figure H1 shows cost data for a spectrum of 1975 automobiles as a function of vehicle curb weight. The upward scatter of data points reflects costs of accessories and luxury items unrelated to basic costs. The curve drawn in Figure H1 might serve as a reasonable representation of the basic vehicle cost (also new vehicle replacement cost for computing repair costs in Appendix G). The curve is a quadratic up to 4000 lbs. and linear beyond:

$$C_V = c_{20} + c_{22}W^2, \quad W \leq W^* \qquad (H\text{-}1)$$

$$C_V = c_{10} + c_{11}W, \quad W > W^*$$

where c_{20} = \$2.4K, $c_{22} = 1\text{x}10^{-7}\$K/lb^2$, c_{10} = \$1.0K, $c_{11} = 7.5\text{x}10^{-4}\$K/lb$, W^* = 4000 lbs.

In view of the scaling of vehicle design [Eqn. (I-7), Appendix I], it is sufficient to relate frontal crush distance to the vehicle weight in Eqn. (H-1). This is given by Eqn. (I-1),

$$\bar{\delta}_{front} = c_f(W-850)^{1/3} \qquad (H\text{-}2)$$

Then $(\delta_i^* - \bar{\delta}_{i1})$ is a measure of incremental weight and thus of incremental cost, as developed below.

Using Eqs. (H-1) and (H-2), $\bar{\delta}_{front}$ may be related to C_V. This is given in Table H1. From Table H1, a difference table is constructed, Table H2, giving, for a family of $\bar{\delta}_{front}$ values, incremental cost ΔC_V as a function of $\Delta\bar{\delta}_{front}$. Table H2 generates the family of dashed curves in Figure H2. This family of curves may be approximated by the equation

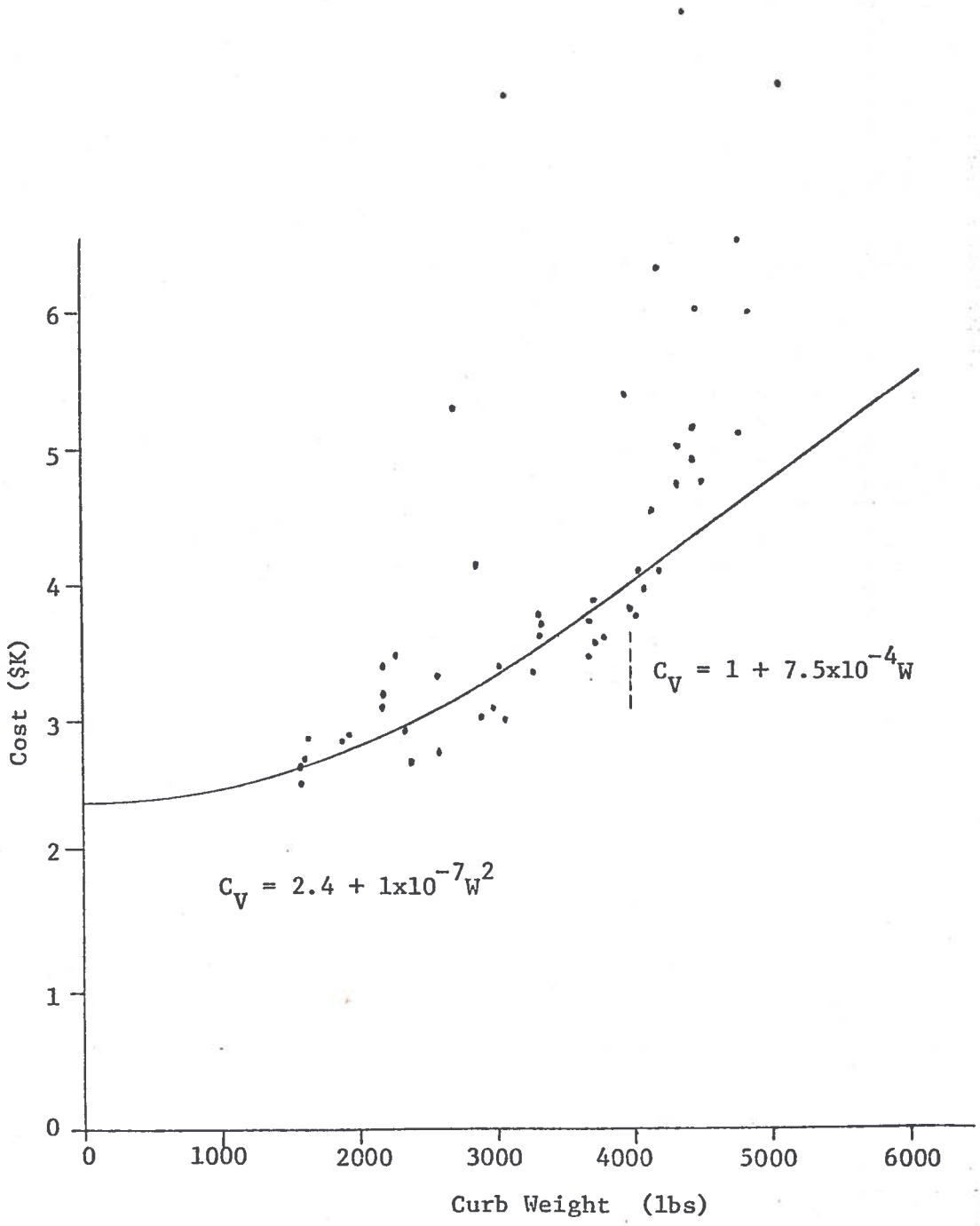

FIGURE H1

Automobile Cost Data

TABLE H1

Vehicle Cost vs. Frontal Crush Distance

$\bar{\delta}_{front}$	1.5	2.0	2.5	3.0	3.5	4.0	4.5	5.0	5.5	6.0	6.5	7.0
C_V	2.489	2.514	2.562	2.649	2.802	3.063	3.492	4.163	4.999	6.001	7.186	8.567

$\bar{\delta}_{front}$ ~ ft; C_V ~ $K

TABLE H2

Incremental Costs, ΔC_V

$\Delta\bar{\delta}$ \ $\bar{c}_1$	1.5	2.0	2.5	3.0	3.5	4.0	4.5	5.0	5.5
0.5	.025	.048	.087	.153	.261	.429	.671	.836	1.002
1.0	.073	.135	.240	.414	.690	1.100	1.507	1.838	2.187
1.5	.160	.288	.501	.843	1.361	1.936	2.509	3.023	3.568

$$\Delta C_V = C_{E1}(\bar{\delta})\Delta\bar{\delta} + C_{E2}(\bar{\delta})\Delta\bar{\delta}^2 \qquad \text{(H-3)}$$

Table H3 gives the values of the coefficients in Eqn. (H-3) which generate the solid approximating curves in Figure H2.

The relationship in Eqn. (H-3) gives the cost of adding crush distance to an automobile, essentially based on current vehicle costs as they relate to vehicle size. Given a weight/size class i vehicle, Eqn. (H-2) is used to compute its frontal crush distance $\bar{\delta}$. Then interpolation in Table H3 gives

$$C_{E1}(i) \quad , \quad C_{E2}(i) \qquad \text{(H-4)}$$

Thus the costs of engineering modifications in terms of added crush distance may be modeled as

$$C_{E/i} = \begin{cases} w_E(i)C_{E1}(i)(\delta_i^* - \bar{\delta}_{i1})^{\gamma} + w_E(i)C_{E2}(i)(\delta_i^* - \bar{\delta}_{i1})^2 & ; \quad \delta_i^* > \bar{\delta}_{i1} \\ 0 & ; \quad \delta_i^* \leq \bar{\delta}_{i1} \end{cases} \qquad \text{(H-5)}$$

where $w_E(i)$ are arbitrary weighting constants, and γ is close to 1.

To approximate the costs of any added stiffness and/or yield strength of materials, the above model is expanded to

$$C_{E/i} = \left\{ \begin{array}{ll} w_E(i)C_{E1}(i)(\delta_i^* - \bar{\delta}_{i1})^{\gamma} + w_E(i)C_{E2}(i)(\delta_i^* - \bar{\delta}_{i1})^2 & ; \quad \delta_i^* > \bar{\delta}_{i1} \\ 0 & ; \quad \delta_i^* \leq \bar{\delta}_{i1} \end{array} \right\}$$

$$+ w_E(i)C_{E3}(i)\sum_{m=1}^{M} \left\{ \begin{array}{ll} s_m(f_{im} - \bar{f}_{im})^2 & ; \quad f_{im} > \bar{f}_{im} \\ 0 & ; \quad f_{im} \leq \bar{f}_{im} \end{array} \right\} \qquad \text{(H-6)}$$

$$+ w_E(i)C_{E4}(i)\sum_{m=1}^{M} \left\{ \begin{array}{ll} s_m(k_{im} - \bar{k}_{im})^2 & ; \quad k_{im} > \bar{k}_{im} \\ 0 & ; \quad k_{im} \leq \bar{k}_{im} \end{array} \right\}$$

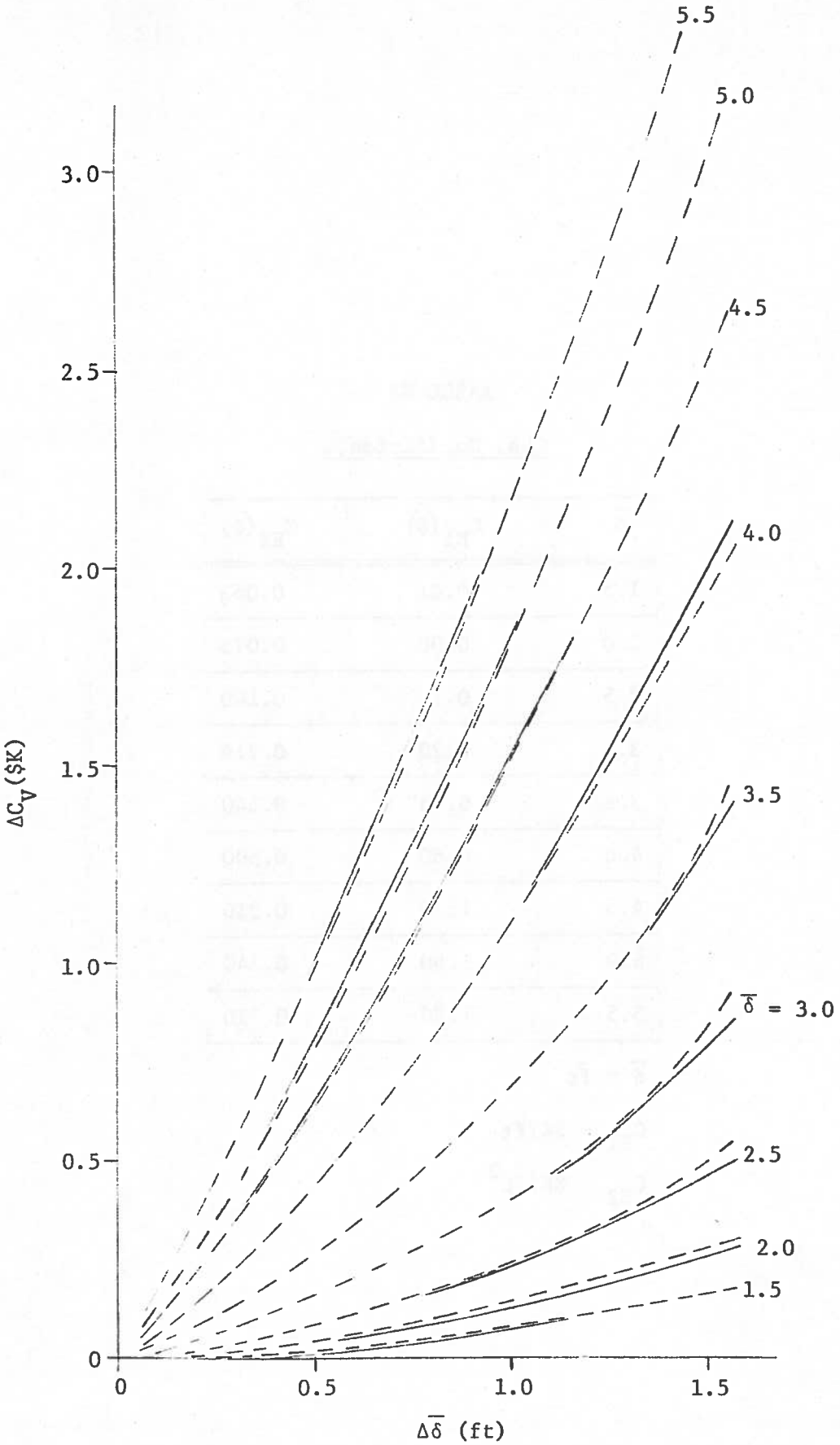

FIGURE H2

Incremental Costs of Added Crush Distance

TABLE H3

Cost Coefficients

$\bar{\delta}$	$C_{E1}(\bar{\delta})$	$C_{E2}(\bar{\delta})$
1.5	0.01	0.063
2.0	0.06	0.075
2.5	0.10	0.140
3.0	0.20	0.214
3.5	0.35	0.340
4.0	0.60	0.500
4.5	1.20	0.310
5.0	1.50	0.340
5.5	1.80	0.390

$\bar{\delta}$ ~ ft

C_{E1} ~ \$K/ft

C_{E2} ~ \$K/ft^2

where $C_{E3}(i)$, $C_{E4}(i)$ and s_m are scaling constants, and $\bar{f}_{im}$, $\bar{k}_{im}$ are nominal values.

APPENDIX I

CRUSH DISTANCE DATA AND DESIGN

The models for occupant compartment penetration cost penalty, repair costs and costs of engineering modifications (Appendices C, G and H) involve data on available crush distance in the various collision modes for the current traffic mix. Also involved is the design (optimization) of vehicle crush distance. Models of available crush distance and crush distance design are developed in this appendix.

A NHTSA study [Ref. 1] presents data on available frontal crush distance (bumper to firewall), and available side crush distance (door thickness) for a spectrum of American, European and Japanese automobiles. These crush distances vary with vehicle weight and very closely satisfy the relations

$$\bar{\delta}_{front} = c_f(W-850)^{1/3} \qquad (I-1)$$

$$\bar{\delta}_{side} = c_s(W-850)^{1/3} \qquad (I-2)$$

where the weight W is in lbs; and if $c_f = 1/3$, $c_s = 0.52/12$, then crush distance is in feet. It is interesting to note that the front to side crush distance ratio, $\bar{\delta}_{front}/\bar{\delta}_{side}$, is independent of vehicle weight and is in fact constant.

Measurements of rear available crush distances at several dealerships (Figure I1 and I2) shows that a similar relationship holds for rear crush distance, so that crush distance ratios of all three directions of impact are constant, independent of vehicle weight.

As a consequence, it is possible to describe the currently available crush distance of a weight/size class i vehicle in collision mode n by

$$\bar{\delta}_{in} = a_n \bar{\delta}_{i,front} \qquad (I-3)$$

where

$$\bar{\delta}_{i,front} = c_f(W_i-850)^{1/3} \qquad (I-4)$$

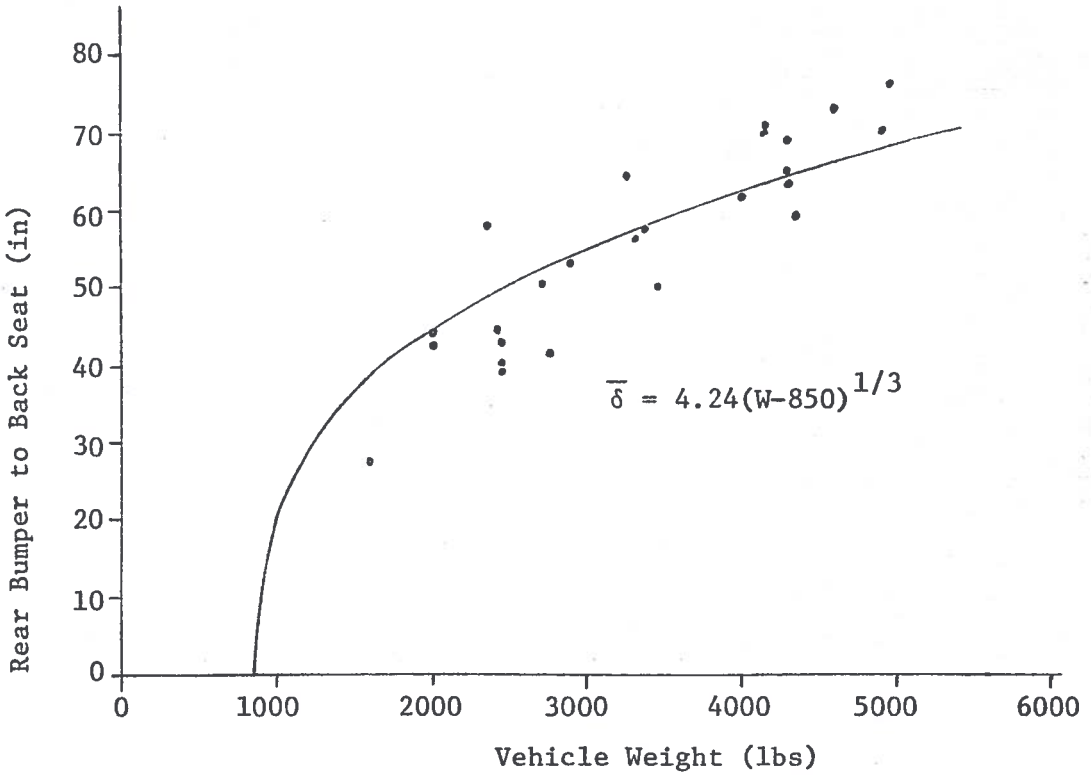

FIGURE I1

Rear (Back Seat) Available Crush

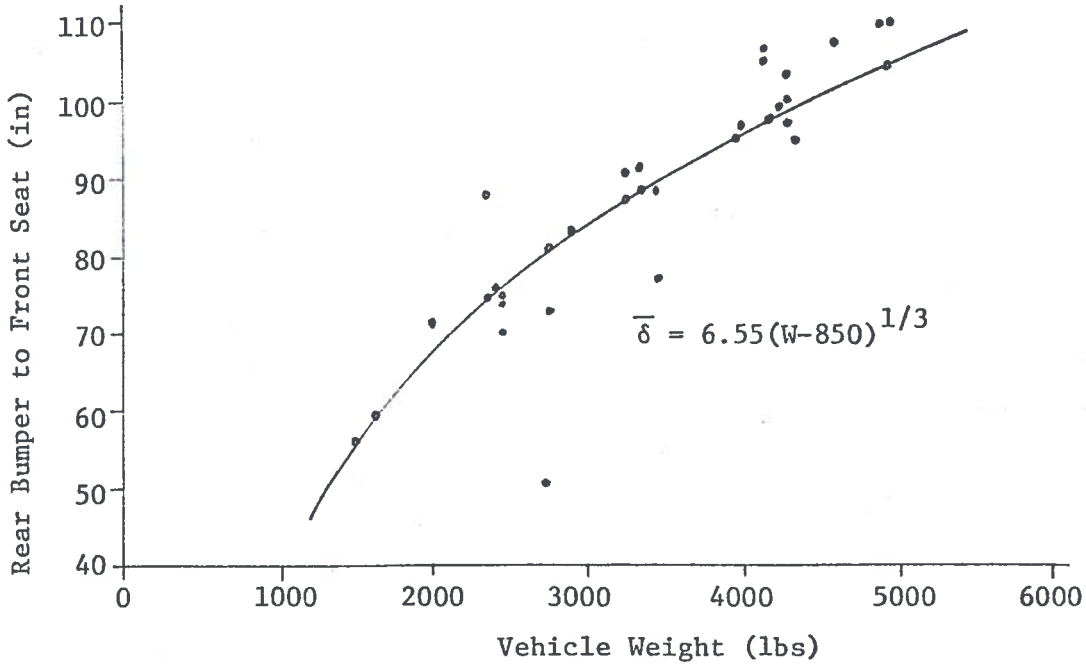

FIGURE I2

Rear (Front Seat) Available Crush

W_i is the weight of the typical class i vehicle. If n=1 is front (f), n=2 is side (s), and n=3 is rear (r); then a_f=1.0, a_s is the side crush distance ratio, and a_r is the rear crush distance ratio. In view of the data presented above,

$$a_s = 0.13, \quad a_r = 1.06 \tag{I-5}$$

Now the total available crush distance is not totally composed of crushable material. For example, in frontal crush the presence of the engine must be considered. Ref. 1 suggests that without engine deflection approximately $0.6\bar{\delta}_f$ is effective crush distance, while with engine deflection the figure approximates $0.85\bar{\delta}_f$. Thus, in general, the effective available crush is

$$k_n \bar{\delta}_{in} \tag{I-6}$$

where the k_n are effective fractions of crush distance in the three collision modes.

Engineering modifications to existing vehicles offer tradeoffs between costs of such modifications and other costs (injury/mortality, etc.). The cost of engineering modifications may be measured in terms of crush distance added (Appendix H). The model chosen for the design crush on a weight/size class i vehicle, in mode n (front, side, rear), is

$$\delta^*_{in} = e_n a_n \delta^*_i + (1-e_n)\bar{\delta}_{in} \tag{I-7}$$

Here, δ^*_i are the design variables. They are also the design frontal crush distances for the several vehicle weight/size classes. The crush distance ratios a_n scale the other aspects of the vehicle (side and rear). The parameters e_n permit the removal from optimization of side and rear crush distances (e_1 is always one). Thus if e_2=1.0, side crush distance is optimized, and if e_2=0.0, the side crush distance remains at the currently available side crush distance.

The model of Eqn. (I-7) permits the design of crush distance in the *current* ratio. There are good reasons for making this restriction, not the least of which is the avoidance of designs which do not fit in existing parking facilities. By fixing the design ratio the dimension of the optimization problem is also reduced. Eqn. (I-7) may be generalized by permitting design in a *fixed* (but not

necessarily current) ratio. Defining any specified crush distance ratios b_n, the model becomes

$$\delta^*_{in} = e_n b_n \delta^*_i + (1-e_n)\bar{\delta}_{in} \qquad \text{(I-8)}$$

REFERENCES

1. J. E. Hofferberth and J. E. Tomassoni, "A Study of Structural and Restraint Requirements for Automobile Crash Survival," Department of Transportation, National Highway Traffic Safety Administration, Motor Vehicle Programs, Office of Crashworthiness, undated and unnumbered report.

APPENDIX J

MODIFIED DAVIDON OPTIMIZATION ALGORITHM

Consider the problem of minimizing the function

$$C_T(x) \tag{J-1}$$

with respect to the parameters $(x_1,\ldots,x_N) = x$. Assume C_T twice continuously differentiable with respect to x. Let

$$x^T = [x_1 \cdots x_N] \tag{J-2}$$*

and the gradient g of C_T

$$g^T = [\frac{\partial C_T}{\partial x_1} \cdots \frac{\partial C_T}{\partial x_N}] \tag{J-3}$$

Denote by subscript i the current (vector) point x_i, and let g_i be the gradient at that point. Let H_i be a symmetric, positive definite NxN matrix.

The Davidon algorithm [Ref. 1] proceeds as follows:

(a) Set $s_i = -H_i g_i$ (J-4)

(b) Find scalar $\lambda>0$ such that

$$C_T(x_i + \lambda s_i) \tag{J-5}$$

is a minimum with respect to λ (one-dimensional search for the minimum).

(c) Set $\sigma_i = \lambda s_i$ (J-6)

$$x_{i+1} = x_i + \sigma_i \tag{J-7}$$

---

* Superscript T denotes the vector (matrix) transpose. Vectors are column vectors.

(d) Evaluate $C_T(x_{i+1})$ and g_{i+1}, where, in view of (b)

$$g_{i+1}^T \sigma_i = 0 \tag{J-8}$$

(e) Set $y_i = g_{i+1} - g_i$ (J-9)

(f) Set $H_{i+1} = H_i + A_i + B_i$, where (J-10)

$$A_i = \frac{\sigma_i \sigma_i^T}{y_i^T \sigma_i}, \quad B_i = -\frac{H_i y_i y_i^T H_i}{y_i^T H_i y_i} \tag{J-11}$$

(g) Set $i = i + 1$ and return to (a).

This algorithm has the following properties [Ref. 1]:

P_1: $H_i > 0$ for all i, so that the algorithm is *stable* (has the descent property). In other words, the method is downhill, guaranteeing a decrease in C_T each iteration.

P_2: For quadratic C_T, the algorithm converges to the minimum in at most N steps, and

$$H_i \to \left[\frac{\partial^2 C_T}{\partial x^2}\right]^{-1}, \text{ for } i = N$$

This is *quadratic convergence.*

Non-quadratic (smooth) functions are almost quadratic sufficiently close to the minimum, so that we may expect quadratic 'terminal' convergence. It is useful, as an option, starting with diagonal H_0, to bypass Eqn. (J-10) for a specified number of iterations. This is the *straight gradient* option.

Property P_1 follows from Eqn. (J-8) which in turn is a result of the one-dimensional minimization in (b). Although straightforward in theory, the accurate location of a one-dimensional minimum is far from trivial in practice. Errors in its location may (and sometimes do) result in loss of positive definiteness of the matrix H_i.

Consider the denominator in A_i of Eqn. (J-11), which can be written as

$$y_i^T \sigma_i = g_{i+1}^T \sigma_i - g_i^T \sigma_i \qquad \text{(J-12)}$$

Replace $y_i^T \sigma_i$ by $-g_i^T \sigma_i$, so that

$$A_i = -\frac{\sigma_i \sigma_i^T}{g_i^T \sigma_i} \quad \text{(Jazwinski modification)} \qquad \text{(J-13)}$$

It can be shown [Ref. 2] that, with this replacement, Property P_1 holds quite independently of the location of the one-dimensional minimum. On the other hand, *if* the one-dimensional minimum is indeed found, then $g_{i+1}^T \sigma_i = 0$ anyway, and the Davidon algorithm remains unaltered.

It has already been noted that accurate location of a one-dimensional minimum can be difficult and (computer) time-consuming. To compensate for errors in this minimum a modified search direction has been developed [Ref. 2]. This modification consists of replacing the search direction of Eqn. (J-4) by

$$s_i = -H_i \left[I - \frac{y_i \sigma_i^T}{y_i^T \sigma_i} \right] g_i \quad \text{(Kelley modification)} \qquad \text{(J-14)}$$

Other, similar modifications are possible [Ref. 2].

REFERENCES

1. R. Fletcher and M. J. D. Powell, "A Rapidly Convergent Descent Method for Minimization," Computer Journal, Vol. 6, No. 2, pp. 163-168, July 1963.

2. A. H. Jazwinski et al, "Midcourse Guidance Optimization," Analytical Mechanics Associates, Inc. Report No. 67-17, December 1967.

APPENDIX K
RESTRAINT SYSTEM MODEL

The motion of a restrained occupant in the colliding vehicle A (Appendix A) is described by

$$m\ddot{x}_{PA} = -f_{PA} \tag{K-1}$$

[and in vehicle B by

$$m\ddot{x}_{PB} = f_{PB} \quad] \tag{K-2}$$

where m is the occupant mass, $\ddot{x}_{PA}$ is the occupant acceleration, and $-f_{PA}$ is the force acting on the occupant due to the restraint system. Equation (K-1) has the initial conditions

$$x_{PA}(0) = 0, \quad \dot{x}_{PA}(0) = V_A \tag{K-3}$$

In order to solve for the occupant motion, the restraint system f-δ characteristics (f_{PA}) must be specified.

A rather general model for restraint system characteristics is given in Figure K1. The dead zone in the model represents the distance the occupant travels before engaging the restraint. d_T is the total distance available to the occupant (e.g. headroom) before encountering a barrier (e.g. dash, door). k_R, f_M describe the restraint system force-crush characteristics; and k_D is a very stiff barrier. The application of this model to various restraint systems is summarized in Table K1. Clearly, the parameters describing the restraint characteristics (in Figure K1) depend on the vehicle weight/size class and collision mode.

It is convenient to formulate the restrained occupant dynamics in terms of the relative displacement (deflection) of the occupant with respect to the vehicle

$$\delta_{PA} = x_{PA} - x_A(t) \tag{K-4}$$

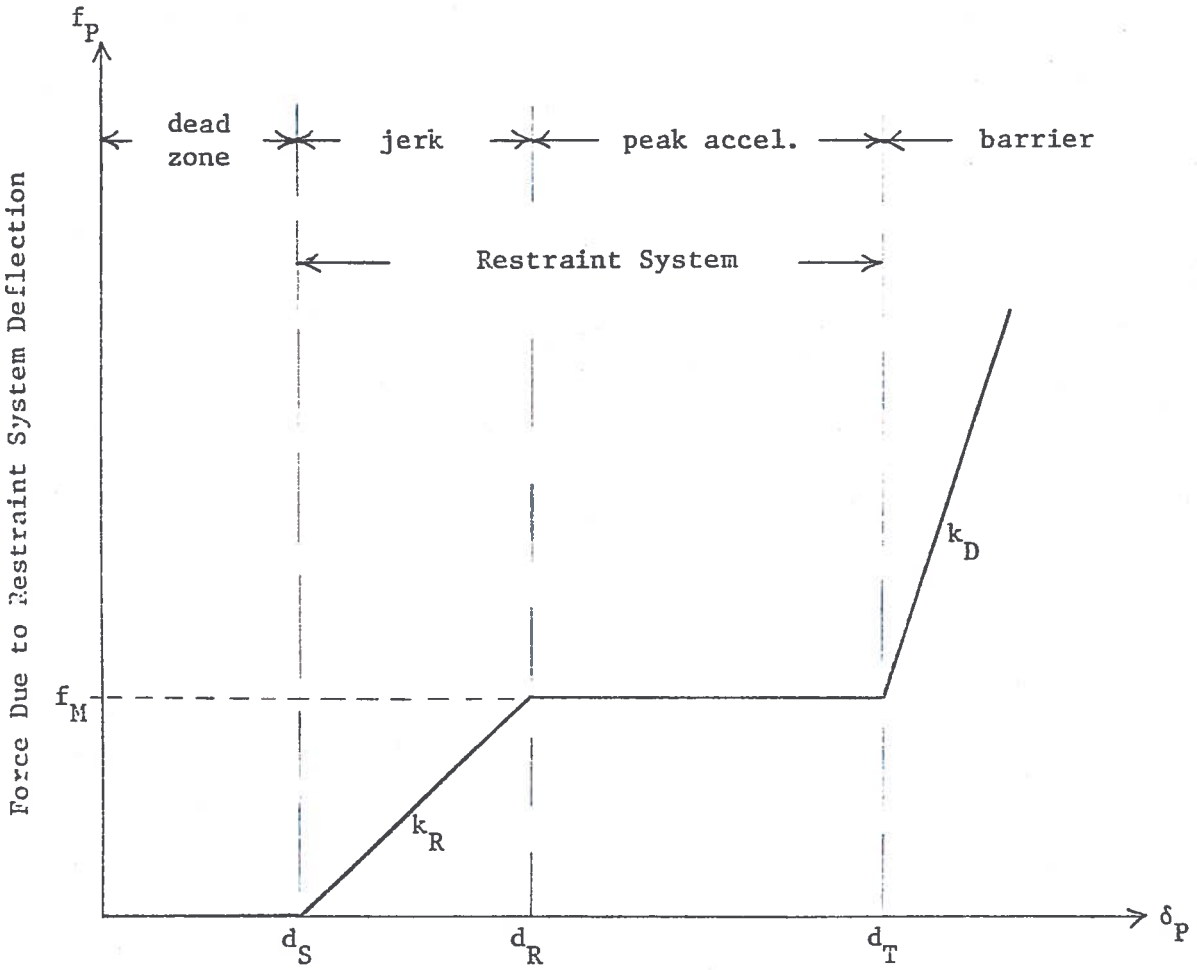

$$d_R = d_S + f_M/k_R$$

FIGURE K1

Restraint System Model

TABLE K1

Application of Restraint System Model

Type of Restraint	Collision Mode		
	Front	Side	Rear
Unrestrained	Slide on seat; hit dash/ windshield $d_S=d_R=0$ $f_M=\mu mg$	Slide on seat; hit door/ window $d_S=d_R=0$ $f_M=\mu mg$ (not symmetric left & right)	Move against back of seat $d_S=0$ f_M=seat strength
Seat Belt	d_S small k_R, f_M specified	1) Driver hit from left-same as above 2) Driver hit from right-seat belt engaged	Same as above
Air Belt	d_S larger f_M smaller than above	Same as above	Same as above
Air Bag	d_S larger yet, f_M smaller than above	Same as above	Same as above

m ~ occupant mass

μ ~ friction coefficient

g ~ gravitational acceleration

where $x_A(t)$ is vehicle A position at any time t. Then from Eqs. (K-4) and (K-1)

$$\ddot{\delta}_{PA} = -f_{PA}/m - \ddot{x}_A(t) \tag{K-5}$$

where $\ddot{x}_A(t)$ is the acceleration of vehicle A. Utilizing the restraint system model of Figure K1, the restrained occupant motion is described by

$$\ddot{\delta}_{PA} = \begin{cases} -\ddot{x}_A(t) & , \quad 0 \leq \delta_{PA} \leq d_S \\ -(k_R/m)(\delta_{PA}-d_S) - \ddot{x}_A(t) & , \quad d_S < \delta_{PA} \leq d_R \\ -f_M/m - \ddot{x}_A(t) & , \quad d_R < \delta_{PA} \leq d_T \\ -f_M/m - (k_D/m)(\delta_{PA}-d_T) - \ddot{x}_A(t) & , \quad d_T < \delta_{PA} \end{cases} \tag{K-6}$$

where, in view of Eqn. (K-3),

$$\delta_{PA}(0) = 0, \quad \dot{\delta}_{PA}(0) = 0 \tag{K-7}$$

Once the vehicle acceleration, $\ddot{x}_A(t)$, is given, Eqn. (K-6) may be solved for the occupant deflection. Then the occupant position x_{PA} is given by Eqn. (K-4), as is the occupant acceleration

$$\ddot{x}_{PA} = \ddot{\delta}_{PA} + \ddot{x}_A(t) \tag{K-8}$$

Similar equations hold for the occupant of vehicle B.

APPENDIX L

SPECIAL SOLUTIONS OF RESTRAINED MOTION

The collision dynamics described in Appendix K, Equation (K-6), can be solved in closed form for each of the three different conditions of vehicle acceleration (vehicle in linear region, vehicle in constant force region, vehicle in zero acceleration region - collision completed). These three different regions of vehicle motion and four different regions of occupant restraint together define twelve distinct regions of occupant motion. The solutions in these regions are given in this appendix.

REGION 1: OCCUPANT IN DEAD ZONE; VEHICLE IN LINEAR REGION

The equation of motion is

$$\ddot{\delta}_{PA} = (1/M_A)\sqrt{\kappa\mu}\, V_c \sin \sqrt{\kappa/\mu}\, t \qquad \text{(L-1)}$$

with initial conditions

$$\delta_{PA}(0) = 0 \; ; \; \dot{\delta}_{PA}(0) = 0 \; .$$

The solution to this equation is

$$\begin{aligned} \delta_{PA}(t) &= \frac{\mu V_c}{M_A}\left[t - \sqrt{\frac{\mu}{\kappa}} \sin\sqrt{\frac{\kappa}{\mu}}\, t\right] , \\ \dot{\delta}_{PA}(t) &= \frac{\mu V_c}{M_A}\left[1 - \cos\sqrt{\frac{\kappa}{\mu}}\, t\right] . \end{aligned} \qquad \text{(L-2)}$$

This is the region in which occupant motion always starts. The occupant remains in this region until

$$t_o = \min(t_{A1}, t_y, t_f) \; ,$$

where t_{A1} is the time when the restraint is contacted ($\delta_{PA}(t_{A1}) = d_s$, assuming that the equation of motion is unchanged) t_y is the time when the vehicle leaves the linear crush region, and t_f is the time when the collision is complete - i.e. vehicle acceleration becomes zero.

These times can then be used to determine the next region. If $t_o = t_{A1}$, the occupant passes to region 4; if $t_o = t_y$, he passes to region 2; if $t_o = t_f$, he passes to region 3.

REGION 2: OCCUPANT IN DEAD ZONE; VEHICLE IN CONSTANT FORCE

The equation of motion is

$$\ddot{\delta}_{PA} = \min(f_A, f_B)/M_A \quad . \tag{L-3}$$

The solution to this equation is

$$\delta_{PA}(t) = \delta_{PA}(t_i) + \dot{\delta}_{PA}(t_i)(t-t_i) + \frac{\min(f_A,f_B)}{M_A} \frac{(t-t_i)^2}{2}$$

$$\dot{\delta}_{PA}(t) = \dot{\delta}_{PA}(t_i) + \frac{\min(f_A,f_B)}{M_A} (t-t_i) \quad , \tag{L-4}$$

where $\delta_{PA}(t_i)$ and $\dot{\delta}_{PA}(t_i)$ are the values of displacement and rate at the time (t_i) when the occupant entered t_i. This time t_i is, of course the same as the time (t_o) when the occupant left the previous region, in this case region 1. This notation will be followed throughout Appendix L. The input time of a region is t_i and is the same as the output time t_o of the previous region.

The occupant remains in region 2 (R2) until

$$t_o = \min(t_{A1}, t_f) \quad .$$

If $t_o = t_{A1}$, occupant goes to R4, otherwise to R3.

REGION 3: OCCUPANT IN DEAD ZONE; VEHICLE UNACCELERATED

The equation of motion is

$$\ddot{\delta}_{PA} = 0 \quad . \tag{L-5}$$

The solution to this equation is, of course,

$$\delta_{PA}(t) = \delta_{PA}(t_i) + \dot{\delta}_{PA}(t_i)(t-t_i)$$
$$\dot{\delta}_{PA}(t) = \dot{\delta}_{PA}(t_i) \qquad \text{(L-6)}$$

The occupant remains in R3 until t_{A1}, the time when the restraint is engaged ($\delta_{PA}(t_{A1}) = d_s$) at which time he goes to R6.

REGION 4: OCCUPANT IN LINEAR REGION; VEHICLE IN LINEAR REGION

The equation of motion is

$$\ddot{\delta}_{PA} = \frac{\sqrt{\kappa\mu}}{M_A} V_c \sin\sqrt{\frac{\kappa}{\mu}}\, t - \frac{k_R}{m}(\delta_{PA}-d_s) \quad . \qquad \text{(L-7)}$$

The parameters in this expression have been defined in Appendix K; m is the occupant mass; k_R is the spring constant of the restraint; and d_s is the length of the dead zone.

The solution to this equation is given by the following, rather extended, formulas:

$$\delta_{PA}(t) = d_s + \left[\delta_{PA}(t_i) - d_s - \frac{\sqrt{\kappa\mu}\, V_c \sin\sqrt{\frac{\kappa}{\mu}}\, t_i}{M_A\left(\frac{k_R}{m} - \frac{\kappa}{\mu}\right)}\right]\cos\sqrt{\frac{k_R}{m}}\,(t-t_i)$$

$$+\sqrt{\frac{m}{k_R}}\left[\dot{\delta}_{PA}(t_i) - \frac{\kappa V_c \cos\sqrt{\frac{\kappa}{\mu}}\, t_i}{M_A\left(\frac{k_R}{m} - \frac{\kappa}{\mu}\right)}\right]\sin\sqrt{\frac{k_R}{m}}\,(t-t_i)$$

$$+\frac{\sqrt{\kappa\mu}\, V_c}{M_A\left(\frac{k_R}{m} - \frac{\kappa}{\mu}\right)} \sin\sqrt{\frac{\kappa}{\mu}}\, t$$

$$\dot{\delta}_{PA}(t) = -\sqrt{\frac{k_R}{m}}\left[\delta_{PA}(t_i) - d_s - \frac{\sqrt{\kappa\mu}\, V_c \sin\sqrt{\frac{\kappa}{\mu}}\, t_i}{M_A\left(\frac{k_R}{m} - \frac{\kappa}{\mu}\right)}\right]\sin\sqrt{\frac{k_R}{m}}\,(t-t_i)$$

$$+\left[\dot{\delta}_{PA}(t_i) - \frac{\kappa V_c \cos\sqrt{\frac{\kappa}{\mu}}\, t_i}{M_A\left(\frac{k_R}{m} - \frac{\kappa}{\mu}\right)}\right]\cos\sqrt{\frac{k_R}{m}}\,(t-t_i)$$

$$+\frac{\kappa V_c}{M_A\left(\frac{k_R}{m} - \frac{\kappa}{\mu}\right)}\cos\sqrt{\frac{\kappa}{\mu}}\, t\ . \qquad \text{(L-8)}$$

The occupant remains in R4 until

$$t_o = \min(t_{A2},\ t_y,\ t_f)$$

where t_{A2} is the time when constant force level on the occupant is reached ($\delta_{PA}(t_{A2}) = d_R$). If $t_o = t_{A2}$, he goes to R7; if $t_o = t_y$, he goes to R5; if $t_o = t_f$, he goes to R6.

We remark that the quantity $\delta_{PA}(t_i) - d_s = 0$.

REGION 5: OCCUPANT IN LINEAR REGION; VEHICLE IN CONSTANT FORCE

The equation of motion is

$$\ddot{\delta}_{PA} = \min(f_A,\ f_B)/M_A - \frac{k_R}{m}\,(\delta_{PA} - d_s)\ . \qquad \text{(L-9)}$$

The solution to this equation is given by

$$\delta_{PA}(t) = d_s + \frac{m \min(f_A, f_B)}{M_A k_R} + \left[\delta_{PA}(t_i) - d_s - \frac{m \min(f_A, f_B)}{M_A k_R}\right] \cos\sqrt{\frac{k_R}{m}}\,(t-t_i)$$

$$+ \sqrt{\frac{m}{k_R}}\ \dot{\delta}_{PA}(t_i)\ \sin\sqrt{\frac{k_R}{m}}\,(t-t_i) \qquad \text{(L-10)}$$

$$\dot{\delta}_{PA}(t) = -\sqrt{\frac{k_R}{m}}\left[\delta_{PA}(t_i) - d_s - \frac{m \min(f_A, f_B)}{M_A k_R}\right] \sin\sqrt{\frac{k_R}{m}}\,(t-t_i)$$

$$+ \dot{\delta}_{PA}(t_i)\ \sin\sqrt{\frac{k_R}{m}}\,(t-t_i)\ .$$

The occupant remains in R5 until

$$t_o = \min(t_{A1}, t_f)\ .$$

If $t_o = t_{A1}$, he passes to R8; if $t_o = t_f$, he goes to R6.

REGION 6: OCCUPANT IN LINEAR REGION; VEHICLE UNACCELERATED

The equation of motion is

$$\ddot{\delta}_{PA} = -\frac{k_R}{m}(\delta_{PA} - d_s)\ . \qquad \text{(L-11)}$$

The solution to this equation is

$$\delta_{PA}(t) = d_s + (\delta_{PA}(t_i) - d_s)\ \cos\sqrt{\frac{k_R}{m}}\,(t-t_i)$$

$$+ \sqrt{\frac{m}{k_R}}\ \dot{\delta}_{PA}(t_i)\ \sin\sqrt{\frac{k_R}{m}}\,(t-t_i)$$

$$\dot{\delta}_{PA}(t) = -\sqrt{\frac{k_R}{m}}\,(\delta_{PA}(t_i) - d_s)\,\sin\sqrt{\frac{k_R}{m}}\,(t-t_i)$$

$$+\,\dot{\delta}_{PA}(t_i)\,\cos\sqrt{\frac{k_R}{m}}\,(t-t_i) \quad . \tag{L-12}$$

The occupant remains in R6 until

$$t_o = \min(t_{A2},\, t_{Af})$$

where t_{Af} is the time such that

$$\dot{\delta}_{PA}(t_{Af}) = 0 \quad ,$$

i.e. he has come to rest. If $t_o = t_{A2}$, the occupant passes into R9; if $t_o = t_{Af}$, the entire collision is complete.

Notice that the collision can be entirely completed - occupant has come to rest - only in regions 6, 9, and 12.

REGION 7: OCCUPANT IN CONSTANT FORCE; VEHICLE IN LINEAR REGION

The equation of motion is

$$\ddot{\delta}_{PA} = \frac{\sqrt{\kappa\mu}}{M_A}\,V_c\,\sin\sqrt{\frac{\kappa}{\mu}}\,t - \frac{f_M}{m} \quad , \tag{L-13}$$

where f_M is the constant force (Figure K-1) applied to occupant A in his class of vehicle and mode of collision.

The solution to this equation is

$$\delta_{PA}(t) = \delta_{PA}(t_i) + \dot{\delta}_{PA}(t_i)(t-t_i) - \frac{f_M}{m}\frac{(t-t_i)^2}{2} + \frac{\mu V_c}{M_A}\cos\sqrt{\frac{\kappa}{\mu}}\,t_i(t-t_i)$$

$$-\sqrt{\frac{\mu}{\kappa}}\,\frac{\mu V_c}{M_A}\left[\sin\sqrt{\frac{\kappa}{\mu}}\,t - \sin\sqrt{\frac{\kappa}{\mu}}\,t_i\right]$$

$$\dot{\delta}_{PA}(t) = \dot{\delta}_{PA}(t_i) - \frac{f_M}{m}(t-t_i)$$

$$- \frac{\mu V_c}{M_A}\left[\cos\sqrt{\frac{K}{\mu}}\,t - \cos\sqrt{\frac{K}{\mu}}\,t_i\right] . \qquad \text{(L-14)}$$

The occupant remains in R7 until

$$t_o = \min(t_{A3},\ t_y,\ t_f) ,$$

where t_{A3} is the time when the barrier is reached ($\delta_{PA}(t_{A3}) = d_T$). If $t_o = t_{A3}$, the occupant passes to R10; if $t_o = t_y$, he goes to R8; if $t_o = t_f$, he goes to R9.

REGION 8: OCCUPANT IN CONSTANT FORCE; VEHICLE IN CONSTANT FORCE

The equation of motion is

$$\ddot{\delta}_{PA} = - \frac{f_M}{m} + \frac{\min(f_A,\ f_B)}{M_A} \qquad \text{(L-15)}$$

The solution to this equation is

$$\delta_{PA}(t) = \delta_{PA}(t_i) + \dot{\delta}_{PA}(t_i)(t-t_i) + \left(\frac{\min(f_A,\ f_B)}{M_A} - \frac{f_M}{m}\right)\frac{(t-t_i)^2}{2}$$

$$\dot{\delta}_{PA}(t) = \dot{\delta}_{PA}(t_i) + \left(\frac{\min(f_A,\ f_B)}{M_A} - \frac{f_M}{m}\right)(t-t_i) . \qquad \text{(L-16)}$$

The occupant remains in R8 until

$$t_o = \min(t_{A3},\ t_f) .$$

If $t_o = t_{A3}$, the occupant passes to R11; if $t_o = t_f$, he goes to R9.

REGION 9: OCCUPANT IN CONSTANT FORCE; VEHICLE UNACCELERATED

The equation of motion is

$$\ddot{\delta}_{PA} = - \frac{f_M}{m} . \qquad \text{(L-17)}$$

The solution to this equation is

$$\delta_{PA}(t) = \delta_{PA}(t_i) + \dot{\delta}_{PA}(t_i)(t-t_i) - \frac{f_M}{m}\frac{(t-t_i)^2}{2}$$

$$\dot{\delta}_{PA}(t) = \dot{\delta}_{PA}(t_i) - \frac{f_M}{m}(t-t_i) \quad . \tag{L-18}$$

The occupant remains in R9 until

$$t_o = \min(t_{A3}, t_{Af}) \quad ,$$

where t_{Af} is the time when the occupant comes to rest,

$$\dot{\delta}_{PA}(t_{Af}) = 0 \quad .$$

If $t_o = t_{A3}$, the occupant goes to R12; if $t_o = t_{Af}$, the entire collision is complete.

REGION 10: OCCUPANT ON THE BARRIER; VEHICLE IN LINEAR REGION

The equation of motion is

$$\ddot{\delta}_{PA} = \frac{\sqrt{\kappa\mu}}{M_A} V_c \sin\sqrt{\frac{\kappa}{\mu}}\, t - \frac{k_D}{m}(\delta_{PA} - d_T) - \frac{f_M}{m} \quad , \tag{L-19}$$

where k_D is the spring constant of the barrier and d_T is the displacement distance at which the barrier is encountered. Note that the equations of motion in regions 10, 11, and 12 have nearly the same form, though different parameters, as the equations in regions 4, 5, and 6. Consequently, the solutions also have the same form. We have taken advantage of this fact in generating the software.

$$\delta_{PA}(t) = d_T - \frac{f_M}{k_D} + \left[\delta_{PA}(t_i) - d_T + \frac{f_M}{k_D} - \frac{\sqrt{\kappa\mu}\, V_c \sin\sqrt{\frac{\kappa}{\mu}}\, t_i}{M_A\left(\frac{k_D}{m} - \frac{\kappa}{\mu}\right)} \right] \cos\sqrt{\frac{k_D}{m}}\,(t-t_i)$$

$$+ \sqrt{\frac{m}{k_D}} \left[\dot{\delta}_{PA}(t_i) - \frac{\kappa V_c \cos\sqrt{\frac{\kappa}{\mu}}\, t_i}{M_A\left(\frac{k_D}{m} - \frac{\kappa}{\mu}\right)} \right] \sin\sqrt{\frac{k_D}{m}}\,(t-t_i)$$

$$+ \frac{\sqrt{\kappa\mu}\, V_c}{M_A\left(\frac{k_D}{m} - \frac{\kappa}{\mu}\right)} \sin\sqrt{\frac{\kappa}{\mu}}\, t \qquad \text{(L-20)}$$

$$\dot{\delta}_{PA}(t) = -\sqrt{\frac{k_D}{m}} \left[\delta_{PA}(t_i) - d_T + \frac{f_M}{k_D} - \frac{\sqrt{\kappa\mu}\, V_c \sin\sqrt{\frac{\kappa}{\mu}}\, t_i}{M_A\left(\frac{k_D}{m} - \frac{\kappa}{\mu}\right)} \right] \sin\sqrt{\frac{k_D}{m}}\,(t-t_i)$$

$$+ \left[\dot{\delta}_{PA}(t_i) - \frac{\kappa V_c \cos\sqrt{\frac{\kappa}{\mu}}\, t_i}{M_A\left(\frac{k_D}{m} - \frac{\kappa}{\mu}\right)} \right] \cos\sqrt{\frac{k_D}{m}}\,(t-t_i)$$

$$+ \frac{\kappa\, V_c}{M_A\left(\frac{k_D}{m} - \frac{\kappa}{\mu}\right)} \cos\sqrt{\frac{\kappa}{\mu}}\, t \ .$$

The occupant remains in R10 until

$$t_o = \min(t_y,\ t_f) \ .$$

If $t_o = t_y$, the occupant goes to R11, otherwise to R12.

We remark that

$$\delta_{PA}(t_i) = d_T \ .$$

REGION 11: OCCUPANT ON THE BARRIER; VEHICLE IN CONSTANT FORCE

The equation of motion is

$$\ddot{\delta}_{PA} = \frac{\min(f_A, f_B)}{M_A} - \frac{k_D}{m}(\delta_{PA} - d_T) - \frac{f_M}{m} \quad . \tag{L-21}$$

The solution to this equation is

$$\delta_{PA}(t) = d_T + \frac{m \min(f_A, f_B)}{M_A k_D} - \frac{f_M}{k_D}$$

$$+ \left[\delta_{PA}(t_i) - d_T - \frac{m \min(f_A, f_B)}{M_A k_D} + \frac{f_M}{k_D} \right] \cos\sqrt{\frac{k_D}{m}}\,(t-t_i)$$

$$+ \sqrt{\frac{m}{k_D}}\,\dot{\delta}_{PA}(t_i) \sin\sqrt{\frac{k_D}{m}}\,(t-t_i)$$

(L-22)

$$\dot{\delta}_{PA}(t) = -\sqrt{\frac{k_D}{m}} \left[\delta_{PA}(t_i) - d_T - \frac{m \min(f_A, f_B)}{M_A k_D} + \frac{f_M}{k_D} \right] \sin\sqrt{\frac{k_D}{m}}\,(t-t_i)$$

$$+ \dot{\delta}_{PA}(t_i) \cos\sqrt{\frac{k_D}{m}}\,(t-t_i) \quad .$$

The occupant remains in R11 until $t_o = t_f$, at which time he goes to R12.

REGION 12: OCCUPANT ON THE BARRIER; VEHICLE UNACCELERATED

The equation of motion is

$$\ddot{\delta}_{PA} = -\frac{k_D}{m}(\delta_{PA} - d_T) - \frac{f_M}{m} \quad . \tag{L-23}$$

The solution to the equation is

$$\delta_{PA}(t) = d_T - \frac{f_M}{k_D} + \left[\delta_{PA}(t_i) - d_T + \frac{f_M}{k_D}\right] \cos\sqrt{\frac{k_D}{m}}\,(t-t_i)$$

$$+ \sqrt{\frac{m}{k_D}}\,\dot{\delta}_{PA}(t_i)\,\sin\sqrt{\frac{k_D}{m}}\,(t-t_i) \qquad \text{(L-24)}$$

$$\dot{\delta}_{PA}(t) = -\sqrt{\frac{k_D}{m}}\left[\delta_{PA}(t_i) - d_T + \frac{f_M}{k_D}\right]\sin\sqrt{\frac{k_D}{m}}\,(t-t_i)$$

$$+ \dot{\delta}_{PA}(t_i)\,\cos\sqrt{\frac{k_D}{m}}\,(t-t_i) \quad .$$

The terminal time for this region, and the entire collision, is the solution, t_{Af}, of

$$\dot{\delta}_{PA}(t_{Af}) = 0 \quad .$$

Similar equations apply for δ_{PB} describing the motion for the occupant in the second vehicle. The parameters describing the occupant restraint, e.g. d_s and k_R, are dependent upon vehicle class and collision mode but subscripts indicating this dependence have been omitted for convenience.

In simulating the equation, we have made the assumption that the restraint system is well tuned to the auto parameters, i.e. it does not increase impact severity. One conclusion from this assumption is that $\delta_{PA}(t)$ is a monotonic function of time; thus the occupant cannot pass from one region to a lower numbered region. This assumption impacts the implementation only in the fact that the solutions used in the program are directly those written above. There is no check to see whether $\dot{\delta}_{PA}$ becomes negative or even to see whether δ_{PA} drops below a region division. This implies that if $\dot{\delta}_{PA}$ is negative, the restraint system continues to provide negative acceleration, i.e. the restraint in all regions (linear, constant, and barrier) is elastic.

APPENDIX M

FIGURE OF MERIT WITH RESTRAINT SYSTEM

The introduction of an occupant restraint system (Appendix K) modifies the Figure of Merit as given in Appendix C. The only cost component of the Figure of Merit which is affected by the restraint system is the Injury/Mortality Cost in Eqn. (C-8). Now, the injury severity indices of Eqn. (C-9) are computed with $a_{0\ell}(t)$ taken as the restrained occupant acceleration. These accelerations are based on the solutions of restrained occupant motion given in Appendix L.

In computing injury severity indices and injury/mortality costs, it is assumed that all the occupant(s)' mass is in the driver's seat. Side involvements are treated in a special way to account for the different side-room to the driver's left and to his right. If one of the vehicles' side is involved (but not both vehicles' sides--not a sideswipe), then that collision is simulated twice, once with the driver's side involved and once with the passenger's side involved. The costs of the latter two simulated collisions are weighted and added to produce a single injury/mortality cost of the collision. In sideswipes, it is assumed that the driver's sides of both vehicles are involved.

In the case $m \neq 2$ and $n \neq 2$ ($2 \triangleq$ side), the injury/mortality cost of a collision is given by Eqn. (C-8)

$$C^{i}_{IM/im/jn/V_{ci}} + C^{j}_{IM/im/jn/V_{ci}}$$

$$= w_{IM}(i)O(i)c_{IM}[1 - \exp(-r_{IM}(SI_i)^4)] \qquad \text{(M-1)}$$

$$+ w_{IM}(j)O(j)c_{IM}[1 - \exp(-r_{IM}(SI_j)^4)]$$

where

$$SI_{\ell} = \int_0^{t_{Af}} a^{\alpha}_{0\ell/im/jn/V_{ci}}(t)\, dt \qquad (\ell=i,j) \qquad \text{(M-2)}$$

and $a_{0\ell}(t)$ is the restrained occupant acceleration. In case m=n=2 (sideswipe), Eqs. (M-1) and (M-2) also hold, and as noted above, it is assumed that the driver's sides of both vehicles are involved.

In the case m=2 *or* n=2 (but not m=n=2), assume for simplicity that m=2. The cost of this collision is given by

$$
\begin{aligned}
&C^{i}_{IM/im/jn/V_{ci}} + C^{j}_{IM/im/jn/V_{ci}} \\
&\quad = w_{IM}(i)O(i)c_{IM}\left\{p_{ds}[1 - \exp(-r_{IM}(SI_i)^4)]_{dr}\right. \\
&\qquad\qquad \left. + (1 - p_{ds})[1 - \exp(-r_{IM}(SI_i)^4)]_{pas}\right\} \\
&\quad + w_{IM}(j)O(j)c_{IM}[1 - \exp(-r_{IM}(SI_j)^4)]
\end{aligned}
\tag{M-3}
$$

In the above, the notation $[]_{dr}$ means that the severity index SI_i is for the involvement of the driver's side of the vehicle, and $[]_{pas}$ means that SI_i is for the involvement of the passenger's side of the vehicle. p_{ds} is the probability that, for a side involvement, the driver's side is involved in the collision.

The acceleration appearing in (M-2) is the occupant acceleration $\ddot{x}_{PA}$ as defined in (K-8) with component $\ddot{\delta}_{PA}$ defined in the twelve regions described in Appendix L and component $\ddot{x}_A$ defined in the linear and constant force regions by (B-38). While the acceleration $\ddot{x}_{PA}$ is readily calculated from the closed form expression in Appendix L and equations (B-38), the integration of this quantity, raised to the α power, is handled by numerical quadrature, using Simpson's Rule with three steps per region.

The choice of three steps (seven function evaluations) was made on the basis that: a) accelerations are composed of sinusoids and constants; b) the vehicle acceleration in the sinusoid region is applied over a maximum of a quarter period; c) the restraint system should be somewhat softer than the vehicle (lower frequency), therefore the integration over the occupant motion should be over less than a quarter period; d) the integration of sinusoids can be performed very accurately with three steps per quarter period. It is noted that

APPENDIX M
FIGURE OF MERIT WITH RESTRAINT SYSTEM

The introduction of an occupant restraint system (Appendix K) modifies the Figure of Merit as given in Appendix C. The only cost component of the Figure of Merit which is affected by the restraint system is the Injury/Mortality Cost in Eqn. (C-8). Now, the injury severity indices of Eqn. (C-9) are computed with $a_{0\ell}(t)$ taken as the restrained occupant acceleration. These accelerations are based on the solutions of restrained occupant motion given in Appendix L.

In computing injury severity indices and injury/mortality costs, it is assumed that all the occupant(s)' mass is in the driver's seat. Side involvements are treated in a special way to account for the different side-room to the driver's left and to his right. If one of the vehicles' side is involved (but not both vehicles' sides--not a sideswipe), then that collision is simulated twice, once with the driver's side involved and once with the passenger's side involved. The costs of the latter two simulated collisions are weighted and added to produce a single injury/mortality cost of the collision. In sideswipes, it is assumed that the driver's sides of both vehicles are involved.

In the case $m \neq 2$ and $n \neq 2$ ($2 \triangleq$ side), the injury/mortality cost of a collision is given by Eqn. (C-8)

$$C^{i}_{IM/im/jn/V_{ci}} + C^{j}_{IM/im/jn/V_{ci}}$$

$$= w_{IM}(i)O(i)c_{IM}[1 - \exp(-r_{IM}(SI_i)^4)] \qquad \text{(M-1)}$$

$$+ w_{IM}(j)O(j)c_{IM}[1 - \exp(-r_{IM}(SI_j)^4)]$$

where

$$SI_{\ell} = \int_0^{t_{Af}} a^{\alpha}_{0\ell/im/jn/V_{ci}}\, dt \qquad (\ell = i,j) \qquad \text{(M-2)}$$

and $a_{0\ell}(t)$ is the restrained occupant acceleration. In case m=n=2 (sideswipe), Eqs. (M-1) and (M-2) also hold, and as noted above, it is assumed that the driver's sides of both vehicles are involved.

In the case m=2 *or* n=2 (but not m=n=2), assume for simplicity that m=2. The cost of this collision is given by

$$
\begin{aligned}
&C^{i}_{IM/im/jn/V_{ci}} + C^{j}_{IM/im/jn/V_{ci}} \\
&\quad = w_{IM}(i)O(i)c_{IM}\left\{p_{ds}[1 - \exp(-r_{IM}(SI_i)^4)]_{dr}\right. \\
&\qquad\qquad \left. + (1 - p_{ds})[1 - \exp(-r_{IM}(SI_i)^4)]_{pas}\right\} \\
&\quad + w_{IM}(j)O(j)c_{IM}[1 - \exp(-r_{IM}(SI_j)^4)]
\end{aligned}
\tag{M-3}
$$

In the above, the notation $[]_{dr}$ means that the severity index SI_i is for the involvement of the driver's side of the vehicle, and $[]_{pas}$ means that SI_i is for the involvement of the passenger's side of the vehicle. p_{ds} is the probability that, for a side involvement, the driver's side is involved in the collision.

The acceleration appearing in (M-2) is the occupant acceleration $\ddot{x}_{PA}$ as defined in (K-8) with component $\ddot{\delta}_{PA}$ defined in the twelve regions described in Appendix L and component $\ddot{x}_A$ defined in the linear and constant force regions by (B-38). While the acceleration $\ddot{x}_{PA}$ is readily calculated from the closed form expression in Appendix L and equations (B-38), the integration of this quantity, raised to the α power, is handled by numerical quadrature, using Simpson's Rule with three steps per region.

The choice of three steps (seven function evaluations) was made on the basis that: a) accelerations are composed of sinusoids and constants; b) the vehicle acceleration in the sinusoid region is applied over a maximum of a quarter period; c) the restraint system should be somewhat softer than the vehicle (lower frequency), therefore the integration over the occupant motion should be over less than a quarter period; d) the integration of sinusoids can be performed very accurately with three steps per quarter period. It is noted that

$$\int_0^{\frac{\pi}{2}} \sin^2 t\,dt = \frac{\pi}{4} = 0.7853981635$$

and

$$\int_0^{\frac{\pi}{2}} \sin^3 t\,dt = \frac{2}{3} \quad ,$$

(the nominal value for α is 2.5).

Using three steps of Simpson's Rule to perform these quadratures, we obtain, respectively, the exact result for the squared problem and 0.6665 for the cubed problem. Further investigation shows that

$$\int_0^{\frac{\pi}{4}} (\sin 2t - \sin t)^2 dt = 0.0639936425$$

while a three-step Simpson's Rule gives 0.064017. Since this is exactly the type of integral occuring in the restraint system, this gives considerable confidence that three steps will result in about three significant figure accuracy.

The fundamental time period is specified by the vehicle. In any one region, the vehicle is either under constant deceleration, or it is under linearly increasing deceleration. In either case, the trajectory stops when zero relative speed is reached or when a new region is reached. If the passenger restraint is softer than the vehicle, as one would expect it to be, then the passenger response has less curvature than the vehicle response, and the above results apply.

Computation of the time at which the occupant leaves a region is simple when the time is determined by the auto collision, i.e. when the end time is t_y or t_f. It becomes a problem which is very complex when the end time is determined by the occupant's reaching a specified position in the auto. For instance, in regions 4 and 10, the end time, t_2, is determined by solving an equation of the type

$$d = a \sin wt_2 + b \sin \nu t(t_2 + \tau)$$

where d, a, w, b, ν, and τ are known, $t_2 \varepsilon [0,T]$, but it is not known if a solution exists.

Because solution for the end time of each region is a *sine qua non* for restraint system operation, these equations have been solved in a generality outreaching the applicability of the system. For instance, the final times of the regions will be computed correctly for all values of the system parameters whereas the passenger injury/mortality cost for restraint systems which are much stiffer than the vehicle (an unrealistic situation) may be in error because of the numerical integration.

APPENDIX N

GRADIENT OF THE FIGURE OF MERIT (M)

This appendix lists the equations for the partial derivatives of the Injury/Mortality cost of Eqn. (M-1). This is the only cost component modified by introduction of the restraint system; further, Injury/Mortality cost is independent of δ_i^* (D-2) so only partials with respect to $f_{\eta\xi}$ and $k_{\eta\xi}$ need be considered. Introduction of the restraint system does not change the form of C_{IM} (Eqs. (M-1) and (C-8) are the same); therefore, equations (D-10) and (D-14) are still applicable,

$$\frac{\partial(C_{IM}^i+C_{IM}^j)}{\partial f_{\eta\xi}} = 4c_{IM}r_{IM}\left[w_{IM}(i)O(i)e^{-r_{IM}(SI_i)^4}(SI_i)^3\frac{\partial SI_i}{\partial f_{\eta\xi}} + w_{IM}(j)O(j)e^{-r_{IM}(SI_j)^4}(SI_j)^3\frac{\partial SI_j}{\partial f_{\eta\xi}}\right] \tag{N-1}$$

$$\frac{\partial(C_{IM}^i+C_{IM}^j)}{\partial k_{\eta\xi}} = 4c_{IM}r_{IM}\left[w_{IM}(i)O(i)e^{-r_{IM}(SI_i)^4}(SI_i)^3\frac{\partial SI_i}{\partial k_{\eta\xi}} + w_{IM}(j)O(j)e^{-r_{IM}(SI_j)^4}(SI_j)^3\frac{\partial SI_j}{\partial k_{\eta\xi}}\right] \tag{N-2}$$

It follows that the crux of the gradient computation is the computation of the partials of the severity indices $\frac{\partial SI_i}{\partial f_{\eta\xi}}$ and $\frac{\partial SI_i}{\partial k_{\eta\xi}}$. These are computed by numerical quadrature and the various regions described in Appendix L are handled by the program flow, so tests such as

$$V_{ci} > \min(f_{im},f_{jn})/\sqrt{\kappa\mu}$$

need not be made explicitly when (N-1) and (N-2) are applied.

The form of the severity index (SI) is given in (M-2)

$$SI = \int_0^{t_{Af}} |\ddot{x}_{PA}(t)|^{\alpha} dt \ .$$

Neither the acceleration $\ddot{x}_A$ nor the final time t_{Af} have any explicit dependence upon the parameters, f_A, f_B, k_A, and k_B. However, $\ddot{x}_A(t)$ can be written in terms of t and $\delta(t)$ when the region is known. The region definition (Appendix L) itself depends upon t, $\delta(t)$, t_y, and t_f while t_y and t_f can be written explicitly in terms of the force-crush parameters.

This completes the overall description of how SI depends upon the parameters. To describe how the partial derivatives of SI are calculated, consider the increment to SI in a single region. From Appendix L, we realize that SI can be written as

$$SI = \sum_{\ell=1}^{12} \int_{t_{\ell-1}(f_A,k_A,f_B,k_B)}^{t_\ell(f_A,k_A,f_B,k_B)} |\ddot{x}_{PA}(\delta(t)|^{\alpha} dt \qquad \text{(N-3)}$$

where $t_0 = 0$ and $t_{12} = t_{Af}$ and some of the integrals are zero because the occupant does not pass through the associated region. Because the equations of occupant dynamics can be written in closed form, there is a representation for δ in the ℓ^{th} region,

$$\delta(t) = g_\ell(t, \delta(t_\ell), \dot{\delta}(t_\ell), f_A, k_A, f_B, k_B) \ .$$

The program has been written so that an increment to SI and its partial derivatives is computed in each region. First, a general description of the method will be given and then the equations involved in each region detailed.

Assume that computations have been completed up to time $t_{\ell-1}$ and the computations required for region ℓ must now be performed. The state, containing all information required to proceed, consists of the five vector

$$\left[\delta(t_\ell), \frac{\partial \delta(t_\ell)}{\partial \lambda_\beta}\right]$$

(where $\lambda_1 = f_A$, $\lambda_2 = f_B$, $\lambda_3 = k_A$, $\lambda_4 = k_B$)

its time derivative

$$\left[\dot{\delta}(t_\ell),\ \frac{d}{dt}\frac{\partial\delta(t_\ell)}{\partial\lambda_\beta}\right] \quad ,$$

the severity index and its partial derivatives,

$$\left[SI,\ \frac{\partial SI}{\partial\lambda_\beta}\right] \quad ,$$

and the following derivatives of time:

$$\frac{\partial(t_y-t_{\ell-1})}{\partial\lambda_\beta} \quad , \quad \frac{\partial(t_f-t_y-t_{\ell-1})}{\partial\lambda_\beta} \quad , \quad \frac{\partial t_{\ell-1}}{\partial\lambda_\beta} \quad .$$

Here t_y refers to the time at which the auto crush dynamics have reached the force value

$$f_m = \min(f_A, f_B) \quad ,$$

while t_f refers to the time at which the two vehicles have zero relative velocity (collision completed).

Transforming the ℓ^{th} component of (N-3) by the time shift

$$t = t_{\ell-1} + \tau \quad ,$$

we obtain

$$\Delta_\ell = \int_0^{t_\ell - t_{\ell-1}} |\ddot{x}_{PA}(\delta(t_{\ell-1}+\tau)|^\alpha d\tau$$

and

$$\delta(t_{\ell-1}+\tau) = g_\ell(t_{\ell-1}+\tau, \delta(t_\ell), \dot{\delta}(t_\ell), f_A, k_A, f_B, k_B) \quad . \qquad \text{(N-4)}$$

In this form, Liebnitz's Rule can be applied to produce

$$\frac{\partial \Delta_\ell}{\partial \lambda_\beta} = \alpha \int_0^{t_\ell - t_{\ell-1}} |\ddot{x}_{PA}(\delta(t_{\ell-1}+\tau))|^{\alpha-1} \frac{\partial \ddot{x}_{PA}}{\partial \delta} \frac{\partial \delta}{\partial \lambda_\beta} \, d\tau$$

$$+ |\ddot{x}_{PA}(\delta(t_\ell))|^{\alpha} \frac{\partial (t_\ell - t_{\ell-1})}{\partial \lambda_\beta} \qquad \text{(N-5)}$$

The expressions for $\frac{\partial \ddot{x}_{PA}}{\partial \delta}$ and $\frac{\partial \delta}{\partial \lambda_\beta}$ will be given below for the twelve regions; in general however, from (N-4),

$$\frac{\partial \delta}{\partial \lambda_\beta} = \frac{\partial g_\ell}{\partial \lambda_\beta} + \frac{\partial g_\ell}{\partial t_{\ell-1}} \frac{\partial t_{\ell-1}}{\partial \lambda_\beta} + \frac{\partial g_\ell}{\partial \delta} \frac{\partial \delta(t_{\ell-1})}{\partial \lambda_\beta} + \frac{\partial g_\ell}{\partial \dot{\delta}} \frac{\partial \dot{\delta}(t_{\ell-1})}{\partial \lambda_\beta} \quad . \qquad \text{(N-6)}$$

The equations for $\frac{\partial (t_\ell - t_{\ell-1})}{\partial \lambda_\beta}$ are obtained by considering how the region is terminated. The region can change because the occupant has come to rest, ($t_\ell = t_{Af}$, $\dot{\delta}(t_{Af}) = 0$). In this case

$$\frac{\partial (t_\ell - t_{\ell-1})}{\partial \lambda_\beta} = - \left. \frac{\partial \dot{\delta}(t_\ell)}{\partial \lambda_\beta} \right|_{t_\ell} / \ddot{\delta}(t_\ell) \qquad \text{(N-7)}$$

The region can change because the occupant reaches a different part of the restraint system ($\delta(t_\ell) = d_S, d_R, d_T$). In this case

$$\frac{\partial (t_\ell - t_{\ell-1})}{\partial \lambda_\beta} = - \left. \frac{\partial \delta(t_\ell)}{\partial \lambda_\beta} \right|_{t_\ell} / \dot{\delta}(t_\ell) \qquad \text{(N-8)}$$

Finally, the region can change because the auto crush force has reached its final value ($t_\ell = t_y$) or because the collision is complete ($t_\ell = t_f$). These partials, as well as $\frac{\partial t_{\ell-1}}{\partial \lambda_\beta}$, are obtained by performing an update in each region:

$$\frac{\partial t_\ell}{\partial \lambda_\beta} = \frac{\partial t_{\ell-1}}{\partial \lambda_\beta} + \frac{\partial (t_\ell - t_{\ell-1})}{\partial \lambda_\beta} \quad ; \qquad \text{(N-9)}$$

$$\frac{\partial (t_y - t_\ell)}{\partial \lambda_\beta} = \frac{\partial (t_y - t_{\ell-1})}{\partial \lambda_\beta} - \frac{\partial (t_\ell - t_{\ell-1})}{\partial \lambda_\beta} \quad , \; (t_\ell < t_y) \; ; \qquad \text{(N-10)}$$

$$\frac{\partial(t_f - t_y - t_\ell)}{\partial\lambda_\beta} = \frac{\partial(t_f - t_y - t_{\ell-1})}{\partial\lambda_\beta} - \frac{\partial(t_\ell - t_{\ell-1})}{\partial\lambda_\beta} \quad , \; (t_y < t_\ell < t_f) \quad . \tag{N-11}$$

At the beginning of the solution for occupant motion, the initial conditions are:

$$\left[\delta(0) \; , \; \frac{\partial\delta(0)}{\partial\lambda_\beta}\right] = 0 \; , \quad \beta = 1,2,3,4$$

$$\left[\dot{\delta}(0) \; , \; \frac{\partial\dot{\delta}(0)}{\partial\lambda_\beta}\right] = 0 \; , \quad \beta = 1,2,3,4$$

$$\left[SI \; , \; \frac{\partial SI}{\partial\lambda_\beta}\right] = 0 \; , \quad \beta = 1,2,3,4$$

$$\left[t_0 \; , \; \frac{\partial t_0}{\partial\lambda_\beta}\right] = 0 \; , \quad \beta = 1,2,3,4$$

$$\frac{\partial t_y}{\partial f_A} = \frac{\partial t_y}{\partial f_m}\frac{\partial f_m}{\partial f_A} \; ,$$

$$\frac{\partial t_y}{\partial f_B} = \frac{\partial t_y}{\partial f_m}\frac{\partial f_m}{\partial f_B} \; ,$$

$$\frac{\partial t_y}{\partial k_A} = \frac{\partial t_y}{\partial \kappa}\frac{\partial \kappa}{\partial k_A} \; ,$$

$$\frac{\partial t_y}{\partial k_B} = \frac{\partial t_y}{\partial \kappa}\frac{\partial \kappa}{\partial k_B} \; ,$$

$$\frac{\partial(t_f - t_y)}{\partial f_A} = \frac{\partial(t_f - t_y)}{\partial f_m}\frac{\partial f_m}{\partial f_A} \; ,$$

$$\frac{\partial(t_f - t_y)}{\partial f_B} = \frac{\partial(t_f - t_y)}{\partial f_m}\frac{\partial f_m}{\partial f_B} \; ,$$

$$\frac{\partial(t_f-t_y)}{\partial k_A} = \frac{\partial(t_f-t_y)}{\partial \kappa}\frac{\partial \kappa}{\partial k_A} \quad ,$$

$$\frac{\partial(t_f-t_y)}{\partial k_B} = \frac{\partial(t_f-t_y)}{\partial \kappa}\frac{\partial \kappa}{\partial k_B} \quad ,$$

where

$$f_m = \min(f_A, f_B) \quad ,$$

$$\kappa = \frac{k_A k_B}{k_A + k_B} \quad ,$$

$\frac{\partial f_m}{\partial f_A, f_B}$ and $\frac{\partial \kappa}{\partial k_A, k_B}$ have been defined in (D-12), (D-13), and (D-7), and

$$\frac{\partial t_y}{\partial f_m} = 1/[\kappa V_c(1-(f_m/V_c\sqrt{\kappa\mu})^2)^{\frac{1}{2}}]$$

$$\frac{\partial t_y}{\partial \kappa} = -\left[\sqrt{\frac{\mu}{\kappa}}\sin^{-1}\frac{f_m}{V_c\sqrt{\kappa\mu}} + \frac{f_m}{\kappa V_c(1-(f_m/V_c\sqrt{\kappa\mu})^2)^{\frac{1}{2}}}\right]\Big/2\kappa$$

$$\frac{\partial(t_f-t_y)}{\partial f_m} = -\frac{\mu V_c}{f_m}\left[\cos\sqrt{\frac{\kappa}{\mu}}\,t_y/f_m + \sqrt{\frac{\kappa}{\mu}}\sin\sqrt{\frac{\kappa}{\mu}}\,t_y\frac{\partial t_y}{\partial f_m}\right]$$

$$\frac{\partial(t_f-t_y)}{\partial \kappa} = -\frac{\mu V_c \sin\sqrt{\frac{\kappa}{\mu}}\,t_y}{f_m}\left[\sqrt{\frac{\kappa}{\mu}}\frac{\partial t_y}{\partial \kappa} + \frac{t_y}{2\sqrt{\kappa\mu}}\right]$$

if

$$V_c > f_m/\sqrt{\kappa\mu} \quad .$$

If

$$V_c \leq f_m/\sqrt{\kappa\mu} \quad ,$$

then t_y is not used and

$$\frac{\partial t_f}{\partial f_m} = 0$$

$$\frac{\partial t_f}{\partial \kappa} = -\frac{\pi\sqrt{\mu}}{4\kappa^{3/2}} \quad .$$

The times, t_y and t_f, are defined in (B-9), (B-37), and (B-44).

This completes the description of the algorithm. The remainder of the appendix gives the equations for $\frac{\partial \ddot{x}_{PA}}{\partial \delta}$ and $\frac{\partial \delta}{\partial \lambda_\beta}$ in the twelve regions.

REGION 1: OCCUPANT IN DEAD ZONE; VEHICLE IN LINEAR REGION

The occupant acceleration is zero,

$$\ddot{x}(t) = 0 \quad .$$

The partial derivatives of occupant position, however, are not identically zero:

$$\left.\frac{\partial \delta(t_1)}{\partial f_m}\right|_{t_1} = 0$$

$$\left.\frac{\partial \dot{\delta}(t_1)}{\partial f_m}\right|_{t_1} = 0$$

$$\left.\frac{\partial \delta(t_1)}{\partial \kappa}\right|_{t_1} = \frac{V_c}{2M}\left(\sqrt{\frac{\mu}{\kappa}}\right)^3\left[-\sin\sqrt{\frac{\kappa}{\mu}}\,t_1 + \sqrt{\frac{\kappa}{\mu}}\,t_1\cos\sqrt{\frac{\kappa}{\mu}}\,t_1\right]$$

$$\left.\frac{\partial \dot{\delta}(t_1)}{\partial \kappa}\right|_{t_1} = \frac{t_1 V_c}{2M}\sqrt{\frac{\mu}{\kappa}}\sin\sqrt{\frac{\kappa}{\mu}}\,t_1 \quad .$$

(For convenience in writing these equations, which are exceedingly complex, we have dropped most subscripts. Thus $\ddot{x}$ is used to denote $\ddot{x}_{PA}$, δ to denote δ_A, M to denote M_A, etc.)

The notation used here for the partial derivatives is intended to indicate that these are the partials evaluated at t_1 on the reference trajectory. The total partial derivative must also reflect the change in t_1,

$$\frac{\partial SI(t_1)}{\partial \lambda_\beta} = \frac{\partial SI(t_1)}{\partial \lambda_\beta}\bigg|_{t_1} + |\ddot{x}(t_1)|^{\alpha}\frac{\partial(t_1-t_0)}{\partial \lambda_\beta}$$

$$\frac{\partial \delta(t_1)}{\partial \lambda_\beta} = \frac{\partial \delta(t_1)}{\partial \lambda_\beta}\bigg|_{t_1} + \dot{\delta}(t_1)\,\frac{\partial(t_1-t_0)}{\partial \lambda_\beta} \qquad \text{(N-12)}$$

$$\frac{\partial \dot{\delta}(t_1)}{\partial \lambda_\beta} = \frac{\partial \dot{\delta}(t_1)}{\partial \lambda_\beta}\bigg|_{t_1} + \frac{\ddot{\delta}(t_1)}{\partial \lambda_\beta}\,\frac{\partial(t_1-t_0)}{\partial \lambda_\beta} \quad .$$

This rectification to the perturbed endpoint, $t_1(\lambda)$, is performed in each region and the equations are identical, so they will not be repeated. As an example of the effect of this rectification, note that

$$\frac{\partial \delta(t_1)}{\partial f_m}\bigg|_{t_1} = 0$$

but if the occupant passes from region 1 to region 2 ($t_1 = t_y$) then, because t_y depends upon f_m, $\dfrac{\partial \delta(t_1)}{\partial f_m}$ will *not* be zero.

REGION 2: OCCUPANT IN DEAD ZONE; VEHICLE IN CONSTANT FORCE

$$\ddot{x}(t) = 0 \quad .$$

$$\frac{\partial \delta(t_2)}{\partial f_m}\bigg|_{t_2} = \frac{\partial \delta(t_1)}{\partial f_m} + \frac{\partial \dot{\delta}(t_1)}{\partial f_m}(t_2-t_1) + \frac{(t_2-t_1)^2}{2M}$$

$$\frac{\partial \delta(t_2)}{\partial f_m}\bigg|_{t_2} = \frac{\partial \dot{\delta}(t_1)}{\partial f_m} + \frac{(t_2-t_1)}{M}$$

$$\frac{\partial \delta(t_2)}{\partial \kappa}\bigg|_{t_2} = \frac{\partial \delta(t_1)}{\partial \kappa} + \frac{\partial \dot{\delta}(t_1)}{\partial \kappa}(t_2-t_1)$$

$$\left.\frac{\partial \dot{\delta}(t_2)}{\partial \kappa}\right|_{t_2} = \frac{\partial \dot{\delta}(t_1)}{\partial \kappa} \quad .$$

REGION 3: OCCUPANT IN DEAD ZONE; VEHICLE UNACCELERATED

$$\ddot{x} = 0.$$

$$\left.\frac{\partial \delta(t_3)}{\partial \lambda_\beta}\right|_{t_3} = \frac{\partial \delta(t_2)}{\partial \lambda_\beta} + \frac{\partial \dot{\delta}(t_2)}{\partial \lambda_\beta}(t_3 - t_2)$$

$$\left.\frac{\partial \dot{\delta}(t_3)}{\partial \lambda_\beta}\right|_{t_3} = \frac{\partial \dot{\delta}(t_2)}{\partial \lambda_\beta} \quad .$$

The occupant motion passes through region 3 only if the collision is complete before the restraint is contacted ($\delta(t_f) < d_s$). If this occurs, then the speed of the occupant $\dot{\delta}(t_f)$, when he encounters the restraint is dependent only upon closing speed, V_c, and the relative vehicle masses, M_A and M_B. It follows that the severity index will be independent of the parameters in such a case.

REGION 4: OCCUPANT IN LINEAR REGION; VEHICLE IN LINEAR REGION

$$\ddot{x} = -\frac{k_R}{m}(\delta - d_s) \quad .$$

Define

$$\frac{\partial \delta(t_4)}{\partial t_3} = \frac{\kappa V_c}{M\left(\frac{k_R}{m} - \frac{\kappa}{\mu}\right)}\left[\cos\sqrt{\frac{\kappa}{\mu}}\,t_4 - \cos\sqrt{\frac{\kappa}{\mu}}\,t_3 \cos\sqrt{\frac{k_R}{m}}\,(t_4 - t_3)\right]$$

$$+ \sqrt{\frac{m}{k_R}}\,\frac{\kappa V_c \sqrt{\frac{\kappa}{\mu}} \sin\sqrt{\frac{\kappa}{\mu}}\,t_3 \sin\sqrt{\frac{k_R}{m}}\,(t_4 - t_3)}{M\left(\frac{k_R}{m} - \frac{\kappa}{\mu}\right)} \quad ,$$

$$\frac{\partial\dot{\delta}(t_4)}{\partial t_3} = -\frac{\kappa V_c\sqrt{\frac{\kappa}{\mu}}}{M\left(\frac{k_R}{m}-\frac{\kappa}{\mu}\right)}\left[\sin\sqrt{\frac{\kappa}{\mu}}\,t_4 - \sin\sqrt{\frac{\kappa}{\mu}}\,t_3\cos\sqrt{\frac{k_R}{m}}\,(t_4-t_3)\right]$$

$$+\sqrt{\frac{k_R}{m}}\,\frac{\kappa V_c\cos\sqrt{\frac{\kappa}{\mu}}\,t_3}{M\left(\frac{k_R}{m}-\frac{\kappa}{\mu}\right)}\sin\sqrt{\frac{k_R}{m}}\,(t_4-t_3)$$

$$D_1 = \left[\frac{\partial\delta(t_3)}{\partial\kappa} - \frac{\sqrt{\frac{\mu}{\kappa}}\,V_c\left(\frac{k_R}{m}+\frac{\kappa}{\mu}\right)}{2M\left(\frac{k_R}{m}-\frac{\kappa}{\mu}\right)^2}\sin\frac{\kappa}{\mu}\,t_3 - \frac{V_c t_3\cos\sqrt{\frac{\kappa}{\mu}}\,t_3}{2M\left(\frac{k_R}{m}-\frac{\kappa}{\mu}\right)}\right]$$

$$D_2 = \left[\frac{\partial\dot{\delta}(t_3)}{\partial\kappa} - \frac{\frac{k_R}{m}V_c\cos\sqrt{\frac{\kappa}{\mu}}\,t_3}{M\left(\frac{k_R}{m}-\frac{\kappa}{\mu}\right)^2} + \frac{V_c\sqrt{\frac{\kappa}{\mu}}\,t_3\sin\sqrt{\frac{\kappa}{\mu}}\,t_3}{2M\left(\frac{k_R}{m}-\frac{\kappa}{\mu}\right)}\right]$$

Then

$$\left.\frac{\partial\delta(t_4)}{\partial f_m}\right|_{t_4} = \frac{\partial\delta(t_3)}{\partial f_m}\cos\sqrt{\frac{k_R}{m}}\,(t_4-t_3) + \sqrt{\frac{m}{k_R}}\,\frac{\partial\dot{\delta}(t_3)}{\partial f_m}\sin\sqrt{\frac{k_R}{m}}\,(t_4-t_3)$$

$$+\frac{\partial\delta(t_4)}{\partial t_3}\,\frac{\partial t_3}{\partial f_m}\,,$$

$$\left.\frac{\partial\dot{\delta}(t_4)}{\partial f_m}\right|_{t_4} = -\sqrt{\frac{k_R}{m}}\,\frac{\partial\delta(t_3)}{\partial f_m}\sin\sqrt{\frac{k_R}{m}}\,(t_4-t_3) + \frac{\partial\dot{\delta}(t_3)}{\partial f_m}\cos\sqrt{\frac{k_R}{m}}\,(t_4-t_3)$$

$$+\frac{\partial\dot{\delta}(t_4)}{\partial t_3}\,\frac{\partial t_3}{\partial f_m}\,,$$

$$\left.\frac{\partial\delta(t_4)}{\partial\kappa}\right|_{t_4} = D_1\cos\sqrt{\frac{k_R}{m}}\,(t_4-t_3) + \sqrt{\frac{m}{k_R}}\;D_2\,\sin\sqrt{\frac{k_R}{m}}\,(t_4-t_3)$$

$$+ \frac{V_c\sqrt{\frac{\mu}{\kappa}}\left(\frac{k_R}{m}+\frac{\kappa}{\mu}\right)}{2M\left(\frac{k_R}{m}-\frac{\kappa}{\mu}\right)^2}\sin\sqrt{\frac{\kappa}{\mu}}\,t_4 + \frac{V_c t_4\cos\sqrt{\frac{\kappa}{\mu}}\,t_4}{2M\left(\frac{k_R}{m}-\frac{\kappa}{\mu}\right)}$$

$$+ \frac{\partial\delta(t_4)}{\partial t_3}\;\frac{\partial t_3}{\partial\kappa}\quad,$$

and

$$\left.\frac{\partial\dot{\delta}(t_4)}{\partial\kappa}\right|_{t_4} = -\sqrt{\frac{k_R}{m}}\;D_1\,\sin\sqrt{\frac{k_R}{m}}\,(t_4-t_3) + D_2\,\cos\sqrt{\frac{k_R}{m}}\,(t_4-t_3)$$

$$+ \frac{V_c\,\frac{k_R}{m}}{M\left(\frac{k_R}{m}-\frac{\kappa}{\mu}\right)^2}\;\cos\sqrt{\frac{\kappa}{\mu}}\,t_4 - \frac{V_c\sqrt{\frac{\kappa}{\mu}}\,t_4\,\sin\sqrt{\frac{\kappa}{\mu}}\,t_4}{2M\left(\frac{k_R}{m}-\frac{\kappa}{\mu}\right)}$$

$$+ \frac{\partial\dot{\delta}(t_4)}{\partial t_3}\;\frac{\partial t_3}{\partial\kappa}$$

Notice that there is an apparent omission in that there is no differentiation performed with respect to the quantity (t_4-t_3). This variation is handled by the rectification (N-12). However, the computation of $\frac{\partial(t_4-t_3)}{\partial\lambda_\beta}$ requires the prior definition of $\left.\frac{\partial\delta(t_4)}{\partial\lambda_\beta}\right|_{t_4}$, so the calculations are performed in the indicated way.

REGION 5: OCCUPANT IN LINEAR REGION; VEHICLE IN CONSTANT FORCE

$$\ddot{x} = -\frac{k_R}{m}\,(\delta-d_s)\quad.$$

$$\left.\frac{\partial\delta(t_5)}{\partial f_m}\right|_{t_5} = \frac{\partial\delta(t_4)}{\partial f_m}\cos\sqrt{\frac{k_R}{m}}\,(t_5-t_4) + \sqrt{\frac{m}{k_R}}\,\frac{\partial\dot{\delta}(t_4)}{\partial f_m}\sin\sqrt{\frac{k_R}{m}}\,(t_5-t_4)$$

$$+ \frac{m}{Mk_R}\left(1 - \cos\sqrt{\frac{k_R}{m}}\,(t_5-t_4)\right)$$

$$\left.\frac{\partial\dot{\delta}(t_5)}{\partial f_m}\right|_{t_5} = -\sqrt{\frac{k_R}{m}}\,\frac{\partial\delta(t_4)}{\partial f_m}\sin\sqrt{\frac{k_R}{m}}\,(t_5-t_4) + \frac{\partial\dot{\delta}(t_4)}{\partial f_m}\sin\sqrt{\frac{k_R}{m}}\,(t_5-t_4)$$

$$+ \frac{1}{M}\sqrt{\frac{m}{k_R}}\sin\sqrt{\frac{k_R}{m}}\,(t_5-t_4)$$

$$\left.\frac{\partial\delta(t_5)}{\partial\kappa}\right|_{t_5} = \frac{\partial\delta(t_4)}{\partial\kappa}\cos\sqrt{\frac{k_R}{m}}\,(t_5-t_4) + \sqrt{\frac{m}{k_R}}\,\frac{\partial\dot{\delta}(t_4)}{\partial\kappa}\sin\sqrt{\frac{k_R}{m}}\,(t_5-t_4)$$

$$\left.\frac{\partial\dot{\delta}(t_5)}{\partial\kappa}\right|_{t_5} = -\sqrt{\frac{k_R}{m}}\,\frac{\partial\delta(t_4)}{\partial\kappa}\sin\sqrt{\frac{k_R}{m}}\,(t_5-t_4) + \frac{\partial\dot{\delta}(t_4)}{\partial\kappa}\cos\sqrt{\frac{k_R}{m}}\,(t_5-t_4)$$

REGION 6: OCCUPANT IN LINEAR REGION; VEHICLE UNACCELERATED

$$\ddot{x} = -\frac{k_R}{m}\,(\delta-d_s)$$

$$\left.\frac{\partial\delta(t_6)}{\partial\lambda_\beta}\right|_{t_6} = \frac{\partial\delta(t_5)}{\partial\lambda_\beta}\cos\sqrt{\frac{k_R}{m}}\,(t_6-t_5) + \sqrt{\frac{m}{k_R}}\,\frac{\partial\dot{\delta}(t_5)}{\partial\lambda_\beta}\sin\sqrt{\frac{k_R}{m}}\,(t_6-t_5)\quad,$$

$$\left.\frac{\partial\dot{\delta}(t_6)}{\partial\lambda_\beta}\right|_{t_6} = -\sqrt{\frac{k_R}{m}}\ \frac{\partial\delta(t_5)}{\partial\lambda_\beta}\ \sin\sqrt{\frac{k_R}{m}}\,(t_6-t_5) + \frac{\partial\delta(t_5)}{\partial\lambda_\beta}\cos\sqrt{\frac{k_R}{m}}\,(t_6-t_5)\ .$$

REGION 7: OCCUPANT IN CONSTANT FORCE; VEHICLE IN LINEAR REGION

$$\ddot{x} = -\frac{f_M}{m}\ .$$

Define

$$\frac{\partial\delta(t_7)}{\partial t_6} = -\frac{\mu V_c}{M}\left[(t_7-t_6)\sqrt{\frac{\kappa}{\mu}}\sin\sqrt{\frac{\kappa}{\mu}}\,t_6 + \cos\sqrt{\frac{\kappa}{\mu}}\,t_7 - \cos\sqrt{\frac{\kappa}{\mu}}\,t_6\right]$$

$$\frac{\partial\dot{\delta}(t_7)}{\partial t_6} = \frac{V_c\sqrt{\kappa\mu}}{M}\left[\sin\sqrt{\frac{\kappa}{\mu}}\,t_7 - \sin\sqrt{\frac{\kappa}{\mu}}\,t_6\right].$$

Then

$$\left.\frac{\partial\delta(t_7)}{\partial f_m}\right|_{t_7} = \frac{\partial\delta(t_6)}{\partial f_m} + (t_7-t_6)\ \frac{\partial\dot{\delta}(t_6)}{\partial f_m} + \frac{\partial\delta(t_7)}{\partial t_6}\ \frac{\partial t_6}{\partial f_m}$$

$$\left.\frac{\partial\dot{\delta}(t_7)}{\partial f_m}\right|_{t_7} = \frac{\partial\dot{\delta}(t_6)}{\partial f_m} + \frac{\partial\delta(t_7)}{\partial t_6}\ \frac{\partial t_6}{\partial f_m}$$

$$\left.\frac{\partial\delta(t_7)}{\partial\kappa}\right|_{t_7} = \frac{\partial\delta(t_6)}{\partial\kappa} + (t_7-t_6)\ \frac{\partial\dot{\delta}(t_6)}{\partial\kappa} + \frac{V_c}{2M}\sqrt{\frac{\mu}{\kappa}}\left[\frac{\mu}{\kappa}\left(\sin\sqrt{\frac{\kappa}{\mu}}\,t_7\right.\right.$$

$$\left.\left. - \sin\sqrt{\frac{\kappa}{\mu}}\,t_6\right) - t_6(t_7-t_6)\sin\sqrt{\frac{\kappa}{\mu}}\,t_6 - \sqrt{\frac{\mu}{\kappa}}\left(t_7\cos\sqrt{\frac{\kappa}{\mu}}\,t_7 - t_6\cos\sqrt{\frac{\kappa}{\mu}}\,t_6\right)\right]$$

$$+\ \frac{\partial\delta(t_7)}{\partial t_6}\ \frac{\partial t_6}{\partial\kappa}$$

$$\left.\frac{\partial \dot{\delta}(t_7)}{\partial \kappa}\right|_{t_7} = \frac{\partial \dot{\delta}(t_6)}{\partial \kappa} + \frac{V_c}{2M}\sqrt{\frac{\mu}{\kappa}}\left(t_7 \sin\sqrt{\frac{\kappa}{\mu}}\, t_7 - t_6 \sin\sqrt{\frac{\kappa}{\mu}}\, t_6\right) + \frac{\partial \dot{\delta}(t_7)}{\partial t_6}\frac{\partial t_6}{\partial \kappa}$$

REGION 8: OCCUPANT IN CONSTANT FORCE, VEHICLE IN CONSTANT FORCE

$$\ddot{x} = -\frac{f_M}{m} \quad .$$

$$\frac{\partial \delta(t_8)}{\partial f_m} = \frac{\partial \delta(t_7)}{\partial f_m} + (t_8 - t_7)\frac{\partial \dot{\delta}(t_7)}{\partial f_m} + \frac{(t_7 - t_6)^2}{2M}$$

$$\frac{\partial \dot{\delta}(t_8)}{\partial f_m} = \frac{\partial \dot{\delta}(t_7)}{\partial f_m} + \frac{(t_7 - t_6)}{M}$$

$$\frac{\partial \delta(t_8)}{\partial \kappa} = \frac{\partial \delta(t_7)}{\partial \kappa} + (t_8 - t_7)\frac{\partial \dot{\delta}(t_7)}{\partial \kappa}$$

$$\frac{\partial \dot{\delta}(t_8)}{\partial \kappa} = \frac{\partial \dot{\delta}(t_7)}{\partial \kappa}$$

REGION 9: OCCUPANT IN CONSTANT FORCE; VEHICLE UNACCELERATED

$$\ddot{x} = -\frac{f_M}{m} \quad .$$

$$\left.\frac{\partial \delta(t_9)}{\partial \lambda_\beta}\right|_{t_9} = \frac{\partial \delta(t_8)}{\partial \lambda_\beta} + (t_9 - t_8)\frac{\partial \dot{\delta}(t_8)}{\partial \lambda_\beta}$$

$$\left.\frac{\partial \dot{\delta}(t_9)}{\partial \lambda_\beta}\right|_{t_9} = \frac{\partial \dot{\delta}(t_8)}{\partial \lambda_\beta}$$

REGION 10: OCCUPANT ON THE BARRIER; VEHICLE IN LINEAR REGION

$$\ddot{x} = -\frac{k_D}{m}\left(\delta - d_T + \frac{f_m}{k_D}\right) .$$

The following equations are of the same form as those for Region 4.

Define

$$\frac{\partial\delta(t_{10})}{\partial t_9} = \frac{\kappa V_c}{M\left(\frac{k_D}{m}-\frac{\kappa}{\mu}\right)}\left[\cos\sqrt{\frac{\kappa}{\mu}}\,t_{10} - \cos\sqrt{\frac{\kappa}{\mu}}\,t_9\,\cos\sqrt{\frac{k_D}{m}}\,(t_{10}-t_9)\right]$$

$$+\sqrt{\frac{m}{k_D}}\;\frac{\kappa V_c\sqrt{\frac{\kappa}{\mu}}\,\sin\sqrt{\frac{\kappa}{\mu}}\,t_9\,\sin\sqrt{\frac{k_D}{m}}\,(t_{10}-t_9)}{M\left(\frac{k_D}{m}-\frac{\kappa}{\mu}\right)} ,$$

$$\frac{\partial\dot{\delta}(t_{10})}{\partial t_9} = -\frac{\kappa V_c\sqrt{\frac{\kappa}{\mu}}}{M\left(\frac{k_D}{m}-\frac{\kappa}{\mu}\right)}\left[\sin\sqrt{\frac{\kappa}{\mu}}\,t_{10} - \sin\sqrt{\frac{\kappa}{\mu}}\,t_9\,\cos\sqrt{\frac{k_D}{m}}\,(t_{10}-t_9)\right]$$

$$+\sqrt{\frac{k_D}{m}}\;\frac{\kappa V_c\,\cos\sqrt{\frac{\kappa}{\mu}}\,t_9}{M\left(\frac{k_D}{m}-\frac{\kappa}{\mu}\right)}\,\sin\sqrt{\frac{k_D}{m}}\,(t_{10}-t_9) ,$$

$$D_1 = \left[\frac{\partial\delta(t_9)}{\partial\kappa} - \frac{\sqrt{\frac{\mu}{\kappa}}\,V_c\left(\frac{k_D}{m}+\frac{\kappa}{\mu}\right)}{2M\left(\frac{k_D}{m}-\frac{\kappa}{\mu}\right)^2}\,\sin\sqrt{\frac{\kappa}{\mu}}\,t_9 - \frac{V_c t_9\,\cos\sqrt{\frac{\kappa}{\mu}}\,t_9}{2M\left(\frac{k_D}{m}-\frac{\kappa}{\mu}\right)}\right] ,$$

and

$$D_2 = \left[\frac{\partial\dot{\delta}(t_9)}{\partial\kappa} - \frac{\frac{k_D}{m}\,V_c\,\cos\sqrt{\frac{\kappa}{\mu}}\,t_9}{M\left(\frac{k_D}{m}-\frac{\kappa}{\mu}\right)^2} + \frac{V_c\sqrt{\frac{\kappa}{\mu}}\,t_9\,\sin\sqrt{\frac{\kappa}{\mu}}\,t_9}{2M\left(\frac{k_D}{m}-\frac{\kappa}{\mu}\right)}\right] .$$

Then

$$\left.\frac{\partial\delta(t_{10})}{\partial f_m}\right|_{t_{10}} = \frac{\partial\delta(t_9)}{\partial f_m}\cos\sqrt{\frac{k_D}{m}}\,(t_{10}-t_9) + \sqrt{\frac{m}{k_D}}\,\frac{\partial\dot{\delta}(t_9)}{\partial f_m}\sin\sqrt{\frac{k_D}{m}}\,(t_{10}-t_9)$$

$$+ \frac{\partial\delta(t_{10})}{\partial t_9}\,\frac{\partial t_9}{\partial f_m}\ ,$$

$$\left.\frac{\partial\dot{\delta}(t_{10})}{\partial f_m}\right|_{t_{10}} = -\sqrt{\frac{k_D}{m}}\,\frac{\partial\delta(t_9)}{\partial f_m}\sin\sqrt{\frac{k_D}{m}}\,(t_{10}-t_9) + \frac{\partial\dot{\delta}(t_9)}{\partial f_m}\sin\sqrt{\frac{k_D}{m}}\,(t_{10}-t_9)$$

$$+ \frac{\partial\dot{\delta}(t_{10})}{\partial t_9}\,\frac{\partial t_9}{\partial f_m}$$

$$\left.\frac{\partial\delta(t_{10})}{\partial\kappa}\right|_{t_{10}} = D_1\cos\sqrt{\frac{k_D}{m}}\,(t_{10}-t_9) + \sqrt{\frac{m}{k_D}}\,D_2\sin\sqrt{\frac{k_D}{m}}\,(t_{10}-t_9)$$

$$+ \frac{V_c\sqrt{\frac{\mu}{\kappa}}\left(\frac{k_D}{m}+\frac{\kappa}{\mu}\right)}{2M\left(\frac{k_D}{m}-\frac{\kappa}{\mu}\right)^2}\sin\sqrt{\frac{\kappa}{\mu}}\,t_{10} + \frac{V_c t_{10}\cos\sqrt{\frac{\kappa}{\mu}}\,t_{10}}{2M\left(\frac{k_D}{m}-\frac{\kappa}{\mu}\right)}$$

$$+ \frac{\partial\delta(t_{10})}{\partial t_9}\,\frac{\partial t_9}{\partial\kappa}\ ,$$

$$\left.\frac{\partial\dot{\delta}(t_{10})}{\partial\kappa}\right|_{t_{10}} = -\sqrt{\frac{k_D}{m}}\,D_1 \sin\sqrt{\frac{k_D}{m}}\,(t_{10}-t_9) + D_2 \cos\sqrt{\frac{k_D}{m}}\,(t_{10}-t_9)$$

$$+ \frac{V_c \frac{k_D}{m}}{M\left(\frac{k_D}{m} - \frac{\kappa}{\mu}\right)^2} \cos\sqrt{\frac{\kappa}{\mu}}\,t_{10} - \frac{V_c\sqrt{\frac{\kappa}{\mu}}\,t_{10} \sin\sqrt{\frac{\kappa}{\mu}}\,t_{10}}{2M\left(\frac{k_D}{m} - \frac{\kappa}{\mu}\right)}$$

$$+ \frac{\partial\dot{\delta}(t_{10})}{\partial t_9}\,\frac{\partial t_9}{\partial\kappa}$$

REGION 11: OCCUPANT ON THE BARRIER; VEHICLE IN CONSTANT FORCE

$$\ddot{x} = -\frac{k_D}{m}\left(\delta - d_T + \frac{f_M}{k_D}\right) \quad .$$

$$\left.\frac{\partial\delta(t_{11})}{\partial f_m}\right|_{t_{11}} = \frac{\partial\delta(t_{10})}{\partial f_m} \cos\sqrt{\frac{k_D}{m}}\,(t_{11}-t_{10}) + \sqrt{\frac{m}{k_D}}\,\frac{\partial\dot{\delta}(t_{10})}{\partial f_m} \sin\sqrt{\frac{k_D}{m}}\,(t_{11}-t_{10})$$

$$+ \frac{m}{Mk_D}\left(1 - \cos\sqrt{\frac{k_D}{m}}\,(t_{11}-t_{10})\right) \quad ,$$

$$\left.\frac{\partial\dot{\delta}(t_{11})}{\partial f_m}\right|_{t_{11}} = -\sqrt{\frac{k_D}{m}}\,\frac{\partial\delta(t_{10})}{\partial f_m} \sin\sqrt{\frac{k_D}{m}}\,(t_{11}-t_{10}) + \frac{\partial\dot{\delta}(t_{10})}{\partial f_m} \cos\sqrt{\frac{k_D}{m}}\,(t_{11}-t_{10})$$

$$+ \frac{1}{M}\sqrt{\frac{m}{k_D}} \sin\sqrt{\frac{k_D}{m}}\,(t_{11}-t_{10}) \quad ,$$

$$\left.\frac{\partial\delta(t_{11})}{\partial\kappa}\right|_{t_{11}} = \frac{\partial\delta(t_{10})}{\partial\kappa}\cos\sqrt{\frac{k_D}{m}}\,(t_{11}-t_{10}) + \sqrt{\frac{m}{k_D}}\,\frac{\partial\dot{\delta}(t_{10})}{\partial\kappa}\sin\sqrt{\frac{k_D}{m}}\,(t_{11}-t_{10})\ ,$$

and

$$\left.\frac{\partial\dot{\delta}(t_{11})}{\partial\kappa}\right|_{t_{11}} = -\sqrt{\frac{k_D}{m}}\,\frac{\partial\delta(t_{10})}{\partial\kappa}\sin\sqrt{\frac{k_D}{m}}\,(t_{11}-t_{10}) + \frac{\partial\dot{\delta}(t_{10})}{\partial\kappa}\cos\sqrt{\frac{k_D}{m}}\,(t_{11}-t_{10})\ .$$

REGION 12: OCCUPANT ON THE BARRIER; AUTO UNACCELERATED

$$\ddot{x} = -\frac{k_D}{m}\,(\delta - d_T + \frac{f_m}{k_D})\quad .$$

$$\left.\frac{\partial\delta(t_{12})}{\partial\lambda_\beta}\right|_{t_{12}} = \frac{\partial\delta(t_{11})}{\partial\lambda_\beta}\cos\sqrt{\frac{k_D}{m}}\,(t_{12}-t_{11}) + \sqrt{\frac{m}{k_D}}\,\frac{\partial\dot{\delta}(t_{11})}{\partial\lambda_\beta}\sin\sqrt{\frac{k_D}{m}}\,(t_{12}-t_{11})\ ,$$

and

$$\left.\frac{\partial\dot{\delta}(t_{12})}{\partial\lambda_\beta}\right|_{t_{12}} = -\sqrt{\frac{k_D}{m}}\,\frac{\partial\delta(t_{11})}{\partial\lambda_\beta}\sin\sqrt{\frac{k_D}{m}}\,(t_{12}-t_{11}) + \frac{\partial\dot{\delta}(t_{11})}{\partial\lambda_\beta}\cos\sqrt{\frac{k_D}{m}}\,(t_{12}-t_{11})\ .$$